Bacton Sandscaping

A process-based modelling study on the morphological response of the Bacton Sandscaping project

J.P.D. van der Veen

Bacton Sandscaping

A process-based modelling study on the morphological response of the Bacton Sandscaping project

by

J.P.D. van der Veen

to obtain the degree of Master of Science
at the Delft University of Technology,
to be defended publicly (online) on Monday August 31, 2020 at 11:00 AM.

Student number:	4319028	
Project duration:	Nov 4, 2019 – Aug 31, 2020	
Thesis committee:	Dr. ir. M.A. de Schipper,	TU Delft
	Prof. dr. ir. S.G.J. Aarninkhof,	TU Delft
	Dr. ir. A.P. Luijendijk,	TU Delft, Deltares
	Dr. ir. B.C. van Prooijen	TU Delft
	Ir. C.M. van der Boon,	Royal HaskoningDHV

An electronic version of this thesis is available at `http://repository.tudelft.nl/`.

The front page image was obtained from:
https://www.maritimejournal.com/news101/dredging/van-oord-completes-norfolk-coastal-works

TU Delft

Royal HaskoningDHV
Enhancing Society Together

Abstract

To counteract the effect of coastal erosion, nourishments are increasingly used to provide resilience to sea level rise. It is essential to better understand and predict the behaviour of these nourishments for both the calculation of cost effectiveness and for the coastal safety of these interventions. The last couple of years, the interest in large nourishments, that also feed the adjacent coast, has increased. A feeder nourishment is suggested to be cost effective as well as ecological more beneficial than traditional nourishments. However, their behaviour is more complex and the need for better morphological predictions has increased. Earlier research has given some insight in the morphological behaviour and the driving forces of these feeder nourishments. Nevertheless, their morphological behaviour is still not fully understood. Moreover, the research on feeder nourishments has been largely focused on one project location at the Delfland coast in the Netherlands. For the current study, a new feeder nourishment will be analysed. This feeder nourishment was constructed in August 2019 at the coast of Bacton (UK) named: *Bacton Sandscaping* (hereafter: BSS). The main research objectives of this thesis are to assess the morphological behaviour of the BSS in the first half year and the capability of a numerical model (Delft3D) to reproduce this behaviour. As a secondary objective, the effect of wave event intensity and grain size on the morphological behaviour is investigated. Lastly, the lifetime of the BSS is predicted using the numerical model. For the purpose of this study, the nourishment at the coast of Bacton is split up into three sections, a sediment feeder section and two sediment receiving sections, see Figure 1.

Figure 1: The feeder nourishment at the coast of Bacton. In yellow different parts of the nourishments are depicted. Number 2 indicates the area that is supposed to feed sediment to the adjacent areas 1 and 3.

The morphological behaviour of the BSS was assessed with the use of full bathymetric surveys. These were conducted three times with echo-sounder, LiDAR scanner and photogrammetry during the first half year of the BSS. These surveys were used to assess volume changes for the sub-aerial beach (beach elevations above +0m Mean Sea Level (MSL)) and submerged beach (beach elevations between +0m MSL and -10m MSL). Furthermore, cross-shore profiles were generated from these surveys to assess the cross-shore behaviour of the BSS. For the first half year, mainly erosion was observed for the sub-aerial beach and mainly accretion was observed for the submerged beach. In addition, the BSS showed a strong initial response; erosion volumes of the first six weeks were 4.5 times higher than the subsequent 4.5 months. Moreover, the volume analysis showed great alongshore variability of the morphological behaviour. Local erosion and accretion volumes can vary up to $100m^3/m$ over alongshore stretches of less than 250m. The alongshore variability of the sub-aerial beach volume changes is linked to the submerged beach volume changes. High erosion volumes of the sub-aerial beach are linked with low accretion rates of the submerged beach. Likewise, low erosion of the sub-aerial beach is linked with high accretion of the submerged beach. Furthermore, the cross-shore profile analysis showed that a scarp of four meters was formed at the end of the first half year. Besides the scarp formation, beach flattening was observed for all sections.

The numerical BSS model was extensively calibrated and validated using the survey data. The validation showed that the erosion and sedimentation intensity locations match very well with the survey data, when compared visually. The model's prediction of the most intense erosion is in line with the location of the scarp in the measurements. Furthermore, the model's capability to simulate the net volume changes is reasonable and it follows the alongshore variability quite good. However, the main strength of the model is to simulate the volume changes of the sub-aerial beach. The model performs excellent and shows the alongshore variability very well. The maxima and minima are also very well represented by the model in both their location and magnitude. For the submerged beach volume changes, the alongshore variability is also very well represented, although scoring just a bit lower than the sub-aerial beach. A similar cross-shore behaviour as in the surveys is observed. High sub-aerial beach erosion areas led to lower sedimentation of the submerged beach. Likewise, low sub-aerial beach erosion areas led to higher sedimentation of the submerged beach. This goes to show that the model is capable of representing the cross-shore connection between the sub-aerial and submerged beach. Lastly, the model predicted that significant wave heights lower than 1 meter are responsible for 59% of the observed erosion of the feeder section and that the erosive behaviour is not dominated by large wave events. Moreover, waves directed from +50 degrees north seem to cause the most erosion overall.

As the model was well capable of simulating the first half year, it was then assumed that the model is also capable of simulating beach volume changes for a different grain size as well as different wave event intensities. The model predicted that grain size and wave event intensity have almost no effect on the alongshore variability of the nourishment and only showed an increase in erosion or sedimentation across the entire alongshore stretch. In addition, the model was used to predict the lifetime of the BSS. The model predicted a lifetime of 5 years, which is shorter than initially expected. However, the model seemed to be sensitive to a calibration factor which determines the erosion of dry cells and no seasonal variability was observed, which means that the model's prediction is very conservative and should be considered as a worst case scenario.

Lastly, the BSS model results were compared to other coastal studies and it was found that for coastal applications, wave calibration factors between 0.2-0.4 gave in general good results. This could be a good starting point for future modelling studies. In addition, the low dependency on grain size in this study could be used for future feeder nourishment projects. If less focus will be put on different grain size alternatives, simulations required to test different grain sizes could be reduced.

Preface

This thesis finalises my master hydraulic engineering at the Delft University of Technology. In the last ten months I have been working on this research in collaboration with Royal HaskoningDHV. Royal HaskoningDHV provided me with all the necessary resources and internal knowledge to conduct this thesis. I am very grateful that they provided me with the opportunity to work on this interesting research of a new feeder nourishment project. I am very proud that I could be part of this project and I hope that my Delft3D model is of great use for Royal HaskoningDHV in the future.

First, I would like to thank my daily supervisor Mariska. She guided and helped me during this graduation and has always provided very positive critical feedback. Even when time was short for her, she always made sure to free up some space for my questions. Furthermore, I would like to thank Jaap Flikweert and Ruben Borsje for providing their knowledge of the project and showing me the UK perspective on the project.

Then I would like to thank my thesis committee. Matthieu, your enthusiasm for nourishments and this project have been of great inspiration. Your positive attitude and the feedback you gave me are very much appreciated. Stefan, thank you for your guidance and insights during meetings. These got me thinking more about the subject and made the report better overall. Arjen, I would like to thank you for your help of getting me started with Delft3D and also for helping me with questions regarding the morphological modelling and morphological analysis. Bram, the feedback during the green light meeting was very constructive and I liked the somewhat different structure of the meeting, thank you for that. It is unfortunate that you're likely not present at my graduation.

Lastly, I want to thank my family and friends for their support during this graduation. Especially my girlfriend has been of great support during the moments I struggled the most.

Jeroen van der Veen
Rotterdam, August 2020

List of Symbols and Abbreviations

Δt	Time step [s]
η	Relative available sediment in mixing layer [-]
γ	Wave breaker coefficient [-]
γ_l	Phase lag coefficient [-]
Ω	Wave energy at foot of cliff [J/m^3]
Ω_c	Energy threshold level [J/m^3]
ρ_s	Sediment density [kg/m^3]
ρ_w	Water density [kg/m^3]
D_h	Horizontal eddy diffusivity [m^2/s]
d_{50}	Median grain diameter [m]
g	Gravitational constant [m/s^2]
H_{m0}	Significant wave height [m]
M	Sediment mobility number due to waves and currents[-]
M_e	Excess sediment mobility [-]
MSE	Mean square error [-]
$MSE_{nochange}$	Mean square error of a no change morphological model [-]
S_p	Steepness parameter [-]
t	Time [s]
T_{m02}	Mean wave period [s]
U_A	Velocity asymmetry value [-]
V_h	Horizontal eddy viscosity [m^2/s]
w_s	Fall velocity [m/s]
1D	One-dimensional
2DH	Two-dimensional, depth averaged
BGT	Bacton Gas Terminal
BODC	British Oceanographic Data Centre
BSS	Bacton Sandscaping
CLR	Cliff line retreat
GPS	General positioning system
LiDAR	Light detection and ranging

morfac	Morphological acceleration factor
MSL	Mean sea level (Ordnance Datum)
SMP	Shoreline management plan
UK	United Kingdom

List of Figures

List of Tables

Contents

1 Introduction

Coastal erosion seriously affects 20.000 km of coast in Europe. The majority of these coasts are continuously retreating, of which 19 % are retreating despite engineering interventions [2]. Such a coast is found in Norfolk (east England), where the shoreline consists of soft Plio-Pleistocene rocks and sediments that shape the cliff dominated coastline [7]. These coastal cliffs are characterised by high erosion rates which can surpass 1 m/year of cliff line retreat[16]. In the past, hard measures (i.e. groynes and seawalls) have been constructed to prevent or decrease the coastal and/or cliff erosion. However, these measures repeatedly introduced new erosion problems at locations further down drift from the intervention and were not able to provide a solution to the erosion[18]. The continuation of erosion ultimately led to an increased danger to the gas infrastructure of the UK. A large gas terminal (providing one third of the total gas production of the UK) close to the edge of these fast retreating cliffs became vulnerable to future large erosion events. Moreover, villages located 1 to 4 km down drift of the gas terminal were also suffering from high erosion rates. Therefore, a large scale beach nourishment was proposed to prevent further cliff erosion. The proposed nourishment was then later constructed and finished in August 2019.

Beach nourishments have been applied in the UK since 1972 to prevent the relocation of erosion due to human interventions[18]. However, the newly constructed nourishment is the largest nourishment in the UK yet. It has a volume of 1.8 million m^3 of sand and is constructed over a length of 6 km and is expected to feed sediment to the villages 1 to 4 km down drift of the gas terminal. Accordingly, the project is called *Bacton Sandscaping* (hereafter: BSS). This feeding concept is a relatively new method of nourishing the coast and is suggested to be cost-effective and ecological beneficial [41]. Traditional beach widening nourishments need regular renourishing, since their effect disappears quite quickly. Contrary, feeder type nourishments require a large starting volume, but will require less renourishments. In this manner, it is expected that financial costs are reduced and less pressure is exerted on the ecosystem [11]. However, the morphological behaviour of feeder type nourishments comes with high uncertainties concerning sediment transport rates.

Considering the uncertainties of the morphological response of large scale nourishments, numerical models are in general used to predict nourishment lifetimes and morphological behaviour. These models are a valuable asset to asses the behaviour of nourishments. Luijendijk et al. [27] showed that a depth averaged (2DH) process-based model is capable of reproducing the morphological behaviour of a mega nourishment (called: the Sand Engine) at the Delfland coast in the Netherlands. Moreover, the model was used to asses individual forcing parameters and their effect on the morphological behaviour. The insight in how forcing parameters affect nourishments is essential in understanding its behaviour. Gaining more knowledge about the range of effect of forcing parameters increases the confidence of predictions.

1.1. Problem definition

The protective capacity of the BSS is largely based on beach width and beach volume. It is used as an indicator for the minimum required safety level for no cliff erosion to be present. Cliff erosion is considered cyclic; as waves remove debris at the bottom of a cliff, it further enhances erosion. Without waves reaching the toe of the cliff, no cyclic recession will be present [37]. Therefore, it is essential that the morphological behaviour of the BSS is fully understood. In order to understand the morphological behaviour of the BSS, first the initial response needs to be evaluated. During the first half year of the BSS project, three surveys were performed. However, these surveys are not yet analysed. This means that volume changes, alongshore variability and cross-shore interactions of the first half year are not yet quantified. Besides the morphological response itself, the capability of a 2DH model to simulate the behaviour of a feeder nourishment outside the Delfland coast

in the Netherlands is still unknown. Moreover, a morphological model can provide more insight in the way the BSS is affected by forcing conditions.

The Bacton coastal area consists of a variety of different sediment classes and is considered to be non homogeneous. It was opted to use the mean d_{50} of the entire area. While the effect of the grain size on the nourishment was evaluated, the effect of the grain size in combination with different wave event intensities was not assessed.

In addition, the morphological evolution of the BSS on a longer time scale has only been evaluated with the use of a 1D model. Further assessment on the lifetime of the nourishment is required.

The following knowledge gaps have been identified: The morphological behaviour of the BSS in the first half year is still unknown. Moreover, the capability of a 2DH morphological model to replicate the behaviour of this feeder nourishment is not quantified. In addition, the effect of grain size and wave event intensity on the beach volume changes is not estimated yet. Finally, the estimated lifetime of the BSS is yet only estimated by the use of a 1D model.

1.2. Project objectives

The design of the BSS is based on a one dimensional model combined with an estimation of the off shore losses provided by a 2DH model (TELEMAC). However, the 2DH model could not be calibrated sufficiently to provide viable data for the coastal section and was therefore not used to simulate the morphology of the BSS. A 1D model is not capable to capture the more complex morphological patterns which are required to asses the behaviour of erosion en sedimentation of a feeder nourishments. Therefore, a depth averaged (2DH) model is set up for the BSS to gain more insight in the morphological behaviour. For a large feeder nourishment (Sand Engine) on the Delfland coast in the Netherlands a model has been successfully set up with the process based model Delft3D and therefore it is chosen to model the BSS with the same model. This combined with the problem definition of the last paragraph leads to the following main objectives:

1. *Assess the morphological behaviour of the BSS in the first half year.*
2. *Evaluate the capability of Delft3D to simulate the first half year of the BSS.*

In addition to the main objectives, two sub-objectives have been defined:

1. *Relate the effect of wave intensities and grain size on beach volume and the morphological behaviour of the BSS.*
2. *Estimate the lifetime of the constructed solution.*

1.3. Research question and sub-questions

The objectives of this thesis leads to the main research questions regarding the Bacton Sandscaping project.

1. *What is the morphological response of the BSS in the first half year?*
2. *How well is Delft3D at simulating the first half year of the BSS?*

The secondary research questions of this research are.

1. *How do wave event intensities and nourishment grain size affect the sub-aerial beach volume behaviour?*
2. *Do the functional requirements of the nourishment still hold at the end of the design lifetime?*

In order to answer these questions, a numerical model will be set up of the BSS. This model will be used to assess different scenarios and also to evaluate the behaviour of the sandscaping nourishment in the future. This numerical model will be validated by field measurements.

1.4. Approach

To answer the main research questions and the secondary research questions it will first be needed to gain a better understanding of the coastal system and the coastal processes present in the area of the BSS. Moreover, a description of the design and the functional requirements will be discussed. Secondly, a morphological model will be set up, which implements the BSS design with the coastal processes present in the area. The

model that is set up will consist of a Delft3D-flow and a Delft3D-wave model that are coupled to get a full morphological model. This model is used to simulate the first half year of morphological change of the BSS. The model is calibrated to the coastal area without the BSS intervention. This will ensure that the coastal processes are incorporated well enough. Furthermore, the model of the original coast, will function as a reference case. Once the model is calibrated, the BSS project will be implemented in the numerical model and is validated afterwards. The validation uses survey data from August 2019, October 2019 and February 2020. These surveys are performed on the field with laser and echo-sounder measurement instruments. Before validation is possible, the surveys are analysed to evaluate the morphological behaviour of the BSS in the first half year. This will answer the first main research question. Afterwards, the validation will provide the capability of Delft3D to simulate the BSS. Hence, the second main research questions will be answered. The validated model is then used to analyse the effect of different wave conditions and different sediment parameters. These conditions are then linked to their effect on the morphological behaviour of the BSS. Lastly, the validated model is used to asses the requirements at the end of the expected lifetime (15 years). The total approach is schematised and showed in Figure 1.1

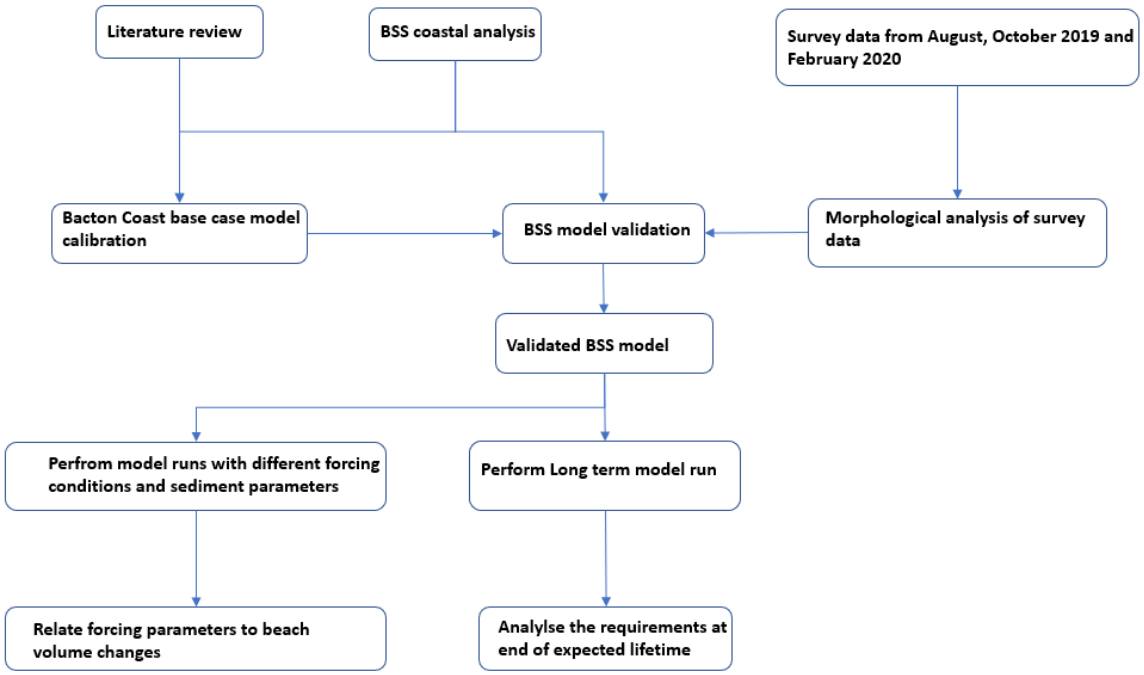

Figure 1.1: Flow diagram of the approach in this thesis. The arrows indicate a connection between the different parts of this thesis

1.5. Outline

This paragraph describes the outline of this thesis and how the approach is divided into the chapters. Chapter 2 discusses the coastal conditions and processes of the Bacton coast. This gives the background information about the study site and the processes that are incorporated in the numerical model. Chapter 3 discusses the methodology of the model approach and which model scenarios are needed to answer the research questions. The following Chapter describes the model calibration procedure of a baseline model. This baseline model will ensure that modelled processes are in line with literature and measurements of the study area. Chapter 5 describes the analysis of the surveys performed for the BSS nourishment. Chapter 6 discusses the validation of the model including the BSS. Chapter 7 describes the results obtained from the different model runs of the BSS. The last chapters of this thesis provide the discussion, conclusions and recommendations.

2
Literature Review

The coastal policy of the UK differs largely from the policy of other European countries and will therefore need some extra elaboration. Moreover, the UK policy is the main driver for the design choices of the BSS and also forms the basis for the requirements for which the lifetime is predicted. Secondly, the morphological and hydraulic processes of the coast of Bacton are discussed to get a foundation of the modelling approach described in Chapter 3. Finally, this chapter will cover the final design of the BSS.

2.1. Coastal policy UK

Before the 1950's the coastal defence strategy of the UK consisted largely of hard engineering solutions (e.g. concrete seawalls, groynes, breakwaters etc.). The hard solutions that were proposed solved the erosion problems locally, but frequently it relocated the problem elsewhere [18]. To reduce the the choice of local solutions and to eliminate the relocation of erosional issues, the UK coast was divided into 22 *coastal cells* (see Figure 2.1). For each of the cells a specific plan for the future of coastal protection was set up. A so called shoreline management plan (i.e. SMP).

Figure 2.1: Shoreline management plans in the UK. The northern part of SMP 6 corresponds with the coastal area of Bacton. Adapted from (Nicholls et al. [30])

These SMP's provided the basis for a coastal system approach by broadening the very local view to a more regional view. However, the country is lacking a plan on national level and coastal decisions are made by local authorities only [30]. Moreover, these SMP's are not coupled to any budget and are not binding in a legal aspect. This implies that there is no obligation to reduce erosion or even flooding along the coast of the country [43].

The SMP's have divided the coast up into smaller sections and for these sections there is a short term, medium term and long term strategy. Respectively, the durations of these terms are 0-20 years, 20-50 years and 50-100 years. For each of the terms a specific strategy is chosen from the below mentioned options:

- **No active intervention**: No intervention will be taken and the shoreline will not be defended any further and loss of land is acceptable.

- **Managed realignment**: The shoreline is allowed to move freely but is managed in such a way that the movement is gradual.

- **Advance the existing defence line**[1]: New coastal defence is build in seaward direction to acclaim new land.

- **Hold the existing defence line**: The existing defence will be kept or improved to current safety standards to keep the shoreline in the same position.

After the 1950's the UK also started implementing beach nourishments. However, the size and amount of nourishing projects have been very limited comparing to other countries in Europe. It can also be concluded that the UK rarely renourishes their project sites, where it is widely accepted that coasts have to be renourished every couple of years to make up for the lack of sediment in the system [17]. A more common approach in the UK is to collect sediment on the downdrift end of the coast and place it up drift again. Often a large groyne on the downdrift end is constructed to simplify this process of redistributing sediment [18]. In Table 2.1 a comparison between the nourishment practices of the UK and other countries of Europe is made which shows the lack of experience in large nourishments in the UK.

Table 2.1: Total nourishment facts of Europe, adapted from Luo et al. [28]

country	Number of sites	Number of projects	Total volume [m^3]	Average volume per nourishment [m^3]
UK	32	35	20,000,000	571,000
Netherlands	30	150	110,000,000	733,000
Germany	60	130	50,000,000	385,000
Spain	400	600	110,000,000	183,000
Italy	36	36	15,000,000	417,000

2.2. Bacton coast

Bacton is located on the coast of East Anglia where coastal cliff erosion has been a major problem. These soft cliffs were formed in poorly consolidated sand and clay and are easily eroded, leading to significant cliff line retreat [21]. To try and reduce the erosion, groynes, revetments and other hard coastal structures have been realised in the past. Despite these structures, coastal erosion remained a significant problem. Moreover, storm surges in 2007 and in 2013 lead to several meters of cliff line loss [43]. This ever increasing retreat became a danger to the natural gas terminal located near the coastline of Bacton. The natural gas terminal provides one third of the total gas supply in the UK [1] and is therefore of vital importance to the country (see Figure 2.2 for the location of the gas terminal, villages, cliffs and a seawall).

[1] Advance the existing defence line is only applicable for areas where large reclamations are planned

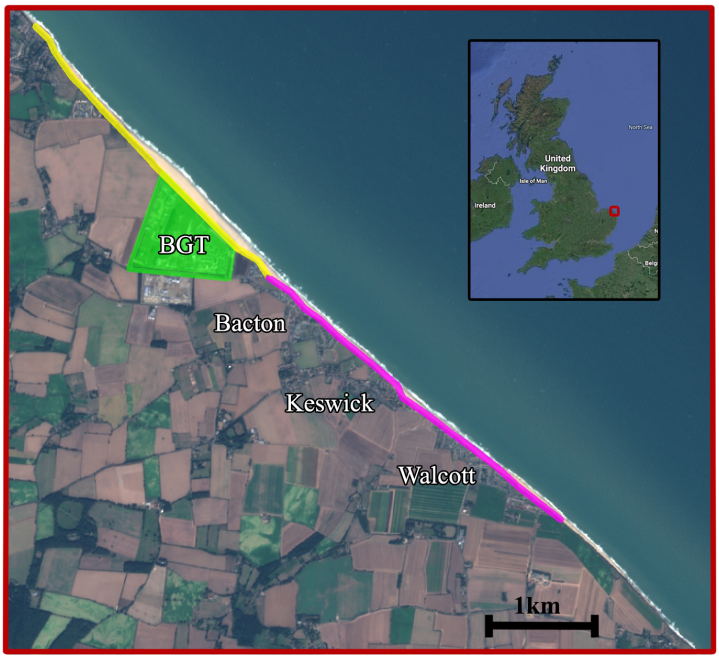

Figure 2.2: Location of the coast of Bacton. Green: Bacton gas terminal (BGT). Yellow: location of cliffs. Magenta: location of the seawall

Additionally, villages and holiday parks located downdrift of the gas terminal were also vulnerable to the coast line retreat. The caravan park in Bacton is directly threatened as the park is situated at the edge of the cliff (see Figure 2.3). The current policy for the location of the gas terminal and the villages downdrift can be found in Table 2.2.

Table 2.2: Strategy for location of interest. *Where 'hold' is defined as: hold the existing defence line*

Location	Short term	Medium term	Long term
Bacton Gas Terminal	hold	hold	hold
Bacton Gas Terminal - Walcott	hold	managed realignment	managed realignment

A difference in strategy for the gas terminal and the villages can be seen and therefore, the protection should provide a solution for the two different strategies. A nourishment of 1.8 million m^3 was constructed in August 2019 and is supposed to protect the gas terminal and feed the adjacent coast. Hence, the project has been called Bacton Sandscaping (BSS). The BSS can be considered as one of the biggest nourishments in UK history, since the volume of the nourishment corresponds with 10% of the total volume of all nourishments since the 1950's. The nourishment consists of large a concentrated volume of sand near the gas terminal with a narrow tail extending to the villages. This provides the immediate protection to both the Gas terminal and the villages, but on the medium/long term it will provide a managed realignment of the coast in front of the villages, through its feeder mechanism. A solution for only a highly concentrated volume of sand in front of the gas terminal was not possible in this case, since this would not provide the necessary immediate protection for the villages.

In order to understand the chosen design of the BSS and ultimately to assess the performance of the BSS, understanding the coastal system is essential. First the location and the coastal policy of the area are described to understand the chosen solution. Secondly, the coastal processes of the area are elaborated.

Figure 2.3: Caravan park located at the edge of the cliff in Bacton

2.2.1. Environmental conditions

The environmental conditions in which the BSS is set provide the information on the relevant hydraulic and morphological processes. In the next part, the coastal profile, wave climate, tide and sediment characteristics are given. Furthermore, the design of the BSS is discussed.

Coastal profile

In a broad context, the east Anglian coast is located on the North Sea continental shelf and it is a relatively shallow area with depths of up to 40 meters at a 40km offshore distance. Besides, a sandbank system can be identified looking at figure 2.4. These sandbanks are characterised by deep troughs and high peaks, where the peaks can reach depths of -4 MSL and the troughs can reach -40 MSL. Since the sandbank system has such high peaks it could have a significant effect on the propagation of waves due to refraction. It could lead to more waves reaching the shores of east Anglia, especially waves coming from the north. The coastline between Bacton and Walcott (i.e. BSS project area) consists of the cliffs described before which have elevations ranging from +5 to +30 meters (reference level: MSL). The toe of the cliff is located between MSL and +4 meters. After the toe the profile advances in a relatively mild slope of 1:100 to a depth of 10 meters below MSL. Finally, the slope mildens further to about 1:1000. A depth of 20 meters is reached approximately 10 kilometres offshore.

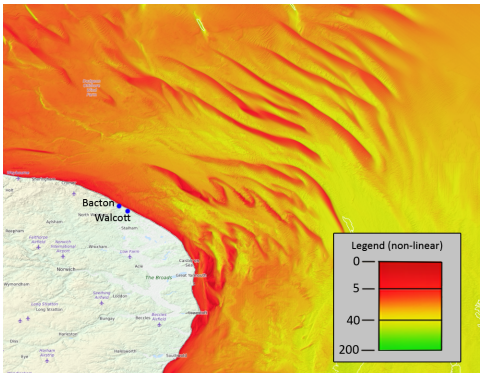

Figure 2.4: Sandbank system near the east Anglian coast (source: EMODnet)

Wave climate

Data for the wave climate is obtained from a point approximately 60 km offshore (see Figure 2.5a) from the Met Office European WaveWatchIII model. This data set covers a period from 1980 until 2015. At this location the depth is around 35 meters. The data set was transformed to nearshore wave conditions just offshore of Bacton. The wave rose for the location just offshore of Bacton can be seen in Figure 2.5b. It can be concluded that most of the waves are coming from the north and north-east. Moreover, the highest waves are coming from these directions as well.

(a) Location of project area and the location of the wave data

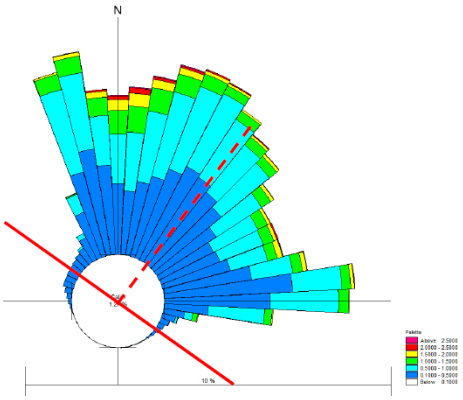

(b) Wave rose just offshore of Bacton

Figure 2.5: Area of interest

Tide

At the coast of east Anglia the tide has a semi diurnal character which means that there is high and low water twice a day. The tide propagates from north to south and decreases in range along the coast. The neap/spring tidal amplitude at Cromer is 0.5/2.5 m and for Winterton it is 0.5/1.5 m. The rising period of the tide is around 5 hours and 30 minutes at both Cromer and Winterton and the falling period is 6.5 hours for Cromer and 7 hours for Winterton, which means that there is a slight asymmetry in the tide.

Sediment

At the Bacton and Walcott beach a sediment study was done by HR Wallingford. Four locations (i.e. the foot of the cliff, upper beach face, lower beach face and shoreface) along the cross-shore profile of Bacton were chosen and multiple samples at each location were taken to estimate the d_{50} in the area. For Walcott only samples of the shoreface were taken. The samples show a variability over the cross-shore profile (see Table 2.3).

Location	Number of samples	d_{50} range [mm]
Bacton toe of cliff	4	0.2 – 0.3
Bacton upper beach face	4	0.3 – 0.45
Bacton lower beach face	3	0.45 – 9
Bacton shoreface	15	0.25 – 0.45
Walcott shoreface	3	0.4 – 0.45

Table 2.3: Sediment samples results

Although the wide variability, the sediment in the area can mostly be characterised as medium sand and gravel with a mean d_{50} of 350μm. This is also the grain size that is used for the construction of the BSS. The nourishment is constructed with sediment from one single source and it is therefore assumed that the d_{50} is constant for the entire nourishment.

2.3. Coastal processes

The coast of Bacton can be considered a complex system, where cliff erosion and alongshore sediment transport interact with each other. Understanding the behaviour of the Sandscaping solution requires a thorough understanding of these processes first. These will be described in the upcoming sections.

2.3.1. Cliff erosion theory

Cliff erosion described in literature is mainly based on soft rocky cliffs. Although the cliffs at Bacton are not made of rock, it shows similar characteristics as that of soft rocks (i.e. compressive strength lower than 5 MPa). Rocky cliffs can be categorised into 3 platform types: Sloping type, horizontal type and plunging type

[37], this is showed in Figure 2.6.

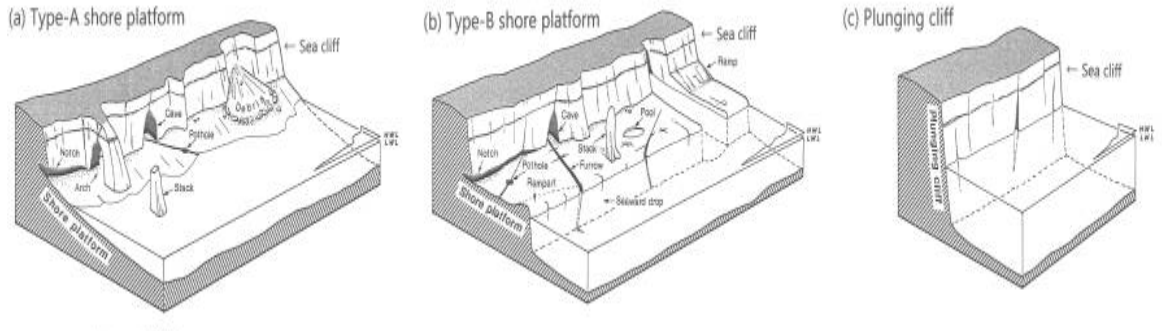

Figure 2.6: Cliff types: sloping type (A), horizontal type (B) and plunging type (C) , adapted from Sunamura [37]

Cliffs consisting of soft rock will form a sloping type platform. This type of cliff is the most rapidly eroding cliff type. The horizontal and plunging type cliffs are always accompanied by stronger rock and will not be formed with softer material. The horizontal cliff type is characterized by an erodible platform in front of the cliff with a seaward drop (scarp) at the end. The plunging cliff is a vertical wall consisting of hard rock which drops immediately in the sea without an erodible platform in front. These cliff types are not applicable for Bacton and they will not be further elaborated. It must be noted that the several features (e.g. cave, arch, stack etc.) of a sloping type cliff are not possible for the cliffs in Bacton which consist of sand and clay, since there is less to no cohesion. However, the slumping type failure accompanied by a debris deposit at the bottom is very similar to the cliff failure type seen at Bacton. Therefore, it is assumed that processes governing the erosion for soft rock will be similar to the processes found at Bacton. The cliff erosion process can be considered both episodic (storm events) and gradual(normal conditions) and contrary to dunes, there is no process as cliff growth and therefore erosion of the cliffs in front of the gas terminal is problematic. Moreover, using a historical extrapolation of cliff recession is generally unreliable, due to the complexity of the mechanisms driving cliff erosion [8]. Accordingly, it is essential to understand the underlying mechanisms that drive the erosion processes. The driving parameters for cliff erosion are described by [8], [45], [21], [33],[37], [16], and [24]. These driving parameters are listed and explained below.

1. *Waves*: Waves are the main force causing the erosion process at the toe of the cliff. The breaking waves exert energy on the toe and start the erosion process. When a large enough amount is eroded at the bottom of the cliff, the cliff becomes unstable and the upper section of the cliff can slide or slump down.

2. *Material strength*: The material strength of the cliffs determines both the shape of the shore platform as well as the erosion rate. It is self-evident that softer material will erode more quickly than harder material. Although it is clear that material strength is an important parameter, it is complicated to quantify the strength of the cliffs due their non-uniform character. Moreover, the sampling of an entire cliff face is a very costly process[16].

3. *Beach slope*: The slope of the beach in front of the cliffs determine the type of waves reaching the toe of the cliffs and therefore, it also largely determines the erosion rate. The slope of the beach combined with the wave steepness determine the breaker type (i.e. Iribarren number), which influences the amount of erosion. Breaker types which exert higher pressure forces on the bottom (e.g. plunging and surging waves) are also more capable of eroding the toe of the cliff.

4. *Beach width*: The beach in front of the cliff can function as a protection. In several studies it has been found that there is a non-linear relation between the width of the beach and the erosion rate of the cliffs. In general, increasing beach width leads to a decrease in erosion of the toe of the cliff.

5. *Beach elevation*: Beach elevation determines to what extend the water level and thus waves can reach the foot of the cliffs. Beach elevation is inextricably coupled to the amount of waves reaching the toe of the cliffs, just as beach width and beach slope.

The aforementioned parameters drive an erosional process at the toe of the cliff. This toe erosion will eventually lead to one of the four different failure mechanisms: slides, flows, topples and falls. See Figure 2.7 and the description below of each individual failure mode.

1. *Slides*: Slides are caused by instabilities in the slope of the cliff and the slide can happen in a circular or linear plane.

2. *Flows*: Flows at cliffs are mostly mudflows or fluidization of the cliff material. Large parts of the cliff flow to the toe and large recession rates are typical for this failure type. [37] These slides are mainly caused by the materials strength and precipitation.

3. *Topples*: A part of the cliffs topples around a turning point higher up in the cliff. This failure mode applies to hard rock cliffs and is therefore not applicable for Bacton.

4. *Falls*: Overhanging clumps of material falling from the top to the bottom of the cliff. Typically this failure mode is only vertical and is applicable for clay and chalk type cliffs but not for the cliffs at Bacton, since no overhanging features are present.

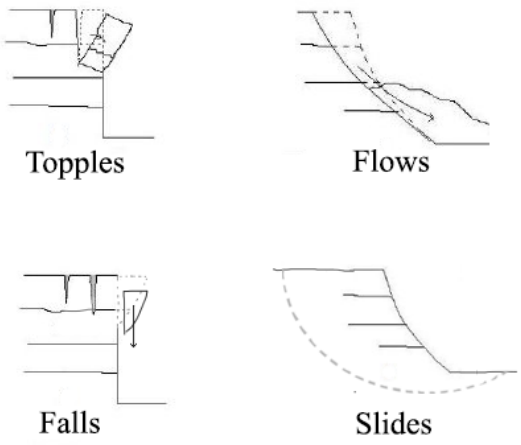

Figure 2.7: Cliff failures modes, modified version from Santos et al. [36]

To summarise, the driving forces lead to erosion of the toe of the cliffs. This leads to mass movement of the total cliff and cliff material is deposited at the bottom (talus). The deposited cliff material is then eroded by the driving forces again until the toe of the cliff is exposed again. New toe erosion happens and the process starts all over again. This feedback loop of cliff erosion is shown in Figure2.8.

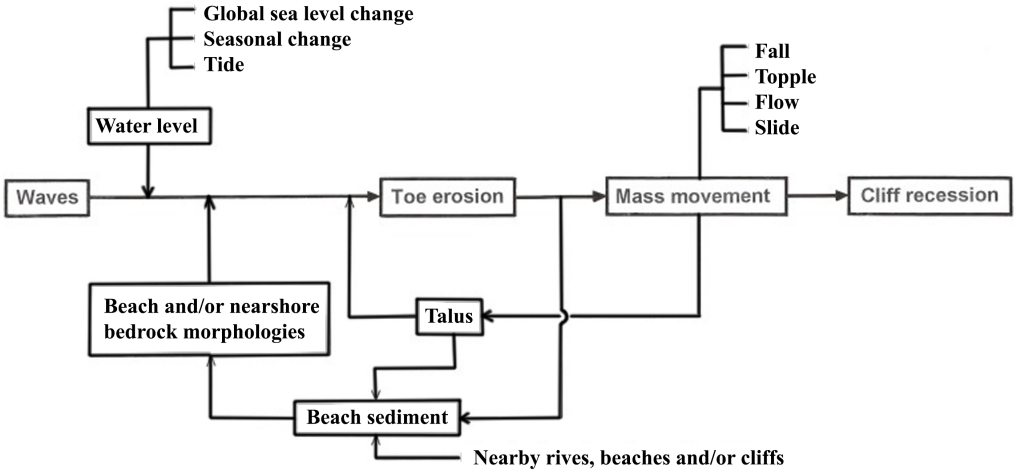

Figure 2.8: Cliff erosion process, including the failure mechanisms and the driving forces, adapted from [37]

2.3.2. Cliff erosion at Bacton

Although it very unreliable to extrapolate satellite imagery to estimate cliff line retreat, due to their complexity and often event driven behaviour [8]. It can still be used to investigate whether the retreat is gradual, episodic or both. Therefore, Royal HaskoningDHV [35] analysed satellite images from 1946, 1992 and 2009 to assess the behaviour of the cliffs in the area. The locations of the toe and the top of the cliffs are marked on the satellite picture of 2009 (see Figure2.9). It can be concluded that the cliff line has been retreating since 1946, but the period between 1992 and 2009 shows little to no erosion at all. Moreover, major cliff line retreats are known to be caused by extreme high water levels which happened in 2007 and 2013. In the duration of the storm events the cliff line retreated several meters. Therefore it is assumed that cliff line retreat is only episodic at the beach front of Bacton.

Figure 2.9: Cliff locations. Dotted lines are the cliff toe positions and the striped lines are the cliff top locations. (Green = 1946, Orange = 1992, Red = 2006). Adapted from [35].

Besides the aerial images, a study of the Northern Norfolk cliff's recession has been performed by Lee [21]. Cliffs from Weybourne up until Mundesley where assessed, the cliffs of Bacton lie just a few hundred meters

east from Mundesley and were not included in the research. From the years 1992-2003 measurements of the cliffs were taken twice a year to estimate the average yearly recession rates. A dependency between beach cross-section area and cliff recession was found. The cross-section area that is linked to the cliff erosion is shown in Figure 2.10. These cross-section areas were determined for 23 different cross-shore profiles across the east Anglian coast.

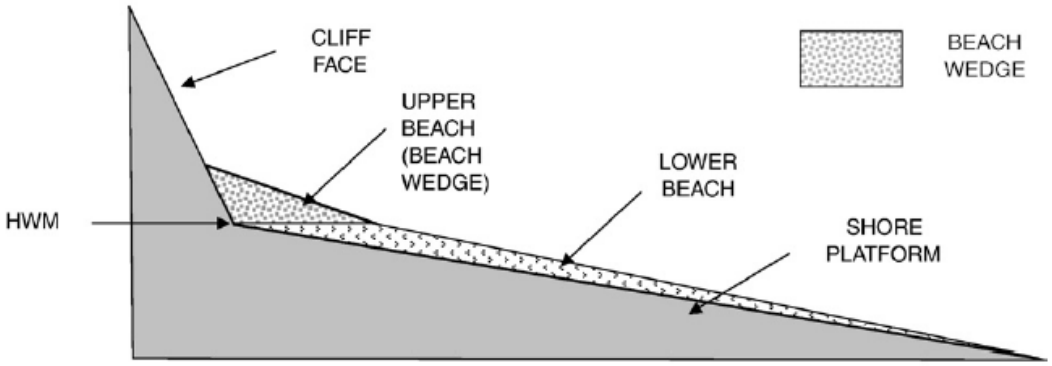

Figure 2.10: The upper beach wedge is the area that is used for the linking beach area with cliff recession. The beach cross-section area is defined as the cross-section area above high mean water (HMW). Adapted from Lee [21]

A wide variability of recession rates was found for small beach cross-sections (i.e. $< 5\text{m}^2$), where the recession rates varied from 0 to 20 meters per year. However, cross-sections larger than $20m^2$ show almost no variability and recession rates are mostly 0 meters/year.Since the cliffs of Bacton are in close proximity of the research area it is assumed that Lee [21]'s research also applies to these cliffs. Considering the large nourishment that is placed in front of Bacton, the beach cross100 section area will be typically much larger than $20m^2$. Combining this with the fact that in the period of 1992-2006 there was no cliff erosion at Bacton, it is presumed that cliff erosion is only episodic.

2.3.3. Alongshore Sediment transport

The sediment alongshore transport has been quantified for the area by a SCAPE (Soft Cliff And Platform Erosion) model by Royal HaskoningDHV in 2017. The model predicted net sediment transport rates for the area of 120,000-140,000 m^3 in southward direction. Also data from literature are available, but this can only be used as an indication since the data are from 1979 and 1983 and only a simple alongshore transport model was used to quantify the transport. Moreover, this model did not incorporate cross-shore processes and off shore losses were not taken into account. In addition, a more recent study by Sutherland et al. [38] provided some alongshore transport data for the area as well. These researches show an increasing transport rate from north to south. At Cromer (see Figure 2.11 for city/village locations) the net sediment transport rate ranges from 24.000 to 54000 m^3/year, at Overstrand it is estimated to be 74.000 m^3/year, at Mundesley it ranges from 10.000 to 300.000 m^3/year and at Happisburgh it extends from 150.000 to 500.000 (See Figure 2.11 for locations). The 3 papers show a large variability in the calculated sediment transport rates and it explains the large ranges for each of the locations. Moreover, the large variability for the area is also due to the year to year difference in net littoral drift and net sediment transport rates can go either east or west from Cromer. According to Sutherland et al. [38] the net sediment transport direction at Cromer is more a statistical process. This means that the net sediment transport rate is depending on the timescale chosen for the average net transport rate and also on how much sediment is transported into eastward direction from Cromer. This explains why the variability of the area is different for different studies. To conclude, the expected net transport rate is in between 100,000 and 150,000 m^3 directed southward. [38].

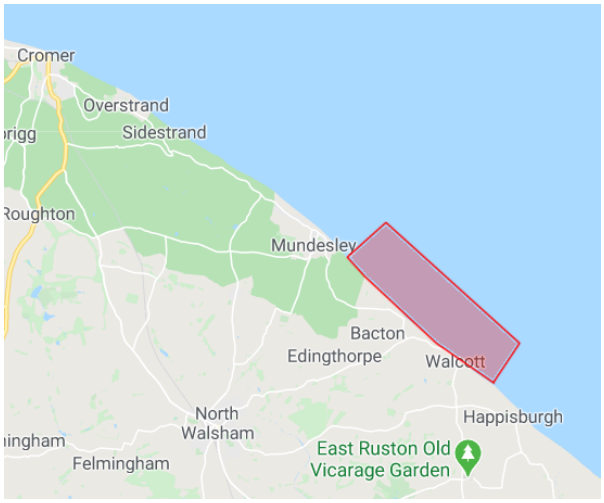

Figure 2.11: Location of Cromer, Overstrand, Mundesley and Happisburgh. In Red the BSS project area

2.4. Sandscaping design and requirements

The design of the BSS consists out of three sections (see figure 2.12), a section that connects the natural coast to the nourishment in front of the gas terminal (Section 1),a section in front of the gas terminal (Section 2) and a section in front of the downdrift villages Bacton, Keswick and Walcott (Section 3). Section 2 will provide immediate protection for the gas terminal and is designed to spread out to the adjacent coast to provide extra protection for Section 1 and Section 3. Section 3 will consist of a more traditional beach nourishment which provides the immediate protection for the villages on the short term. The design originates from the SMP strategy found in Table 2.2.

The nourishment size of Section 1 and 2 combined is approximately 1 million m^3 and is spread out over 2 kilometres which corresponds with a nourishment density of 500 m^3/m. Whereas, the nourishment volume of section 3 is approximately 0.5 million m^3 spread out over 3.6 km, which corresponds with a nourishment density of 138 m^3/m. The profiles of each section consists of 3 elements: The berm, the steep front and the mild slope. The berm is located at the toe of the cliff and the other two elements follow respectively in seaward direction. Further elaboration on the design can be found in Section 2.4.2. First the requirements of each section will be discussed.

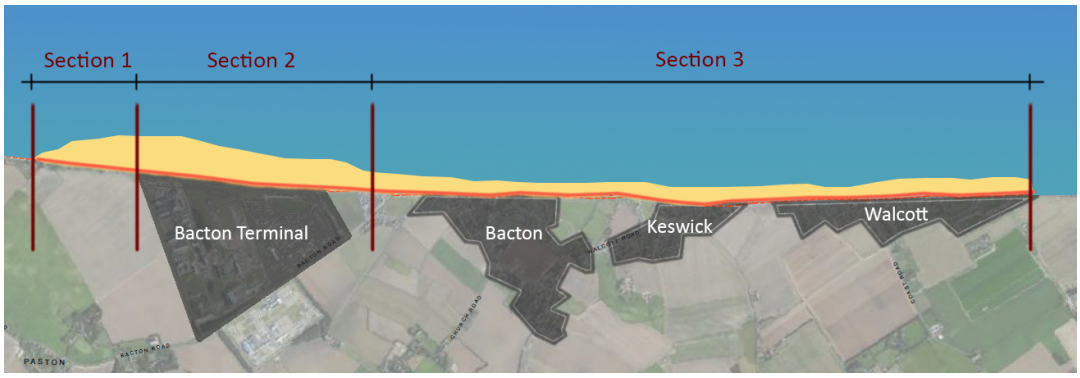

Figure 2.12: initial design. Sections are indicated by the red lines. Villages and Bacton gas terminal are marked in gray. The nourishment itself is marked in yellow.

2.4.1. Requirements

For each section requirements were set up (by Royal Haskoning DHV) for the lifetime of the BSS. Section 1 has the purpose to connect Section 2 to the original coast and therefore has no requirement. Section 2 provides the protection for the gas terminal and has therefore the most strict requirements regarding beach width and no toe erosion. Section 3 protects the existing seawall construction and accordingly its requirement is based on the structure. The requirements from Royal Haskoning DHV were changed to more parametric

requirements in the purpose of this research. These parametric requirements per section are listed in Table 2.4.

Table 2.4: Requirements

Section 1	Section 2	Section 3
1. No requirement	1. Maintain a beach width of 20 m at +7m MSL 2. No erosion at the toe of the cliffs, therefore the water level may not reach the toe of the cliffs	1. No erosion at the toe of the seawall

2.4.2. Design

The design of the BSS is based on a combination of a 1D (LitLine) and a 2DH model (TELEMAC). Due to difficulties of calibrating the 2DH model it could only be used to make an estimation of the offshore losses and could not be used to simulate the total area. The offshore losses of the 2DH model were then incorporated in the 1D model as a sink, since a 1D model is not able to predict these losses. The 2D model predicted an offshore loss of 100,000m^3/year and has been an important design parameter in the expected lifetime of the nourishment. The 1D model with the offshore losses from the 2DH model was then used to predict the nourishments behaviour over time. This lead to the following design for each section.

Section 1

Section 1 has the main function to connect the current beach to section 2. A berm height of +7.00m MSL is maintained at this area. The width of the berm gradually increases from the original beach width to the width of section 2. In cross-shore direction the berm descends with a slope of 1:15 until it reaches the initial bottom profile.

Section 2

The Berm of section 2 is located at an elevation of +7.00m MSL and is in between 5 and 80 meters wide. However,in front of the terminal the berm is always wider than 20 meters. In cross-shore direction the berm descends with a slope of 1:5 for 5 meters after which it descends in a slope of 1:15 until it reaches the initial bottom profile. A typical cross-section of section 1 can be found in Figure 2.13.

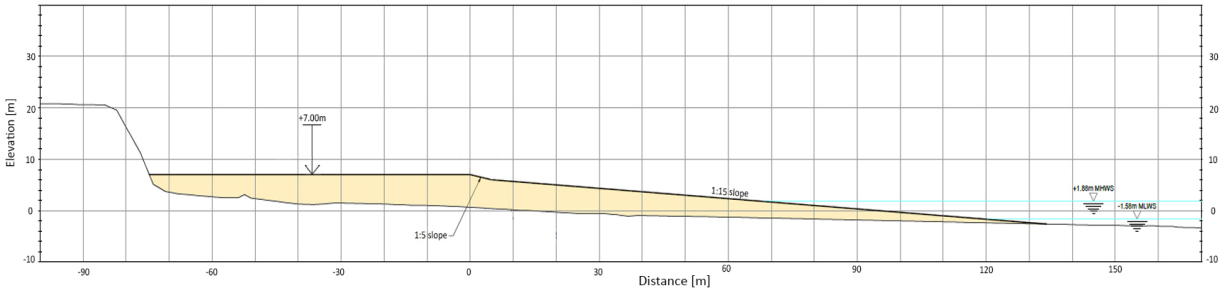

Figure 2.13: Cross-section of Section 2

Section 3

The design of Section 3 is quite similar to the one in section 2 in its shape, although the size is significantly smaller. The berm of section 2 is at a lower elevation and is also less wide. Over section 3 the elevation of the berm decreases from +5m MSL at Bacton (village) to +3m MSL at Walcott. The width of the berm is typically between 5 and 27 meters and in cross-shore direction the berm of the nourishment descends again in a slope of 1:5 for 5 meters and subsequently in a slope of 1:15 until it reattaches the initial bottom. *Note: the cliff height in this area is typically much lower than in Section 2*

3
Methodology

One of the main objectives of this thesis is to asses the ability of a process based model to simulate the morphological behaviour of the BSS. Therefore, a morphological model is set up. Moreover, the same model is used to evaluate the secondary research questions regarding the lifetime of the nourishment and the sensitivity of grain size and wave event intensity on the morphological behaviour of the BSS. The Delft3D software has successfully been used to model the mega feeder nourishment at the Delfland Coast in the Netherlands (i.e. The Sand Engine) [27]. Its capabilities to provide reliable results for modelling large scale nourishments gives confidence in its ability to model the BSS as well.

First, paragraph 3.1 discusses some general concepts of Delft3D and acceleration techniques to speed up numerical simulations. This gives a general idea about the software being used to simulate the BSS. Secondly, paragraph 3.3 discusses the model approach. It describes which processes are incorporated in the Delft3D model and further describes how the grid, bathymetry, boundary conditions and other model parameters are implemented. Paragraph 3.4 discusses how the model is calibrated and validated using measurements. The calibration and validation methods are important as they determine the skill of the model to predict the behaviour of the BSS and answers one of the main research questions. Paragraph 3.5 discusses the required model runs to answer the main research questions and the secondary research questions. The final paragraph discusses how the results are analysed and how the results are used to answer the main research questions. The methodology chapter follows the same structure as the chapters of this thesis. The calibration results are described in Chapter 4, the measurements that are used for validation are described in Chapter 5. The validation results are discussed in Chapter 6 and the results of all the model runs are described in Chapter 7.

3.1. Delft3D

Delft3D is a process-based model that can perform hydraulic and morphological computations. The flow module solves the unsteady shallow water equations in either depth averaged mode (2DH) or in 3D. These equations include the: continuity equation, momentum equation, transport equation and turbulence. The shallow water equations assume that vertical accelerations are small compared to the gravitational acceleration and that water is incompressible. Therefore, the water pressure can be assumed hydrostatic. Furthermore, it implies that pressure differences as a result of rapid bed level changes and acceleration due to buoyancy effects are not taken into account [23]. Besides the flow computations, Delft3D is also capable of computing the morphological changes. It includes several empirical transport relations (e.g. van Rijn, Bijker etc.) in the morphology module. The most commonly used transport relations in nourishment applications are the ones proposed by van Rijn (2004). The formulation of Van Rijn (2004) These transport formulations by van Rijn can be split up into two situations. A situation without waves and a situation including waves. Since the BSS is situated in a coastal area, the transport relations used are the ones including waves. The van Rijn equations are empirical and a separation is made between the bed load transport and the suspended load transport. The magnitude of the bed load transport by waves and currents is formulated as:

$$|S_b| = \eta 0.006 \rho_s w_s M^{0.5} M_e^{0.7} \tag{3.1}$$

With:

η	=	Relative available sediment in mixing layer	[-]
ρ_s	=	Density of sediment	[kg/m^3]
w_s	=	Fall velocity	[m/s]
M	=	Sediment mobility number due to waves and currents	[-]
M_e	=	Excess sediment mobility	[-]

In this relation the sediment mobility is determined by the effective near bed velocity that is present due to waves and currents and the excess mobility is determined by both the effective velocity and the critical velocity. The only input for the sediment characteristics is the d_{50} which is incorporated in both M and M_e. This means that grading effects of the sediment are not taken into account. Besides the bed load transport there is also the suspended load transport. The suspended load is transported via waves and currents via different methods. For currents the concentration present in the water column follows the advection diffusion equation and for waves the suspended transport is determined via:

$$|S_{s,w}| = \gamma_l U_A 0.007 \rho_s d_{50} M \tag{3.2}$$

With:

γ_l	=	Phase lag coefficient	[-]
U_A	=	Velocity asymmetry value	[m/s]
d_{50}	=	median grain diameter	[m]

To perform both the hydraulic and morphological computations simultaneously a staggered computational grid is used. This allows for a hydraulic computation on each whole time step and morphological computations on each half time step. In this manner an efficient and stable scheme is created which is also second order accurate. The structure of the processes included in Delft3D are shown in Figure 3.1

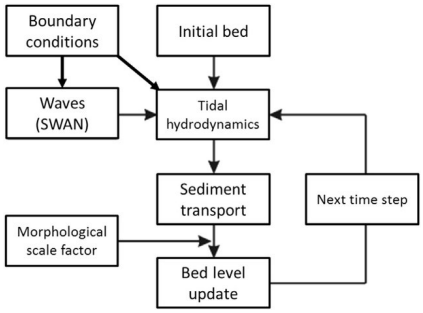

Figure 3.1: Structure of the interaction between hydrodynamics and morphodynamics from Luijendijk et al. [27]

3.2. Acceleration techniques

If no acceleration or upscaling techniques are used and all conditions are run to simulate the morphological changes, the simulation is regarded as a *Brute Force* simulation. The brute force method simulates all the conditions at every time step [26]. Although, the brute force simulation represents the most accurate solution, it is very time consuming and computationally expensive. Acceleration techniques have been developed to reduce the computational time, but maintaining a satisfactory level of accuracy is crucial. In the upcoming paragraphs the most common techniques are described. The acceleration techniques that are used for all the different model scenarios are described per scenario in paragraph 3.5.

3.2.1. Wave input reduction

Several methods of wave input reduction techniques are present, but here only the main concept of the input reduction is discussed. The objective of wave input reduction is to reduce the full wave climate (i.e. distribution of wave height, period, and direction averaged over time [19].) to a wave climate with far fewer wave conditions that still represents the full wave climate. Ultimately, the morphological changes of the reduced climate should sufficiently reproduce the full climate's morphological changes [10]. A framework for wave input reduction is given by Walstra et al. [47] and is as follows:

1. Select the period over which the input reduction should be applied
2. Select representative wave conditions for the chosen period based on the weighted average of the frequencies that occur in the full climate
3. Sequence the selected wave conditions
4. Determine the duration of the chosen conditions

Another more simpler way to reduce the wave input, is to omit the wave conditions that hardly cause any morphological change. A significant wave height lower than 1 meter can be considered as such a condition [27]. Removing these conditions can be considered as the *Brute force filtered* method.

3.2.2. Morphological acceleration factor

The morphological acceleration factor, *morfac*, is used to increase the morphological time step and to decrease computational time [23]. For very uniform conditions only, morfac allows for simulations on the millennial timescale, whereas for conditions of waves or currents a decadal timescale can be reached [32]. The computational advantage is gained by multiplying the bed changes with a constant factor at the end of each time step (see figure 3.1). Thereby, the morphological time step is increased by a factor equal to the *morfac*. The upper limit for coastal applications of *morfac* is dependent on its capability to accurately represent the simulation where no *morfac* is used. Luijendijk et al. [26] mentioned that a *morfac* of 5 and higher gave instabilities for the computed bed levels for a large feeder nourishment.

3.3. Model approach

In Delft3D a combination of the flow, morphology and wave module is used to model the morphological response. In this model the cliff erosion process will not be taken into account. As is described in section 2.3 cliff erosion at Bacton can be assumed to be highly episodic and will not influence the behaviour of the BSS as long as the water level will not reach the toe of the cliffs. The BSS has a beach level of +7.0m MSL and therefore the water level will not reach the toe of the cliffs before a large part of the berm width has eroded. The requirement in front of the gas terminals is to keep a minimum berm width of 20 meters. Therefore, cliff erosion is unlikely to happen before renourishment and will therefore not contribute sediment to the system. Consequently, cliff erosion will not be incorporated into the Delft3D model as a sediment source. Yet, cliff erosion is still possible to happen due to high precipitation with the consequence of a flow failure mode. However, the BSS will not have any effect on the precipitation and the flow failure mode, since it is not governed by the water level reaching the toe of the cliffs. Moreover, no data on flow failure events in the region is present unfortunately. In addition, cliff erosion models are largely based on either water levels reaching the toe of the cliff or on continuous erosion and are therefore also not applicable to implement in the Delft3D model (for further elaboration on model strategies for Cliff erosion see Appendix A). First a base case is set up to simulate the coastal behaviour of the coast without the BSS. In this manner the model parameters can be calibrated for the alongshore transport rates and tidal currents found in literature and other model studies. When the model is calibrated satisfactory, the same model is then used with the bathymetry including the BSS. This model is then validated by measurements done in the field. The analysis on the measurements are described in Chapter 5 and the validation is described in Chapter 6.

3.3.1. Model implementation

The domain of the BSS is schematized using a curvi-linear grid with an area of approximately 16 km^2. The grid extends 8 km in alongshore direction and 2 km in offshore direction. It stretches from the south of Mundesley up until the north of Happisburgh (see Figure 3.2a). The resolution of the grid increases from 17 meters near the coast to 165 meters offshore and consists of 200 by 36 grid points (i.e. 7200 grid points in total). The bathymetry used in the model implementation is a combination of the survey before construction and the survey after construction. These bathymetries only extend 1 km offshore and is therefore expanded with bathymetry from the open source data set from EMODnet. Wave data is obtained from the ERA5 model from a point offshore with coordinates 53.0E 1.5N. The wave data point lies 18 km of the grid described before and therefore a larger wave grid is used to generate wave boundary conditions for the flow model. The grid is rectangular instead of curvi-linear and has a resolution of 500 meters by 500 meters. The wave grid consists of 3066 grid points and has an offshore width of 36 km. Storm surge levels are not incorporated into the Delft3D model as no data is available in ERA5 for the simulation period.

(a) Location of flow model at the coast of Bacton

(b) Location of the wave grid (flow model in blue and wave point is marked in red)

Figure 3.2: The flow and wave grid locations

Tidal boundary conditions are generated using astronomical data from the TPXO 8.0 tidal model. The tidal boundary is imposed at the offshore boundary. The lateral boundaries are imposed with Neumann boundaries as is described by Roelvink and Walstra [34]. The Neumann boundary conditions prescribe a water level gradient at the boundary instead of a defined water level. Therefore, the water levels at the lateral boundaries have not to be determined beforehand. Lastly, there are multiple groynes present in the area of Bacton. These are wooden open structures which are largely covered by the construction of the nourishment. For this thesis it is assumed that the groynes are not affecting the morphology of the BSS in the first half year. Therefore, the groynes are also not incorporated in the Delft3D model.

3.4. Model calibration and validation

This paragraph discusses the calibration and validation method of the BSS. First the calibration procedure is discusses and secondly the validation.

3.4.1. Model Calibration

Model calibration is required to ensure the basic coastal processes are incorporated and that the magnitude of morphological processes are correct. A base case for the Delft3D model without BSS is set up. This results in the initial coast before construction of the BSS. This model is checked to show the right hydrodynamics and alongshore sediment transport. Measurements of current velocities in 2006 are used to calibrate the current velocities of the base case model. The alongshore sediment transport rate is calibrated by use of values found in literature. Finally, the model is calibrated with use of the beach volume changes of the years 2005,2006 and 2007. The choice of the years that are selected for the calibration procedure is further described in Chapter 4.

3.4.2. Validation

The model validation will be done on the basis of surveys that are performed during the first half year of the BSS. An in depth analysis on the surveys is discussed in Chapter 5. These surveys provide the bed levels up until a depth of around -10m MSL. The erosion and sedimentation patterns of the surveys are visually compared to the model predicted patterns. Also, the volume changes of the nourishment that are observed in these surveys are compared to the predicted volume changes by the model. The Brier skill score is used to assess the model's skill in predicting these volume changes. In addition, the model's capability to assess the requirements at the end the predicted lifetime of the BSS is discussed as well.

3.5. Model scenario's

This paragraph describes the scenarios that are used with the BSS Delft3D model. Five different types of scenarios are used to answer the main and secondary research questions. First the base case scenario is discussed, where the scenario simulates the original coast (so without BSS). This scenario is used to for the initial calibration of morphology and flow. Secondly, the reference scenario is discussed, where the base BSS

model is used to validate the BSS model and quantify its performance. Thirdly, different wave scenarios are described. These wave scenarios are used to quantify the effect of waves on the beach volume. Subsequently, the different sediment grain diameter runs are discussed. Finally, the two long run scenarios are defined to evaluate the requirements at the end of the expected lifetime of the BSS.

3.5.1. Base case scenario

The base case scenario simulates the coast before construction of the BSS. The survey just before construction is used to set up the bathymetry of this model. Three different years are used to calibrate current speeds, alongshore transport and beach volume changes. The calibration factors obtained from these scenarios function as a basis for the calibration of the model including the BSS. This scenario uses a brute force simulation to obtain the most accurate representation of reality. The simulations used for calibration are shown in Table 3.1.

Scenario	Description	Grain size	Simulation period	*morfac*
0.1	No BSS	350 μm	2005	1
0.2	No BSS	350 μm	2006	1
0.3	No BSS	350 μm	2007	1

Table 3.1: Base case scenarios

3.5.2. Reference scenario

The reference scenario is a simulation of the period August 2019 until March 2020. August 2019 is the date of the first survey and March 2020 is the date of the latest available survey. The reference case uses wave data for the same period. This scenario is used to calibrate and validate the model. Once the model is fully calibrated and validated, the calibration parameters will stay the same during all the other model scenarios. In this manner the effect of different wave conditions and sediment settings can be related to the reference scenario. The reference scenario will provide several outputs that are used to evaluate the model. These outputs are:

1. Volume changes per running meter for the sub-aerial and submerged beach
    - This output describes the morphology above and below the waterline separately. It gives insight in the total maintained beach volume of the BSS.
2. Net volume changes per running meter
    - This output describes the net sediment changes across the entire domain.
3. Volume changes per section
    - This outputs reflects the absolute differences between the model and the measurements and gives insight in the amount of sediment that is interchanged between the sections.

The aforementioned volume changes are determined by subtracting the bed levels before simulation from the bed levels after simulation. This generates the bed level differences for the entire simulation. These differences are then averaged over each grid cell and multiplied by the area of the grid cell. This generates the volume changes per grid cell. These volumes are then used to calculate the volume changes per running meter. All the volume outputs are checked with the survey performed in March 2020 to validate the reference model. In addition, these outputs are used to analyse relative differences with other scenarios. These outputs then also answer the main research question of how well Delft3D is capable of simulating the BSS. Similar to the base case, brute force simulations are used for the reference scenario. The simulation period is only half a year and accuracy is of great importance in calibrating and validating the reference scenario.

3.5.3. Wave scenarios

Three different wave scenarios are used to analyse the effect of waves on the beach volume behaviour. These three different wave scenarios include an intensified wave climate, a reduced wave climate and the reference wave climate. The reference wave climate contains the wave conditions used for the reference case. The intensified and reduced climate are fictional conditions and are created from the reference conditions. First the

transformation of the reference conditions to the intensified and reduced conditions is described. Afterwards the specific conditions of both climates are discussed.

The reference wave conditions are portrayed in Figure 3.3 and are obtained from the ERA5 hourly reanalysis which is generated using Copernicus Climate Change Service information. The first period between August 2019 and October 2019 show relatively average conditions with one event with significant wave heights reaching to almost 3 meters. The period between October and March show a more dynamic and stormier period. Three wave events surpass the 3 meter significant wave height and also the storm Ciara in the beginning of February is notably present. For this event the significant wave height reaches up to 4.5 meters.

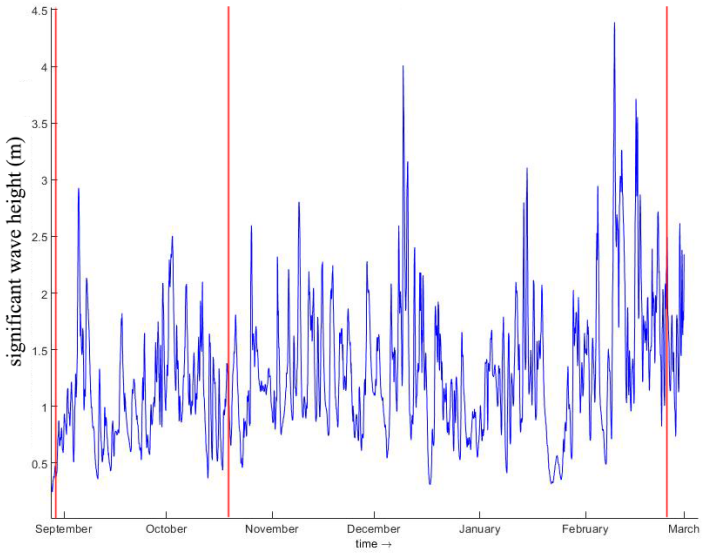

Figure 3.3: Significant wave heights of the ERA5 point described in chapter 3. Red vertical lines indicate the survey dates.

The model is then used to evaluate which conditions cause the most alongshore sediment transport. The selection for these events is discussed in paragraph 3.5.4. These events are considered as the wave events which cause the major alongshore morphological changes of the BSS. These storm events are then extracted and either intensified or reduced (hereafter the intensification or reduction of the wave events is called wave transformation). These wave conditions cannot be simply multiplied or divided by a single factor. The wave conditions are also linked to their wave periods. Jäger and Nápoles [20] uses a wave steepness function to find the relation between the significant wave height and the mean wave period. The wave steepness is defined as:

$$S_p = \frac{2\pi H_{m0}}{g T_{m02}^2} \tag{3.3}$$

The wave period and the wave height are plotted against each other and the steepness value is then visually estimated. Such a steepness curve including wave data is shown in Figure 3.4. First, the wave event selection is described and afterwards the wave transformation is discussed.

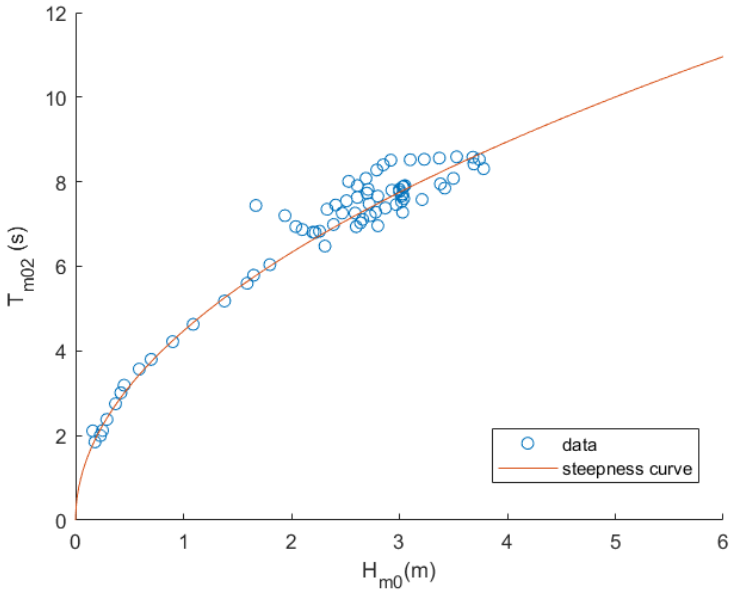

Figure 3.4: The significant wave height plotted against the corresponding wave period. The steepness curve gives the relation between the significant wave height and the wave period, assuming full dependence

3.5.4. Event selection

The alongshore transport rate is an important parameter for the BSS nourishment, since the BSS is designed to feed the adjacent coast with sediment. Therefore, the wave events that cause the most alongshore sediment transport are chosen. The wave events that are individually responsible for more than 20% of the total alongshore transport are selected. By either intensifying or reducing the effects of these events, the feeder behaviour of the nourishment can be analysed for different event intensities. Their effect is quantified by calculating the volume changes per section and per running meter. This indicates the quantity and effect of the feeder behaviour. The wave events that are responsible for more than 20% of the total alongshore transport are shown in Figure 3.5. Three major alongshore transport events are identified which cause roughly 80% of the total alongshore transport and can therefore be considered as significant. The events that cause the most alongshore sediment transport are:

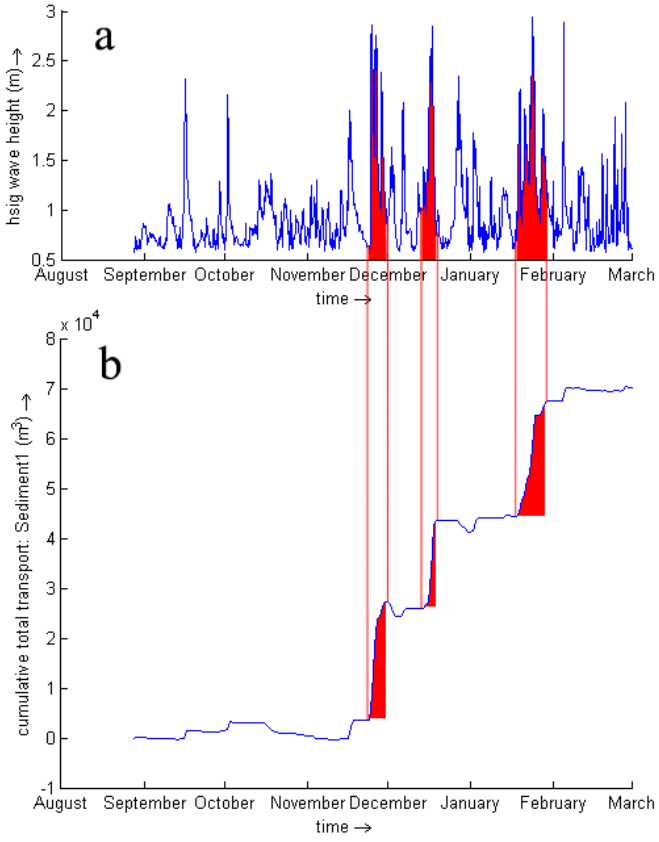

Figure 3.5: (a):Significant wave heights at the boundary of the flow model. Selected wave events are marked in red (b): Alongshore sediment transport rate during the simulation. The highest alongshore transport events are marked in red

1. 24 until 29 November 2019
2. 16 until 19 December 2019

3. 18 until 31 January 2019

For all these events an intensified and reduced time series is created. This means that 2 separate extra time series are created. In these time series all wave conditions are kept exactly the same, but the three events are either intensified or reduced. This process is defined as wave transformation in this thesis.

After the steepness value is estimated, a relation between the significant wave height and the wave period is obtained. Now the wave heights can be increased or decreased by a certain percentage and a new wave period automatically follows from the steepness function. The selected wave events are then transformed. These events are now included in the separate time series. The different wave scenarios that are used in the wave analysis are shown in Table 3.2.

scenario	Description	Value
1.1	Reference wave conditions	+-0%
1.2	Wave conditions intensified	+20%
1.3	Wave conditions reduced	-20%

Table 3.2: Wave scenarios

For the wave scenarios, brute force simulation are used. This is to ensure no differences are caused by acceleration techniques. Moreover, the wave events that undergo an intensification or reduction need the highest accuracy possible to simulate their effects properly.

3.5.5. Wave transformation

The wave transformation is performed for all three events from the preceding paragraph. To intensify or reduce a wave event, the wave heights are either reduced by 20% or increased by 20%. As wave heights are also dependent on the wave period, the wave period also needs adjustment. As described in Chapter 3, the wave transformation is performed by using a steepness relation between the significant wave height and the wave period. The steepness parameter 'S_p' is defined for each of the three events. The S_p value for each of the events is determined by visual estimation, a similar approach as Jäger and Nápoles [20]. This gives a relation between the significant wave height and the wave period. The significant wave heights are then multiplied or reduced by 20% and the related wave period is then calculated via the steepness curve formula (assuming full dependence). The result of the transformation for the event of January is shown in Figure 3.6. As the other transformation follow the same procedure their transformations are not shown in this paragraph but in Appendix E.

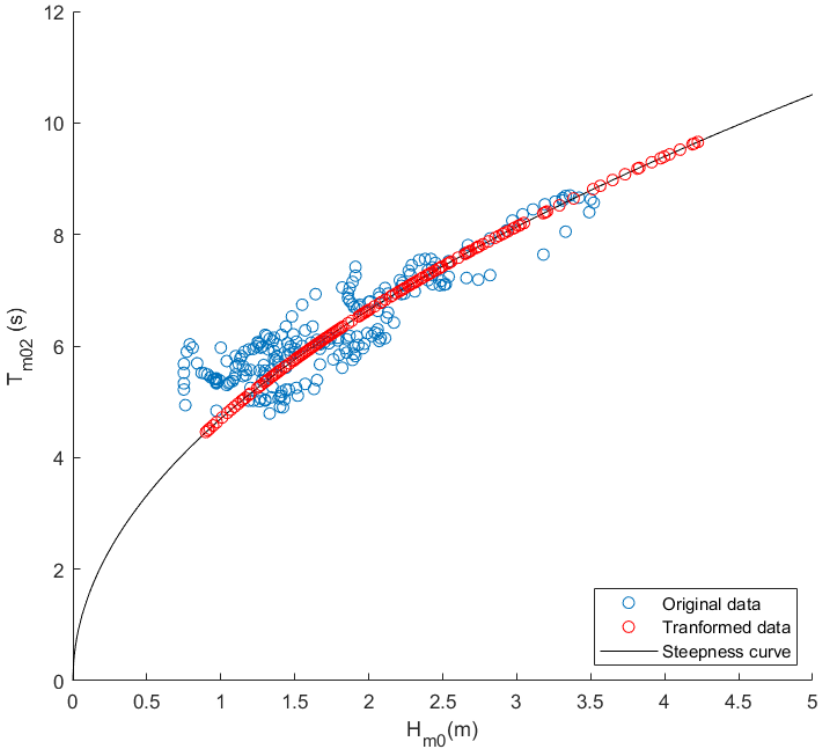

Figure 3.6: The wave transformation process. Blue: Original significant wave height plotted against the original wave period of the wave event in January with corresponding steepness curve. Red: Intensified significant wave height with corresponding wave period following the same steepness curve for January.

The accompanying S_p values used for the transformation of the three events are listed in Table 3.3. The S_p values differ only slightly for the three events. This shows that the events are very similar in properties. In addition, the wave direction during these events are all directed from 0-90° North. Waves from these directions transport sediment southward. This in combination with the high significant wave heights of these events explain why these particular events cause the most alongshore transport in the southern direction.

Wave event	S_p [-]
November 2019	0.032
December 2019	0.029
January 2020	0.029

Table 3.3: 'S_p' values for individual wave events

3.5.6. Sediment scenarios

Three different sediment scenarios are used to evaluate the effect on the morphological behaviour of the BSS. Grain size was an important parameter in the design phase of the BSS. There is a wide variety of sediment sizes present in the area (see Table 2.3) and in the design phase the mean d_{50} of 350 μm was chosen. This sediment size is the reference scenario for sediment. The two other scenarios use sediment sizes of 300 μm and 400μm. These sediment sizes are still in the range of the sediment sizes in the area, but significantly differ from the reference scenario. The sediment scenarios are shown in Table 3.4

scenario	Description	Value
1.1	Reference grain size	350 μm
2.1	Increased grain size	400 μm
3.1	Reduced grain size	300μm

Table 3.4: Sediment scenarios

Identical to the earlier described scenarios, the sediment scenarios make use of brute force simulation and the same time frame as the preceding scenarios.

3.5.7. Long run scenario

To evaluate the requirements at the end of the expected lifetime of the BSS, a run of 15 years is required. To resemble future wave conditions, it is chosen to use wave conditions of the past 15 years. As no prediction can be made of future wave conditions it seems satisfactory to use the wave conditions of the past 15 years instead. However, the first few months of wave data which are available can still be used. To assess the BSS, one long run is performed including the BSS, see Table 3.5. This scenario requires morphological acceleration, since a simulation without acceleration would require 37.5 days. A combination of *morfac*, wave input reduction and wave compression is used to downscale the simulation time to 7-14 days.

Scenario	Description	Grain size	Years of wave conditions	Morfac
4.1	Including BSS	350 μm	2005-2020	4

Table 3.5: Long run scenario

3.5.8. Scenarios combined

The earlier described wave and sediment scenarios are combined to get a full image of the effect of both waves and grain size. The scenarios will be combined in such a way that all sediment scenarios are performed for all wave scenarios and vice versa. Resulting in a total of nine runs to combine the three sediment scenarios with the three wave scenarios. A sensitivity analysis of the combined effect is now possible. Hence, not only the separate effects of waves and grain size can be analysed, but also the connection between waves, grain size and beach volume. The combined scenarios, the base case scenarios and the long run scenarios are summarised in Table 3.6.

Scenario	Description	Grain size	Wave event description	Simulation period	*morfac*
0.1	No BSS	350 μm	Wave conditions +-0%	2005	1
0.2	No BSS	350 μm	Wave conditions +-0%	2006	1
0.3	No BSS	350 μm	Wave conditions +-0%	2007	1
1.1	Including BSS	350 μm	Wave conditions +-0%	Aug 2019-Mar 2020	1
1.2	Including BSS	350 μm	Wave conditions +20%	Aug 2019-Mar 2020	1
1.3	Including BSS	350 μm	Wave conditions -20%	Aug 2019-Mar 2020	1
2.1	Including BSS	400 μm	Wave conditions +-0%	Aug 2019-Mar 2020	1
2.2	Including BSS	400 μm	Wave conditions +20%	Aug 2019-Mar 2020	1
2.3	Including BSS	400 μm	Wave conditions -20%	Aug 2019-Mar 2020	1
3.1	Including BSS	300 μm	Wave conditions +-0%	Aug 2019-Mar 2020	1
3.2	Including BSS	300 μm	Wave conditions +20%	Aug 2019-Mar 2020	1
3.3	Including BSS	300 μm	Wave conditions -20%	Aug 2019-Mar 2020	1
4.1	Including BSS	350 μm	Filtered & compressed	15 years	4

Table 3.6: All scenarios that are simulated using Delft3D

3.6. Concluding remarks

This chapter described how a morphological model is implemented and which model runs are required to answer the main and secondary research questions. First, a model calibration without the BSS is performed to assess the model's capability of implementing the hydrodynamics and morphology of the original coast. Afterwards, surveys are analysed to assess the behaviour of the BSS in the first half year. These surveys are

then used to validate the BSS model and assess the capability of Delft3D model to simulate the first half year. The validated BSS model is finally used to answer the secondary research questions as well. The scenarios that are used for this thesis are listed below and a short explanation on how the scenarios are analysed is summarised as well.

- Base case scenarios:
  The base case scenario is analysed based on the alongshore transport, current velocities and volume changes of the sub-aerial beach. The results of the alongshore sediment transport are compared to the values found in literature. The current velocities are compared to measured current velocities. The volume changes of the sub-aerial beach are compared to the profile changes from 2005,2006 and 2007. Further explanation on the choices of these years is explained in Chapter 4.

- Reference scenario:
  The volume changes per running meter of the sub-aerial beach and the submerged beach of the reference scenario are compared to the volume changes of the measurements described in Chapter 5. The model skill is determined with this data comparison. Moreover, the volume changes per section are also compared as well as the exact bed level elevations.

- Wave scenarios:
  The wave scenarios are evaluated on the basis of volume changes for both the sub-aerial beach and the submerged beach. These volumes are determined per running meter and per section.

- Sediment scenarios:
  The sediment scenarios have the same analysis as the wave scenarios.

4

Model calibration

In order to simulate the Bacton coastline with the BSS nourishment it is first necessary to assess the capability of the model to accurately simulate the coastal processes without the Sandscaping project. In this way it can be assessed if the model captures the main trends of the existing coastline development. This includes the net sediment transport rate and erosion and sedimentation patterns. Since the net sediment transport rates are highly variable and uncertain in this region [38], it is chosen to evaluate the trends rather then absolute values. First, the methodology of the calibration is described, followed by the results of the calibration process.

4.1. Calibration methodology

The parameters that require calibration are categorised in five different categories, flow, waves, morphology, roughness and numeric. The effect of the model parameters and their final value is described for each of the categories.

1. Flow

    - For the model a simple background horizontal diffusivity and viscosity was chosen. No 2D turbulence model was used and therefore the eddy viscosity concept as defined by Prandtl [31] is not included (this also means that the Prandl-Schmidt number is not used). The value for the horizontal eddy viscosity (V_h) has a numerical stability condition: $\Delta t V_h(\frac{1}{\Delta x} + \frac{1}{\Delta y}) < 1$. In which Δt is the time step, Δx the grid size in x direction and Δy the grid size in y direction. This condition is always met with the default value. The horizontal eddy diffusivity (D_h) was changed from its default value. The horizontal eddy diffusivity influences the flow. Similar values as Luijendijk et al. [27] were used, this did not create the optimal calibration of the current velocities and was slightly adjusted until the best result was obtained.
    - The water density (ρ) is changed from the default value of 1000 kg/m^3 to 1025 kg/m^3. The area is located at the shore and the model is simulating salt water. 1025 kg/m^3 is generally considered the density for salt sea water and 1000 kg/m^3 is the density of fresh water.

2. Waves

    - The wave stress relation and the wave breaking parameter (γ) were kept at their default. It was opted to use the wave roller model of Delft3D to better simulate the delayed breaker effect [27]. However, the computational cost was too high to implement this and is therefore not used. No further calibration was performed for waves.

3. Morphology

    - The median grain diameter (d_{50}) was changed from 200 μm to 350 μm as this is the grain size of the nourishment as well as the mean grain size of the area.
    - The transport relation used for calibration is the van Rijn (2004) formulation. Luijendijk et al. [27] describes that the Van Rijn formulation provided the best results for the Delft3D sand engine model. Moreover, the van Rijn (2004) equation is reported to be better at predicting deposition areas Luijendijk et al. [27]. No further calibration tests are done with other transport relations

- The factor for erosion of adjacent dry cells (ThetSed) is changed from 0 to 1. Delft3D normally only allows erosion of grid cells that are considered wet. The ThetSed parameter allows for erosion of dry cells that are adjacent to wet cells with a factor equal to ThetSed. The ThetSed parameter seemed to be an important parameter for the beach volume changes. A ThetSed of 0 resulted in not enough erosion and a ThetSed of 1 provided the best results.

- The calibration factors: current related reference concentration factor (fSUS), current-related transport vector magnitude factor (fBED),wave-related suspended transport factor ($fSUS_w$) and the wave-related bed-load transport factor ($fBED_w$) influence the sediment transport by waves and currents. Undertow is not fully resolved in 2DH simulations and therefore the calibration factors are largely used to influence the behaviour of onshore and offshore sediment transport. In the Bacton coastal area high offshore sediment transport rates are observed. A lower $fSUS_w$ value corresponds with lower onshore sediment transport due to waves and a higher fSUS value corresponds with higher offshore suspended sediment transport due to currents. To minimise the effect of the under predicted undertow a decreased value of $fSUS_w$ (0.35) and an increased value of fSUS (3.5) is chosen. $fBED_w$ and fBED are chosen similar to their suspended counterpart. In addition, in other coastal application studies from Luijendijk et al. [27] and Walstra et al. [46], $fSUS_w$ is typically lower than 0.4, which justifies the choice of 0.35. The fSUS and fBED are also largely influencing the alongshore sediment transport. The values used for fSUS en fBED by Luijendijk et al. [27] are 0.5, while Walstra et al. [46] uses values above 1. Compared to these studies this calibration resulted in fairly high fSUS and fBED values. However, no upper bounds of these values are mentioned in coastal application studies. For the alongshore variability and net sediment transport rate the values of both these studies were not satisfactory and were therefore increased.

4. Roughness

- The Chézy value is changed from 65 $\sqrt{m}/s$ to 38.5 $\sqrt{m}/s$. The Chézy value is actually a smoothness factor and lower value means a rougher bed. The bed roughness influences shear stresses that are exerted on the bottom. For lower Chézy values, a higher shear stress is observed. The Chézy value also influences the depth averaged velocity. As it is obvious that water flows faster over a smooth surface than over a rough surface. The obtained Chézy value gives the most optimal result for the current velocities mentioned in paragraph 4.2. Moreover, the default Chézy value assumes a sandy bottom, but in Bacton the sediment is not only sand, but also contains shingle and gravel. These sediments are considered more rough than sand, hence a lower Chézy value seems applicable here.

5. Numeric

- The time step (Δt) is changed from 60 to 30 seconds to satisfy the CFL condition of $\frac{u \cdot \Delta t}{\Delta x} < 1$, in which u is the depth averaged velocity, Δt is the time step and Δx is the grid size resolution.

All the preceding calibration parameters are listed in Table 4.1. The end results of the calibration processes are described in the next paragraphs. Paragraph 4.2 discusses the result of the hydrodynamic calibration, where the roughness and flow parameters were calibrated to obtain the optimal hydrodynamic results. Paragraphs 4.3 and 4.4 discuss the results of the morphological calibration. The results of the numeric calibration are not discussed as this concerns only the CFL condition that needs to be met.

Table 4.1: Model parameters

	Parameter	Default value	Used value	Unit	Description
Flow	D_h	10	0.5	m^2/s	Horizontal eddy diffusivity
	V_h	1.0	1.0	m^2/s	Horizontal eddy viscosity
	ρ_w	1000	1025	kg/m^3	Water density
Waves	γ	0.73	0.73	-	Wave breaking parameter
	Wave stress relation	-	-	-	Fredsoe (1984) wave stress relation
Morphology	d_{50}	200	350	μm	Median grain diameter
	Transport relation	-	-	-	Van Rijn (2004) transport relation
	ThetSed	0	1.0	-	Factor for eroding adjacent dry cells
	Morfac	1.0	1.0	-	Morphological acceleration factor
	fSus	1.0	3.5	-	Calibration factor for suspended sediment transport
	fBed	1.0	3.5	-	Calibration factor for bed load sediment transport
	$fSus_w$	1.0	0.35	-	Calibration factor for suspended sediment transport by waves
	$fBed_w$	1.0	0.35	-	Calibration factor for bed load sediment transport by waves
Roughness	Chézy	65	38.5	$m^{1/2}/s$	Chézy roughness parameter, constant for whole domain
Numeric	Δt	60	30	s	flow time step

4.2. Hydrodynamics calibration

Measured current velocities are obtained from the British Oceanographic Data Centre (BODC) at a location 4 kilometers outside the model domain at a depth of 7 meters. The data used spans a period of 14 days in 2006 and is the only available measured current velocity data in the area. This short period is simulated in the Delft3D model and the depth-averaged current is compared with the measured data in a linear regression analysis (see Figure 4.1). The modelled current velocities are obtained from a southward point located 1 km from the boundary (to eliminate boundary effects) at the same depth as the measured current velocities. The linear regression analysis is needed since the model data cannot be directly compared to the measured data, since the measured data is not a point located in the model domain. However, since the measured data is quite close to the model domain, it is assumed that the model results will not differ significantly.

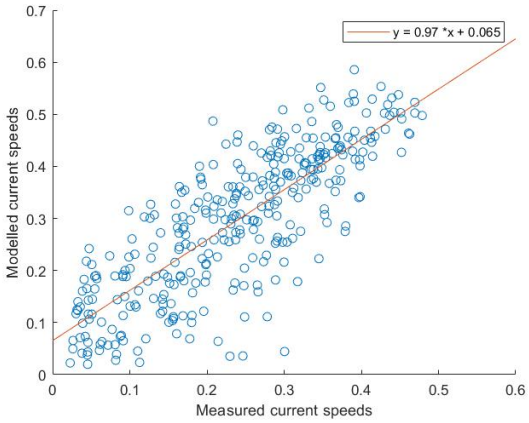

Figure 4.1: Measured and modelled current velocities from april 7th until april 21st in 2006. In red the least squared regression line. Note: least regression line does not go through origin as the residual current in the measured data is not totally filtered out.

Overall, it can be concluded that the model is in good agreement with the measurements. The minimums of the measurements are slightly under predicted by the model and the maximums are both under predicted and over predicted marginally by the model. The Pearson R value of the least squared regression is 0.82. This indicates that the model shows a fairly strong positive correlation with the measured data. It is regarded that the model sufficiently represents the hydrodynamics of the coastal area. Especially, when it is considered that the measured current velocities are outside the model domain. In the calibration process the Chézy roughness parameter was observed to be the most sensitive to the results of the hydrodynamics. The Chézy value largely affected the peak velocities, with higher Chézy values, higher peak velocities were observed and for lower Chézy values lower peak velocities were observed. The horizontal eddy diffusivity and horizontal eddy viscosity had less effect on the model results and were tweaked to obtain the most optimal least regression fit.

4.3. Net alongshore sediment transport calibration

Across the east Anglian coast several different transport rates have been calculated by Sutherland et al. [38], Clayton et al. [9] and Vincent [44]. For the exact values of the alongshore sediment transport rate, see paragraph 2.3.3. The locations that are used in this analysis are again shown in Figure 4.2

The literature shows an increase in alongshore sediment transport going southward of Cromer. The modelled transport rates in combination with the shoreline orientation and wave climate are shown in Figure 4.3a. This shows the overall positive trend, but there is also a negative trend found in the net sediment transport (see cyan shaded area in Figure4.3a) . To check if this decrease is explicable, the coastal orientation in combination with the wave climate will be evaluated.

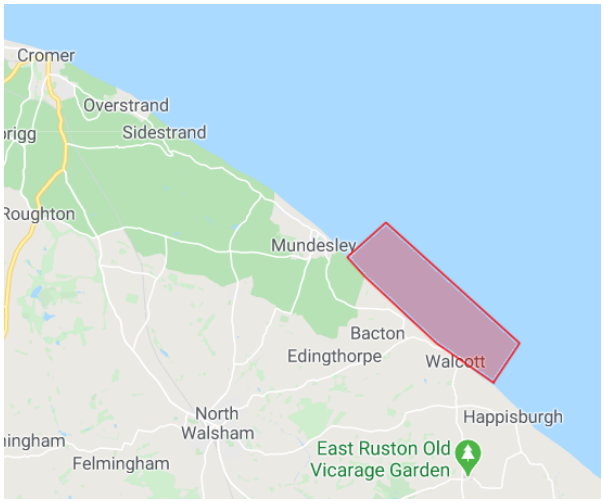

Figure 4.2: Location of Cromer, Overstrand, Mundesley and Happisburgh. The model domain is shaded in red.

The coastal orientation relative to the North and the wave climate of the coast are shown in Figure 4.3. The wave climate is obtained from the nearshore modelling by HR Wallingford at a location in front of the gas terminal 750 meters offshore. These figures will be used to explain the possible decrease of the cyan shaded area of Figure4.3a. The coastal orientation of the Bacton coast varies from -42 degrees north to -56 degrees north and most waves originate from the north and north-east (see Figure 4.3a and 4.3b). Moreover, the highest waves are also originating from these directions. Maximum alongshore transport happens for waves making a 45 degree angle with the shoreline orientation when using the empirical CERC formula [6]. Therefore the main sediment transport direction is directed southward. However, also a small amount of waves are coming from the east and these will provide northward directed sediment transport.

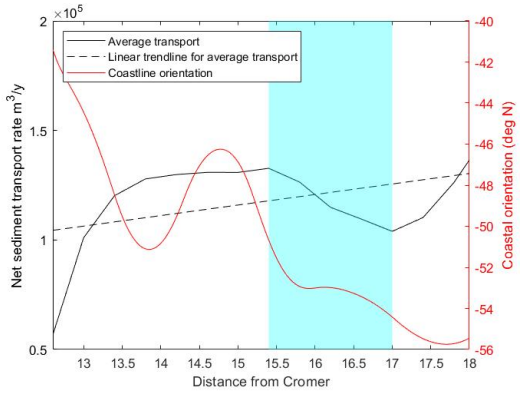

(a) Coastline orientation plotted with the average transport of 2005,2006 and 2007. The cyan shaded area shows a decrease in transport

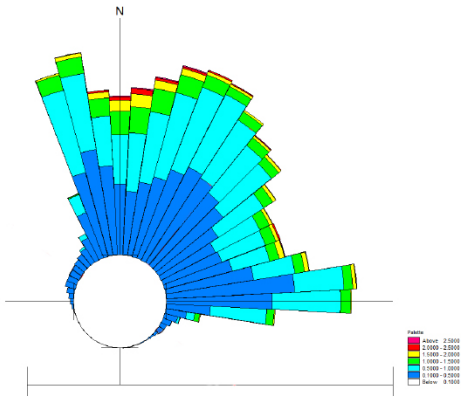

(b) Wave rose just offshore of Bacton for the period 1984-2014

Figure 4.3: Coastline orientation and wave climate for Bacton

The cyan shaded area in Figure 4.3a shows a decrease in net sediment transport. This area also shows an increase of shoreline orientation from -50.5 degrees north to -54 degrees north. East from the cyan shaded area, the net sediment transport starts increasing again. Hence, the decrease in net sediment transport is only found for angles between -50.5 and -54 degrees north. An explanation for this decrease is that the highest waves the waves from the north-east are losing their transport capacity with an increase in shore angle (i.e. higher angle relative to the north) as these waves are now oriented more perpendicular to the coast than for the smaller shore angles. To assess these trends the years 2005, 2006 and 2007 will be used in the calibration process. The year 2006 has already been used to calibrate the current velocities and is therefore convenient to use here as well. In addition the years 2005 and 2007 are chosen to check the variations for different years. The choice for 2005 and 2007 For an adequate calibrated model, it has to show the increase in net sediment

transport rate going southward. First the sediment transport rates across the coast will be calculated for all 3 years and compared to the values found in literature. The modelled net sediment transport rates for 2005, 2006 and 2007 are shown in Figure 4.4. A positive trend is present across the domain.

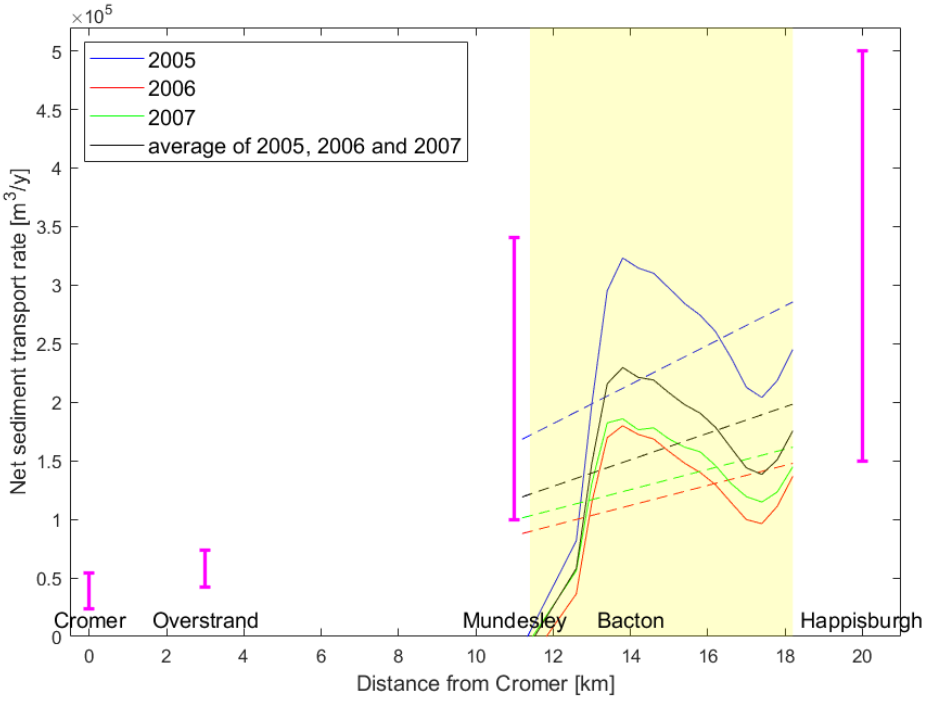

Figure 4.4: The net sediment transport of the years 2005,2006 and 2007 along the Bacton coast. The yellow shaded area is the project area. The magenta bars indicate the minimum and maximum found values of net sediment transport rate found in literature. The Bacton gas terminal is located between 13 and 14 km. Trend lines are indicated with dotted lines

The modelled transport rates are then compared to the trend of the entire coast in Figure 4.4 as well. The positive trend modelled for the years 2005,2006 and 2007 is in line with the trend of the entire Anglian coast. The large variability for Mundesley and Happisburgh is also reflected in the model results for the coastal area between these two cities. The absolute net sediment transport rates of 2007 and 2006 are on the lower side of what might be expected for the coastal stretch of Bacton. However, the model predicts a much higher transport rate for 2005, which further confirms the high variability between the yearly transport rates. Moreover, similar calibration factors will be used to model the BSS. If the model provides good results with these transport rates, it is assumed that the alongshore transport rate is calibrated sufficiently. However, due to lacking data of sediment transport rates across the rest of the model area, no further calibration is possible for the sediment transport rate. The BSS model will also confirm if the negative trend found in the blue shaded area of Figure 4.3a is plausible.

4.4. Dry beach volume behaviour

In addition to literature, 6-monthly coastal profiles between Mundesley and Happisburgh are available from 1991 to 2013. These profiles are spaced with approximately 1km distance. However, these coastal profiles only cover the dry beach and the intertidal area. These profiles will be used to assess the sedimentation and erosion processes in alongshore direction of the sub-aerial beach. These profiles are from 5 different location with roughly 1 km spacings. The profiles are then used to calculate the profile differences in m^2 for the calibration years of 2005,2006 and 2007. For the model, volume changes are calculated in m^3/m so they can directly be compared to the observed profile changes in m^2. The minimums,maximums and average values of the observed coastal profile changes are shown Figure 4.5. The modelled profile changes are also included in Figure 4.5. For both the model and the observed changes a negative trend can be found for the first 1500 meters of the model. After the first 1500 meters a positive trend is observed for the model. Both the negative and the positive trend are captured well in the model. However, the observed positive volume

changes are under predicted by the model.

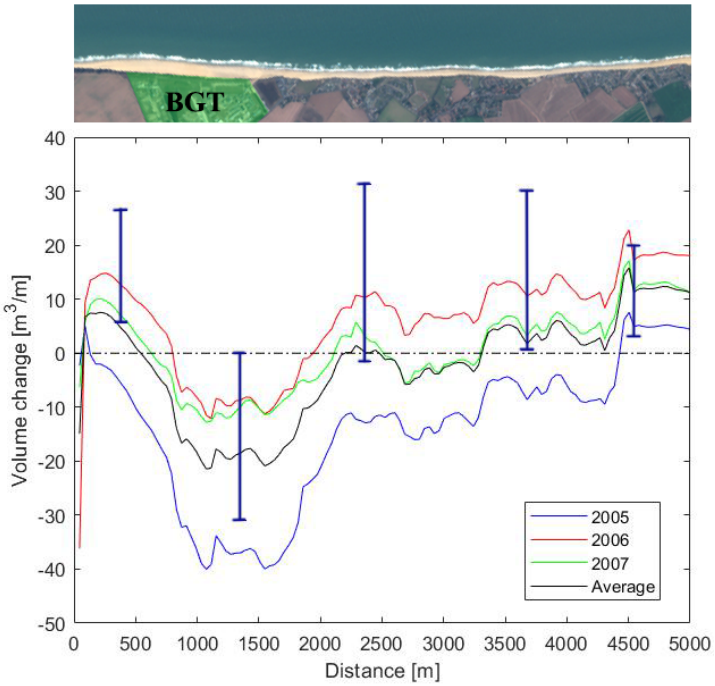

Figure 4.5: The modelled sub-aerial beach volume changes are plotted for each year continuously.The error bars indicate the maximums and minimums per profile, but do not indicate a confidence interval. The map corresponds with the distance of the graph.

The model seems to capture the overall sub-aerial beach volume changes quite well and it is therefore assumed that it is possible to use the model to analyse the sub-aerial beach volumes. For the case including the BSS, it will be much more evident if the model performs satisfactory, as the behaviour can be validated with survey data covering the entire sub-aerial and submerged beach. As measurements of the entire area give a much clearer view on the coastal behaviour.

4.5. Concluding remarks

The Bacton model shows plausible results for the alongshore sediment transport, hydrodynamics and the sub-aerial beach volume changes. Therefore, it is expected that the model is well able to simulate the morphological behaviour of the coastal area in a robust way. The bed level accuracy of the model cannot be evaluated after the model calibration as not enough bathymetric data is available. It is expected that the model is better at predicting the beach volume changes, as this is robust and the dry beach volume behaviour calibration seems to match quite well with the measurements. In the next chapter a data analysis of all the performed surveys is presented. This data is later on used in the model validation of the BSS model. The combination of the data analysis and the model validation will prove if the model performs sufficiently for beach volume changes.

5
Data analysis

The Bacton Sandscaping project was surveyed four times between the period of July 2019 and March 2020. Before construction a presurvey (July 2019) was done from the tops of the cliffs until a depth of -12m. Right after construction (August 2019) a second (as built) survey was conducted from the tops of the cliffs until depths varying between -2m and -4m MSL. This survey is combined with the survey of July 2019 before construction to obtain a full bathymetric survey reaching the depth of -12m. The other surveys are conducted in October 2019 and March 2020 and contain a bathymetric survey from the tops of the cliffs until a depth of approximately -15m MSL. In this paragraph the surveys will be discussed in more detail and they will be used to analyse the morphological behaviour. First, the method of surveying is discussed and afterwards the analysis of the data is described.

5.1. Method

The surveys of both July 2019 and August 2019 are conducted by a multibeam echo-sounder and a two drone system using photogrammetry. The survey of August 2019 was conducted over a longer period of time during the construction phase. The multibeam echo-sounder is attached to the bottom of a vessel and used to measure the water depths. It sends out multiple sound pulses with a frequency of 2 Hz to the bottom. These pulses are then reflected back to the echo-sounder. The time between sending the pulse and receiving the pulse is measured. The speed of sound (in the current salinity and temperature of the water), combined with the time difference, is then used to determine the current water depth. The vessel contains a GPS device which registers the location and elevation of the vessel itself. Subtracting the GPS elevation from the water depth measured by the multi beam, results in the current bed level. In addition, a motion sensor, attached to the vessel, is used to correct for the roll, pitch and yaw motions of the vessel. The drones are used to measure the dry beach and make use of photogrammetry. One drone makes flat images of the area and the other drone makes oblique images. These can then be combined to obtain elevations of the entire area. For a more thorough explanation on photogrammetry see Zhang et al. [48]

The surveys conducted in October 2019 and March 2020 consist of two different measurement methods. One method uses a single beam echo-sounder to measure the water depths and a mobile LiDAR scanner is used to survey the dry beach. The single beam echo-sounder sends out single sound pulses and works similar to the multibeam echo-sounder. The device is attached to the bottom of a jetski. Similarly to the multibeam vessel, the jetski contains GPS and a motion sensor. The echo-sounder will survey the cross-shore profile with spacings between the profiles of 100 meters. To assure no major depth difference occur in between the spacing, crossings between the profiles are made (see Figure 5.1). The 100 meter spaced cross profiles will then be interpolated to obtain the full bathymetry, which can be used on a grid to evaluate and analyse the morphological behaviour.

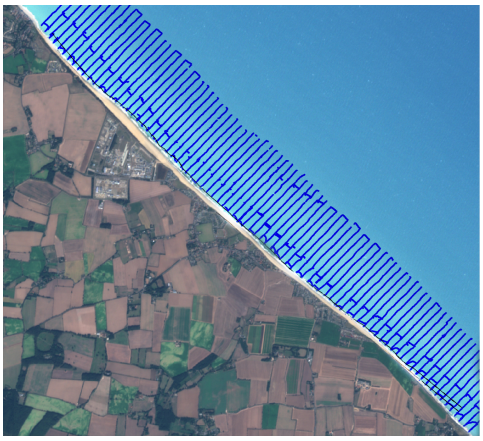

Figure 5.1: Scanning trajectory of the jetski marked in blue. Crossings are visible as shore parallel lines.

The LiDAR system also measures the elevation. However, it uses light instead of sound to measure the elevation. It is attached to either a car or a drone and can measure up to 700,000 points per second. This generates a point cloud which is then transferred onto a grid for further analysis. The

accuracy of the LiDAR system is 2mm and therefore provides very accurate results of the dry beach. After the measurements, the LiDAR data is combined with the jetski data to obtain a full survey of the bathymetry and topography.

5.2. Analysis

The four surveys are used to analyse the morphological behaviour of the BSS. The change in bed level elevation between surveys will be calculated. This will result in the bed level change for the period of August 2019-October 2019, October 2019-March 2020 and the combined period of August 2019-March 2020. The bed level changes are then used to calculate the volume changes in each of the sections (mentioned in paragraph 2.4). First the erosion and sedimentation patterns are discussed. Secondly, a volume analysis is performed and lastly cross-shore profiles are analysed.

5.3. Erosion and sedimentation patterns

The differences between the surveys of August 2019, October 2019 and March 2020 are used to asses the morphological behaviour between these periods. The erosion and sedimentation patterns are shown in Figure 5.2. The first period between August 2019 and October 2019 shows mainly erosion between +7m MSL and 0m MSL (hereafter this area is called: sub-aerial beach) which implies a decrease in the dry beach volume and therefore the beach width. Erosion of up to 2 meters locally is measured in front of the gas terminal (Section 2). The area between the +0m MSL and -5m MSL (hereafter: submerged beach) shows accretion across the entire alongshore stretch. This could indicate that a large part of the eroded sediment of the dry beach is deposited on the foreshore. Between the -5m MSL and -8m MSL almost no significant changes are present for the period. The area below -8m MSL is rather stable across the domain and shows a few spots of both minor erosion and accretion.

For the period of October 2019-March 2020, a slightly different pattern is observed. Accretion is now observed between +0m and +7m for Section 1 and 3. For Section 2 erosion is found at the front of the +7m contour line in front of the Gas terminal. Less erosion is found between the +7m and 0m line for this Section compared to the period of August 2019-October 2019. Across the entire domain, erosion is found around the +0m contour line. Between the +0m and -5m contour line sedimentation is found across all sections which is similar to the period of August 2019-October 2019. Similarly to the first period, the period October 2019-March 2020 shows no significant bed level changes below -5m. Therefore it is assumed that the dynamically active zone for this area is up until a depth of -5m.

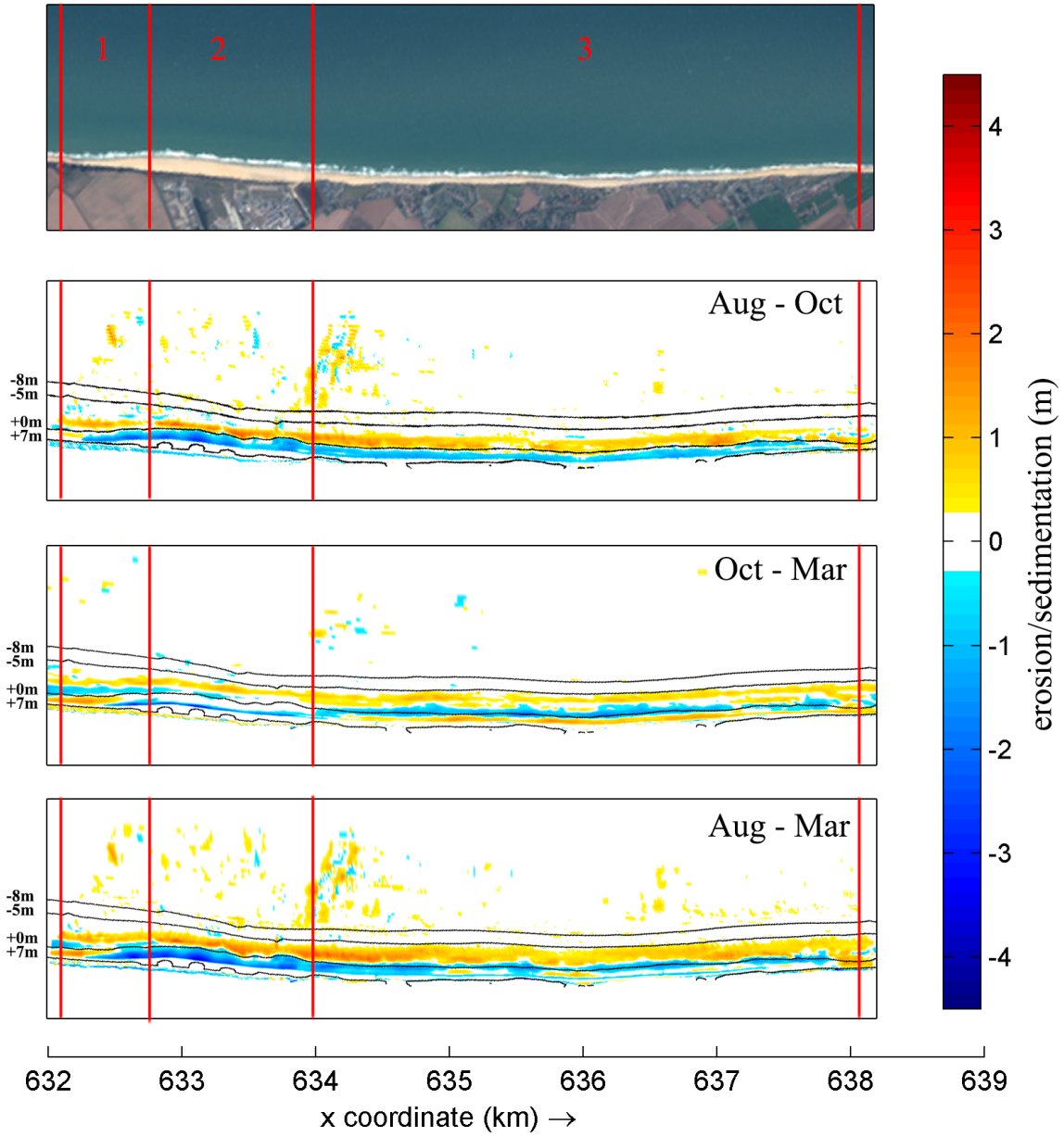

Figure 5.2: Erosion/sedimentation patterns for the three different periods. The blue color indicates erosion and the red color indicates sedimentation. Contour lines of -8m MSL,-5 m MSL, +0m MSL and +7m MSL are included. sections are marked and numbered in red.

5.4. Volume analysis

To gain a better understanding of the morphological patterns, the volume changes for all sections are evaluated. Volume changes of the sub-aerial beach are calculated for each section as well as the volume changes of the submerged beach. These volumes make up the total volume changes of each section and are shown in Table 5.1 and Table 5.2. All the volume changes are referenced to the 0m contour line location of the survey in August 2019. This implies that the volume changes are always calculated from the same points in space. In this way the volumes are checked in a consistent way and it results in the net sedimentation and erosion of the initial survey.

Period	Section	Volume change sub-aerial beach	Volume change submerged beach	Total volume change
Aug 2019-Oct 2019	Section 1	-41,413	+38,119	-3,294
Aug 2019-Oct 2019	Section 2	-100,606	+97,236	-3,369
Aug 2019-Oct 2019	Section 3	-128,663	+330,956	+202,293
Aug 2019-Oct 2019	Combined	-270,682	+466,311	+195,629
Oct 2019-Mar 2020	Section 1	-2,612	+6,264	+3,652
Oct 2019-Mar 2020	Section 2	-37,905	+31,820	-6,085
Oct 2019-Mar 2020	Section 3	-22,787	+48,458	+25,671
Oct 2019-Mar 2020	Combined	-63,304	+86,542	+23,238

Table 5.1: Volume changes for the sub-aerial beach, submerged beach and the total volume changes per section in m^3 for the periods Aug 2019-Oct 2019 and Oct 2019-Mar 2020

Period	Section	Volume change sub-aerial beach	Volume change submerged beach	Total volume change
Aug 2019-Mar 2020	Section 1	-44,025	+44,383	+358
Aug 2019-Mar 2020	Section 2	-138,511	+129,056	-9455
Aug 2019-Mar 2020	Section 3	-151,450	+379,414	+227,964
Aug 2019-Mar 2020	Combined	-333,986	+552,854	+218,867

Table 5.2: Volume changes for the sub-aerial beach, submerged beach and the total volume changes per Section in m^3 for the periods Aug 2019-Mar 2020

The combined section volumes in Table 5.1 show a significant difference between the period August 2019-October 2019 and the period October 2019-March 2020. The first period is characterised by considerably higher erosion rates. As 270,000m^3 was eroded of the sub-aerial beach in the first months. This is 4.5 times more than what has eroded (i.e. 63,000 m^3) in the 4.5 months afterwards. The area of the submerged beach is characterised by sedimentation for both periods. The combined total volume of August 2019 - March 2020 shows an increase in sediment volume over the entire domain, which indicates that a large volume of sediment has transported into the domain. The majority of this sedimentation happened on the submerged beach in Section 3 for the period August 2019-October 2019. As the volume decreases for the sub-aerial beach and increases for the submerged beach, it is expected that a large part of the eroded sediment is transported in cross-shore direction. On the other hand, the first period (August 2019-October 2019) shows a net decrease in volume for Section 1 and 2 and a net increase of volume for Section 3, indicating also alongshore transport of the eroded sediment. A total sediment loss of roughly 334,000 m^3 for the sub-aerial beach and a total sediment gain of approximately 553,000 m^3 for the submerged beach are observed. This means that 219,000 m^3 of sediment located outside the domain is transported into the domain, resulting in net accretion of the area. Normally, it is expected that sediment is transported out of the domain. Therefore, possible causes of the net sediment import are described. Cliff erosion events inside the survey domain could be responsible for the extra input of sediment in the system. The cliff erosion was calculated for the period August 2019 - March 2020 and was found to be 13,920 m^3. Therefore, the local cliff erosion is not enough to provide the overall extra sediment input. A cliff erosion event outside the domain could also be an explanation of this extra sediment surplus. According to Vincent [44] cliff erosion events are able to add 400,000 m^3 of sediment yearly to the coastal system between Cromer and Happisburgh. However, this seems to be a very large amount as this would results in more than a meter cliff retreat over the entire coast between Cromer and Happisburgh.

Furthermore, information regarding cliff erosion events in the surrounding area is not available.

Another part of the explanation for the extreme sedimentation in Section 3 could be caused by errors in the combined survey of July 2019 and August 2019. The survey of July 2019 and August 2019 are inspected through the entire domain to check for possible errors. During this inspection several mismatches between the surveys were observed. An example of both a mismatch and a good match between between the surveys is shown in Figure 5.3.

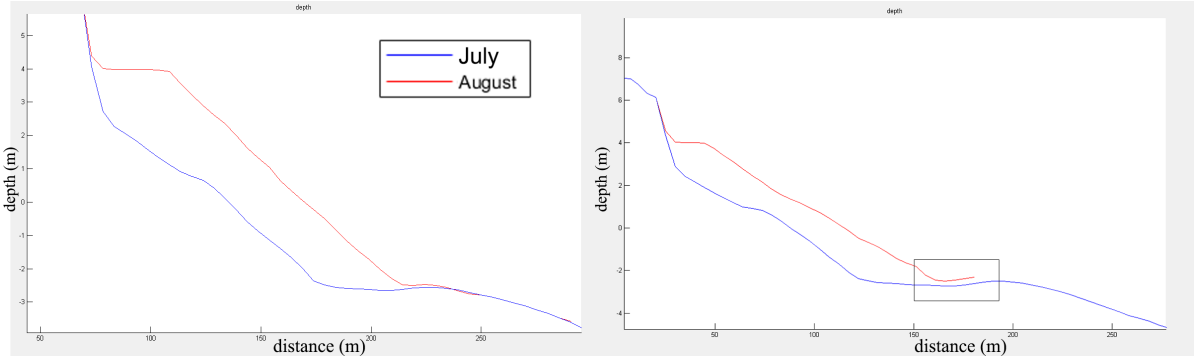

Figure 5.3: The left figure shows a good connection between the survey of July 2019 and August 2019. The right Figure shows no connection between the survey of July 2019 and August 2019. The mismatch is roughly 25 cm and is marked by the black box

The mismatch shown in Figure 5.3 may seem insignificant, however these mismatches are detected over areas which span several hundred meters. Therefore, large over predictions of sedimentation and erosion of the lower areas of the submerged beach are possible. In Figure 5.5 and 5.6 the black shaded areas mark these areas that are affected by the mismatches. The total length of the mismatches in alongshore direction is roughly 2km. If a mismatch is of the order 25cm and spans over 50-100 meters in cross-shore direction, it already leads to an overestimation of the accretion of 25,000-50,000 m^3. All the cross-sections which contain these mismatches are marked and shown in Appendix D as well. In addition, the survey that was conducted in August 2019 was performed over a longer period of time during the construction phase and the survey sometimes just reaches -2m MSL. It could well be that during construction sediment has slided to lower areas than -2m MSL. This would result in missing this particular amount of sediment in the lower submerged beach. This sediment is than later found in the survey of October 2019 and leads to the extreme sediment input found. Figure 5.4 illustrates this problem.

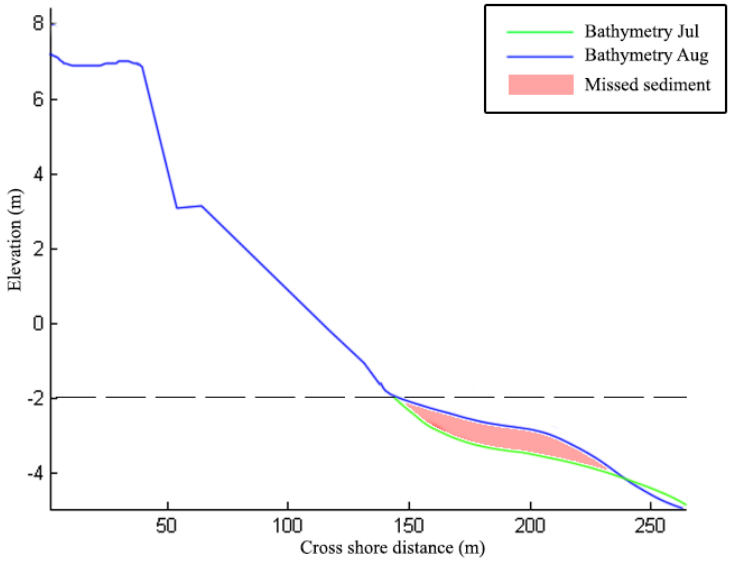

Figure 5.4: The real bathymetry in August 2019 (blue) is measured up until a depth of -2m MSL. The sediment that has slided below this level is not present in the survey and extended with the bathymetry of July 2019 (green). This will result in the missing sediment (red) in the survey of August 2019. This Figure purely indicative and it is unknown how big the effect is.

A combination of the mismatches and the missed sediment in August 2019 could be a viable explanation of the sediment surplus found.

The volumes are now further analysed per running meter and these volume changes are shown in Figure 5.5. The figure shows the volume changes for the sub-aerial beach and the submerged beach per running meter, whereas Figure 5.6 shows the net volume changes per running meter. Figure 5.5 shows that Section 1 is overall less reliable for the period August 2019 - October 2019, this unreliability extends for small part to Section 2. In Section 3, four more less reliable parts are present for the submerged beach and could accordingly be an explanation to the large amount of accretion in Section 3. The period of October 2019 - March 2020 is reliable, since these surveys contain the entire domain and are measured at one point in time. The period August 2019 - March 2020 is an summation of the periods August 2019-October 2019 and October 2019-March 2020 and therefore, the same areas are affected as in the first period.

For the period August 2019 - October 2019 only erosion is observed for the sub-aerial beach and sedimentation is observed for the submerged beach. For the period October 2019 - March 2020 a different pattern is found. In Table 5.1 no accretion can be found for the sub-aerial beach. However, when using an analysis per running meter, local accretion is observed for Section 1 and 3. Yet, only erosion is observed for Section 2. This could be an indicator of the feeding mechanism of Section 2. As the BSS was designed to feed sediment from Section 2 to both Section 1 and Section 3.

Figure 5.6 shows this in a more evident way as Section 2 shows mainly net erosion and Section 3 shows overall net accretion. Furthermore, Figure 5.6 shows that Section 1 has a large accreting area near the end of the domain. This is another indicator of the feeder mechanism of Section 2 for the period October 2019 - March 2020. Section 3 shows large variability during in both net erosion and accretion for the same period. Finally, during the period August 2019 - October 2019 it can be concluded that also Section 2 has an area which shows accretion and is therefore not only eroding and serving as a feeder for Section 1 and 3.

In the period August 2019-March 2020 great alongshore variability is observed for both the sub-aerial and submerged beach. Local changes of more than $100 m^3/m$ are observed over alongshore stretches of less than 250m. This alongshore variability shows similar behaviour for the periods August 2019-October 2019 and October 2019-March 2020. The largest alongshore variability is observed for Section 2, whereas Section 1 and Section 3 show less variability.

Besides the alongshore variability a cross-shore connection between the sub-aerial and submerged beach is observed. High local erosion of the sub-aerial beach leads in general to lower accretion of the submerged beach at the same alongshore location. Likewise, low local erosion of the sub-aerial beach leads in general to higher accretion of the submerged beach.

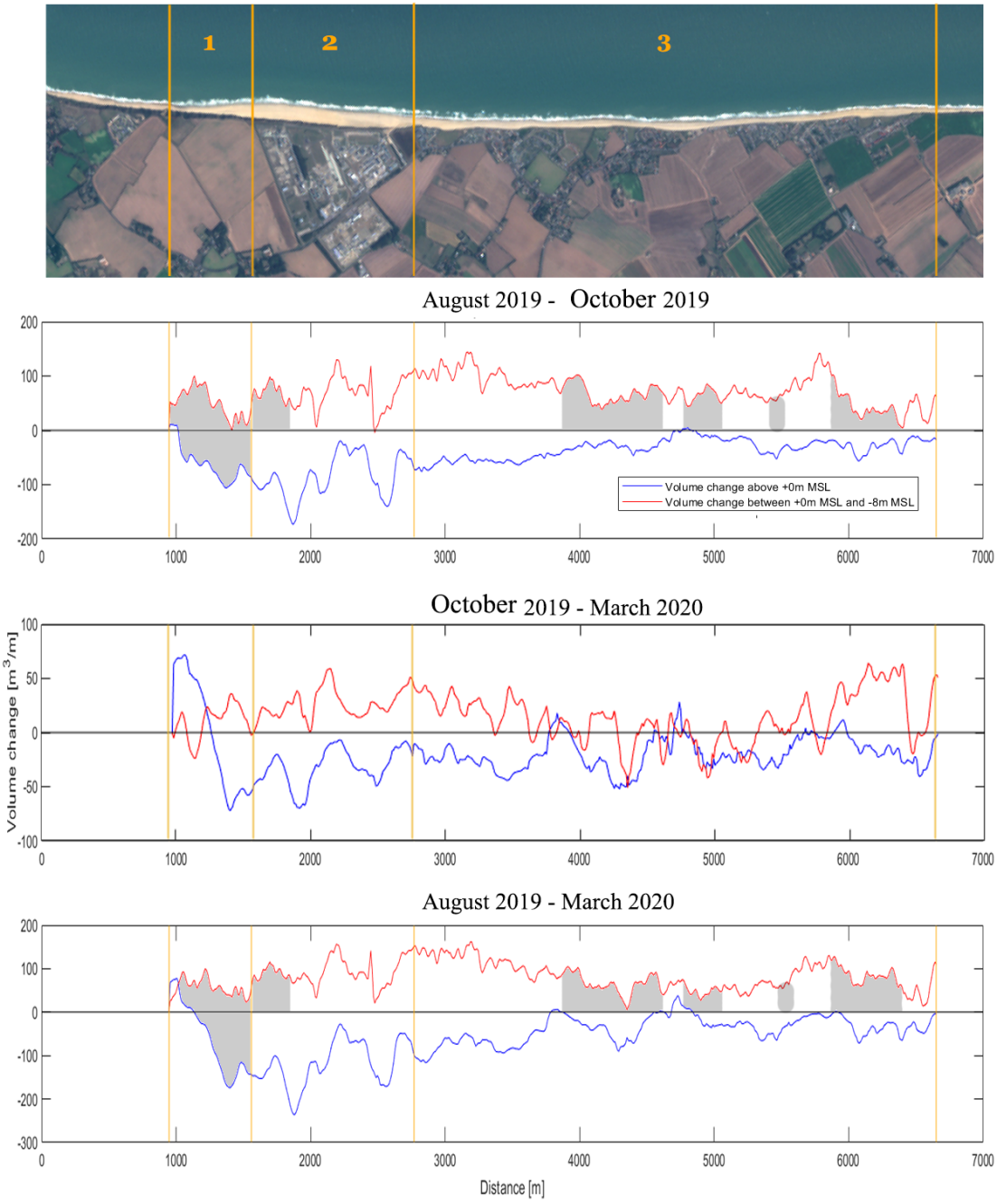

Figure 5.5: volume changes for the sub-aerial beach (blue) and the submerged beach (red) across the total domain in m^3/m for the periods in between surveys. In yellow the section numbers and lines are indicated. Grey shaded parts indicate the areas that are affected by mismatches.

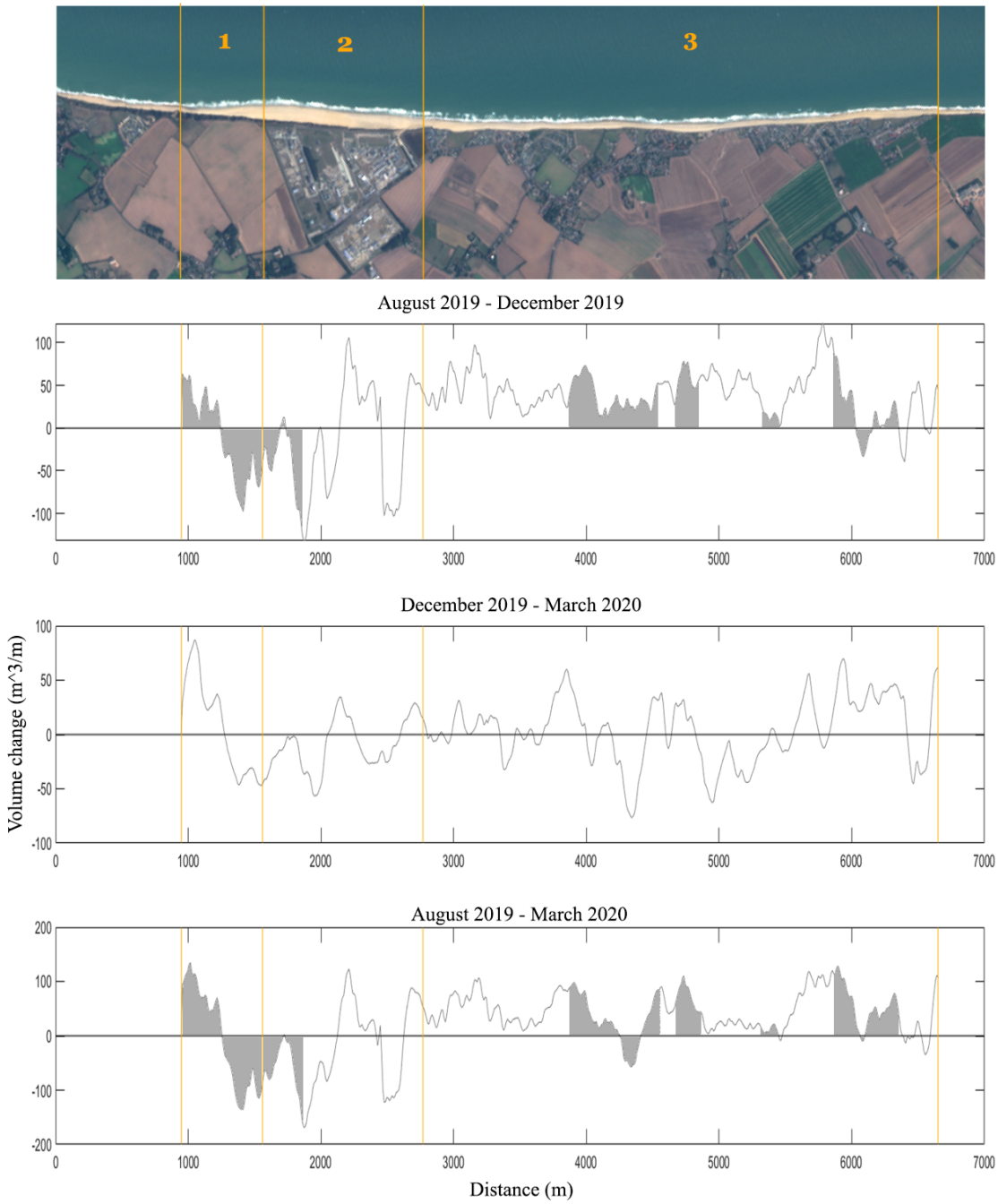

Figure 5.6: Net volume changes across the total domain in m^3/m for the periods in between surveys. In yellow the section numbers and lines are indicated. Grey shaded parts indicate the areas that are affected by mismatches.

5.5. Profiles

The erosion and sedimentation patterns are further analysed using cross-sections of each section (see Figure 5.7 for the cross-sections and see Figure 5.8 for the locations of these cross-sections). The erosion/sedimentation patterns seen in Figure 5.2 are indisputably present in the cross-sections as well. However, the cross-sections give a more apparent view in the slope evolution of the nourishment which is not visible on the erosion and sedimentation map of Figure 5.2.

For the period August 2019 - October 2019, all sections show a flattening of the sub-aerial beach for this period. However, a scarp of approximately 2 meters has formed in Section 2 and extends partly into Section 1. Pictures of the scarp are shown in Figures C.1 and C.2 in appendix C . Moving cross-shore from the scarp, the profile flattens until it reaches the initial bottom slope at -5m MSL. Flattening of the beach slope can also be recognised for Section 1. Differently, Section 3 shows no major slope changes and also no scarp is present in this section.

For the period October 2019 - March 2020, the scarp formed in Section 2, increases in this period to a height of 4 meters and has retreated several meters. Section 1 and 3 show a significant increase of sub-aerial beach volume. This could again be an indication of sediment spread from Section 2 to both of the other sections. Indicating that the feeder mechanism is present. However, sediment has eroded from the lower intertidal zone for all sections, so part of the sedimentation on the higher beach could be originated from the lower areas due to onshore sediment transport processes. Nevertheless, it is not expected that all the sedimentation is caused by onshore transport of the lower beach, but also due to the alongshore feeding mechanism of Section 2.

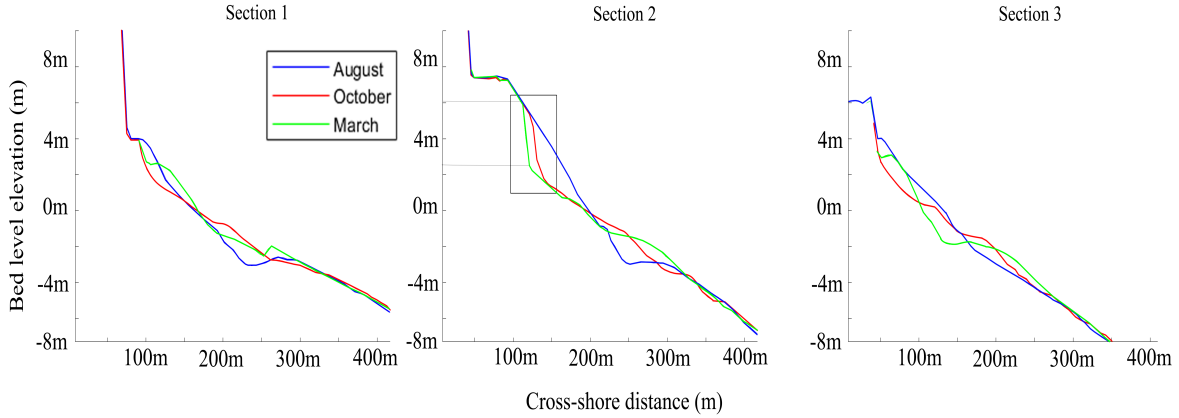

Figure 5.7: Cross-sections of a typical profile of each section. In Section 2 a significant scarp of 4 meters can be identified (marked with the black square)

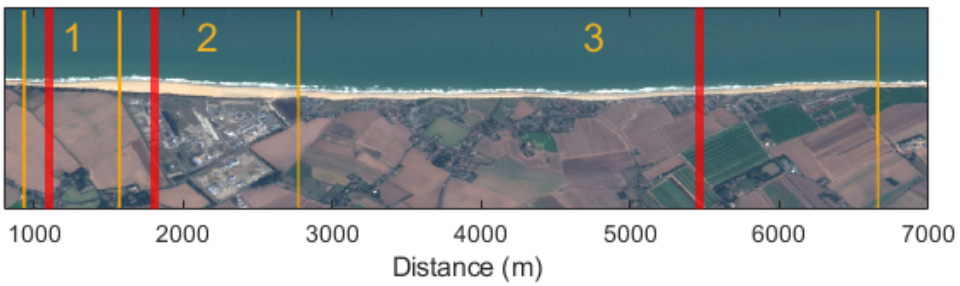

Figure 5.8: cross-section locations of Figure 5.7 are marked in Red. Sections are indicated by the yellow numbers and yellow vertical lines.

5.6. Concluding remarks

The surveys conducted in August 2019, October 2019 and March 2020 show the behaviour of the BSS in the first half year. The visual inspection of the erosion and sedimentation patterns showed that erosion mainly occurred between +7m MSL and +-0m MSL, while accretion was observed for the area between +-0m MSL and -5m MSL. The area between -5m MSL and -8m show no significant erosion or sedimentation. Depths below -8m MSL show minor adjustments of the shore profile.

The volume analysis further showed that he sub-aerial is eroding while the submerged beach is accreting. Section 2 shows the most erosive behaviour, while Section 1 and 3 also show some accretion. The erosion volumes of the sub-aerial beach shows quite some alongshore variation. Erosion volumes per running meter can vary more than $100m^3/m$ locally in Section 2. It is therefore important that the BSS numerical model is able to capture this alongshore variability. In addition, a link between the erosion of the sub-aerial beach and the accretion of the submerged beach is found. Higher erosion volumes of the sub-aerial beach lead in general to lower accretion volumes of the submerged beach. Also lower erosion volumes of the sub-aerial beach lead to higher accretion levels of the submerged beach.

The profile analysis showed a scarp formation in Section 2 which grew from 2 meters height to 4 meters height from October 2019 to March 2020. Moreover, beach flattening is observed for all section. For Section 2 the beach flattening is observed for the area in seaward direction from the scarp.

6

Bacton Sandscaping model validation and analysis

This chapter describes the validation and performance of the BSS model compared to the measurements described in Chapter 5. This provides the models capacity to simulate the morphological behaviour up until the survey performed in march 2020. Also, its predictive capacity to estimate other scenarios including different wave events, different grain sizes and longer time periods.

First, the method of validation is discussed. This describes how the model is verified and how the skill of the model can be scored. Subsequently, the model behaviour is described. In particular, morphological patterns such as sediment deposition and erosion locations are elaborated. These patterns are visually compared to the earlier described measurements.

One of the main research objectives is to assess the capability of Delft3D to simulate the first half year of the BSS. This is mainly answered by the model validation. A large part of this model validation is based on visual interpretation of the model results and measurements. Shape formation, erosion patterns and sedimentation patterns are discussed. This includes the model's capability of reproducing the scarp formation, the sedimentation of the submerged beach and the erosion of the sub-aerial beach described in Chapter 5. In addition to the visual verification of the results of the model, a quantitative score to validate the model's performance will be used.

The secondary objectives of this thesis are to asses the BSS requirements after 15 years and to assess the effect of different wave events and grain size on the beach volume of the BSS. The predictive capabilities of the model will determine how well it is able to simulate other forcing conditions as well as long term behaviour. This is discussed in the last paragraph of this chapter.

6.1. Qualitative validation

To evaluate the model performance it is essential to understand the strengths and limitation of the BSS model. Several different characteristics of the model are described in this paragraph, such as the morphological patterns simulated by the model, the volume changes and the capability of the model to erode higher parts of the beach. Finally the model's predictive capacity is summarised.

6.1.1. Morphological pattern prediction of the BSS model results

The erosion and sedimentation patterns of the model are compared to the measured erosion and sedimentation patterns described in Chapter 5. Both the measured patterns as the modelled patterns are shown in Figure 6.1. Both the model and the observations show a similar erosion front between +0m MSL and +7m MSL. The model captures the overall intensity of the erosion adequately in Section 1 and Section 2. Erosion in Section 3 is slightly less dynamic in the model results compared to the measurements. The model is likely too coarse to show these minor dynamics. However, the erosion band in Section 3 is still captured sufficiently considering the size of the erosion band. Observations show also erosion above +7m MSL, indicating cliff erosion and possibly aeolian transport. The model cannot capture this erosion as the water does not reach the cliffs. In addition, episodic cliff events and aeolian transport processes are not incorporated in the Delft3D model. Between +0m MSL and -5m MSL both the model and measurements show a sedimentation band. The model is largely under predicting the sedimentation that is found in the observations. In Chapter 5 it is described that a net sediment input to the system is observed. The model is not able to represent this net sediment input as the model is based on a sediment balance. To resemble a net sediment input, a sediment

boundary conditions would have to be implemented in the model. This would require more data concerning sediment influx and sediment transport of the area, these are however not available. Moreover a new calibration procedure would have be required. Therefore, this has not been implemented in the model. On the other hand the model is well capable of representing the locations of sedimentation. As the darker yellow and red sedimentation areas of the observations match with the darkest areas of sedimentation in the model. So the model is capturing the pattern quite well, but not the intensity.

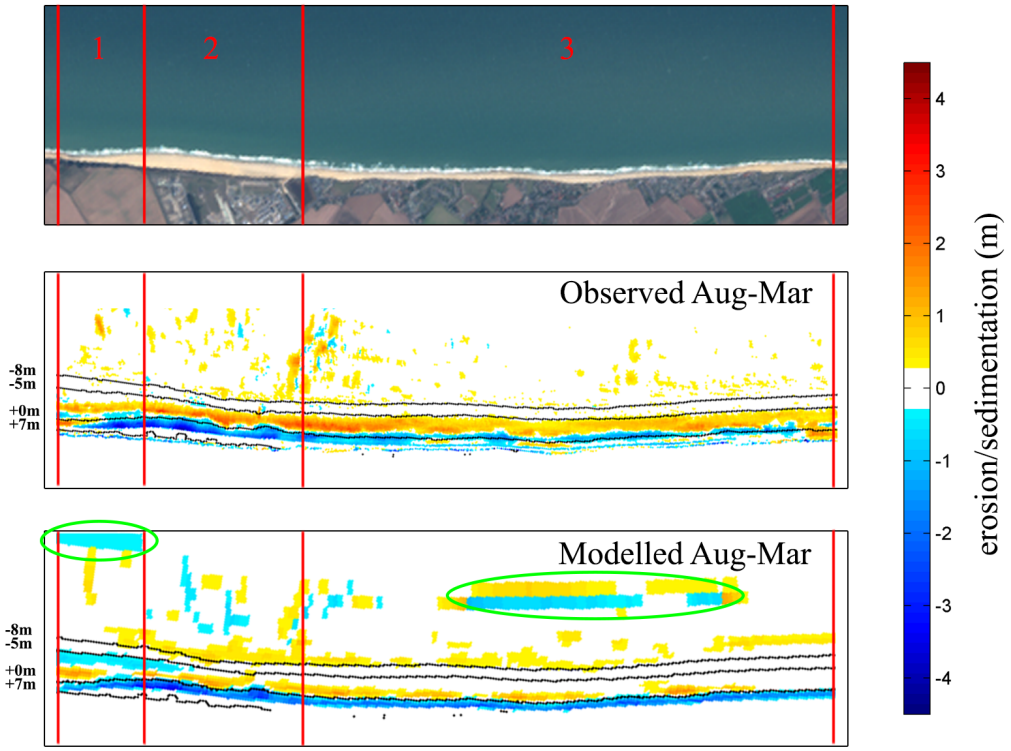

Figure 6.1: The observed and modelled erosion and sedimentation patterns. The blue color indicates erosion and the red color indicates sedimentation. Contour lines of -8m MSL,-5 m MSL, +0m MSL and +7m MSL are included. Sections are marked and numbered in red. The two green circles indicate profile adjustments of the model and are not affecting the volume calculations.

Between -5m MSL and -8m MSL the observations show no significant changes and this is captured by the model as well. In deeper areas the model shows more dynamics than the observations. But overall the model shows similar behaviour in these deeper areas as the observation. As the model's grid resolution decreases in offshore direction small local changes as in the observations are not possible and therefore the areas that show either erosion or sedimentation are more pronounced.

In conclusion, the model accurately presents the patterns and intensity of erosion for the sub-aerial beach. The model is less accurate predicting sedimentation intensity of the submerged beach, but it is adequately capable of representing the location and patterns of sedimentation.

6.1.2. Higher beach erosion capabilities

The capability of the BSS model to erode the higher parts of the dry beach is evaluated in this paragraph. The standard Delft3D parameters allow sediment calculations for cells that are considered wet. The depth for a cell to be considered wet is a predetermined parameter and is set to a value of 0.3m. Cells that are permanently dry will therefore not show any morphological changes during simulations. However, Delft3D incorporates a parameter which allows dry cells to be eroded as well. This parameter (called: ThetSed) is a factor which determines the rate of erosion of dry cells adjacent to wet cells. This allows dry cells to be eroded and later allows them to be active wet cells after enough sediment has eroded. The factor can range from 0 to 1. If ThetSed is set to 0, dry cells will not be able to erode and if ThetSed is set to 1, dry cells erode at the

same rate as active adjacent wet cells. Therefore, a factor between 0 and 1 gives the relative erosion rate that is transferred from a wet cell to a dry cell. The BSS model is once run with the parameter set to 0 and once run with the parameter set to 1. The result is shown in Figure 6.2.

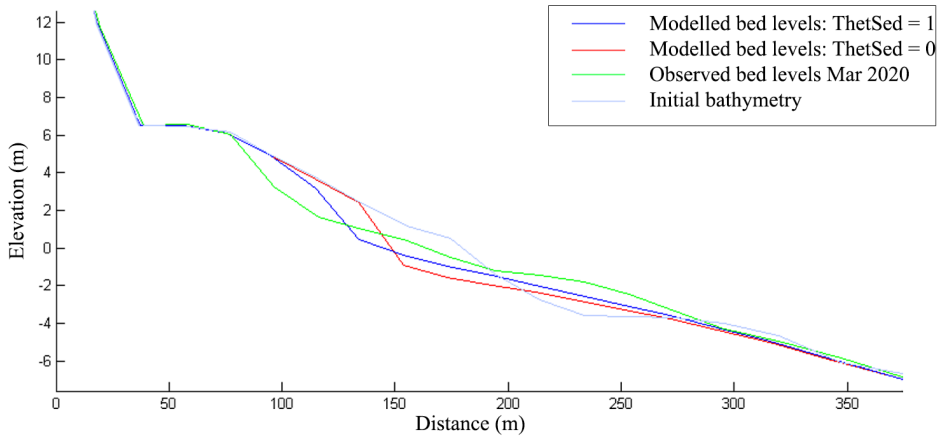

Figure 6.2: Modelled bed levels for Thetsed = 1 and ThetSed = 0 at the end of the simulation, compared to the observed bed levels in March 2020 and the initial bathymetry August 2019

Figure 6.2 shows a clear difference between the runs with a different Thetsed parameter. The run with Thetsed set to 0 shows no erosion above the highest astronomical tide (HAT=+2.71m MSL) level. Whereas the simulation with Thetsed set to 1 shows erosion up to a level of +5MSL. Therefore, showing the capability of eroding the higher parts of the BSS. The simulation with a ThetSed of 0 would eventually lead to a very steep front at the location of the HAT and would cause the model to further erode only the levels below HAT. The measurements show that higher beach levels are eroding and it is therefore essential that the model captures this behaviour. However, measurements show that the BSS is eroding more rapidly than that the model is predicting. At the location of the scarp, the model resolution is 17 meters. Therefore,the BSS model has a limiting grid resolution and can therefore not predict the same steep slopes that are present in reality. Moreover, this version of Delft3D has no slope avalanching and this also limits its ability to accurately model these scarps. This might also be the explanation as to why the model is predicting less erosion above HAT. The resolution is not allowing for enough wet cells to reproduce the same amount of erosion of the levels above +5m MSL

6.2. Quantitative validation

The skill of the morphological model is commonly evaluated by comparing a morphological model prediction to a model prediction without morphological changes [5]. This provides the relative improvement of the morphological prediction to a model that would predict no change at all. A common score which is used for model verification is the Brier skill score [5] [27]. The Brier skill score is defined as:

$$\text{Brier skill score} = 1 - \frac{MSE}{MSE_{no\ change}} \tag{6.1}$$

In this formula, the MSE is the mean squared error of the morphological prediction compared the measured bed elevations. The $MSE_{nochange}$ is the mean squared error of the prediction without morphological changes. Subtracting the ratio of MSE and $MSE_{nochange}$ from 1, will result in the relative improvement of the model prediction compared to the no change prediction. A score of 0 represents a morphological model performance similar to a model without any changes at all. A score of 1 represents a morphological model performance which perfectly represents reality. A score between 0 and 1 gives the relative improvement of the morphological model compared to the no change model. Negative scores indicate that a morphological model prediction is performing worse than a model predicting no change. According to Sutherland et al. [39] the model performance can be categorised in five different scores (see Table 6.1).

Table 6.1: Brier skill score ratings

Brier skill score	Performance
≤0	Bad
0 − 0.1	Poor
0.1 − 0.2	Reasonable
0.2 − 0.5	Good
0.5 − 1	Excellent

The traditional Brier skill score uses the bed level changes at all grid locations across an entire domain. As the grid resolution of the model is quite large in comparison to the nourishment size, this method is not very robust. The performance of the model to predict exact bed levels shows is therefore lower than for the volume changes. The Brier skill score for the predicted bed levels is 0.19. This means that the models still performs reasonable to almost good. However, the capability to predict volume changes scores much better. Therefore, the brier skill score is also used to asses the model performance regarding volume changes. Volume changes are calculated per running meter and are compared to the volume changes per running meter of the observations in Chapter 5.4. These volume changes are then compared to the zero change reference model to obtain the volume Brier skill score.

6.2.1. Model performance and volume analysis

This paragraph focuses on the model performance regarding the net volume changes and the volume changes of the sub-aerial and submerged beach. The beach volume behaviour is discussed, volume changes per section are described as well as volume changes per running meter. These results are then compared to the measurements and used to score the performance of the BSS model. The first check on the model performance is done on the net volume changes per running meter. The net volume changes for the model results compared to the observations is shown in Figure 6.3.

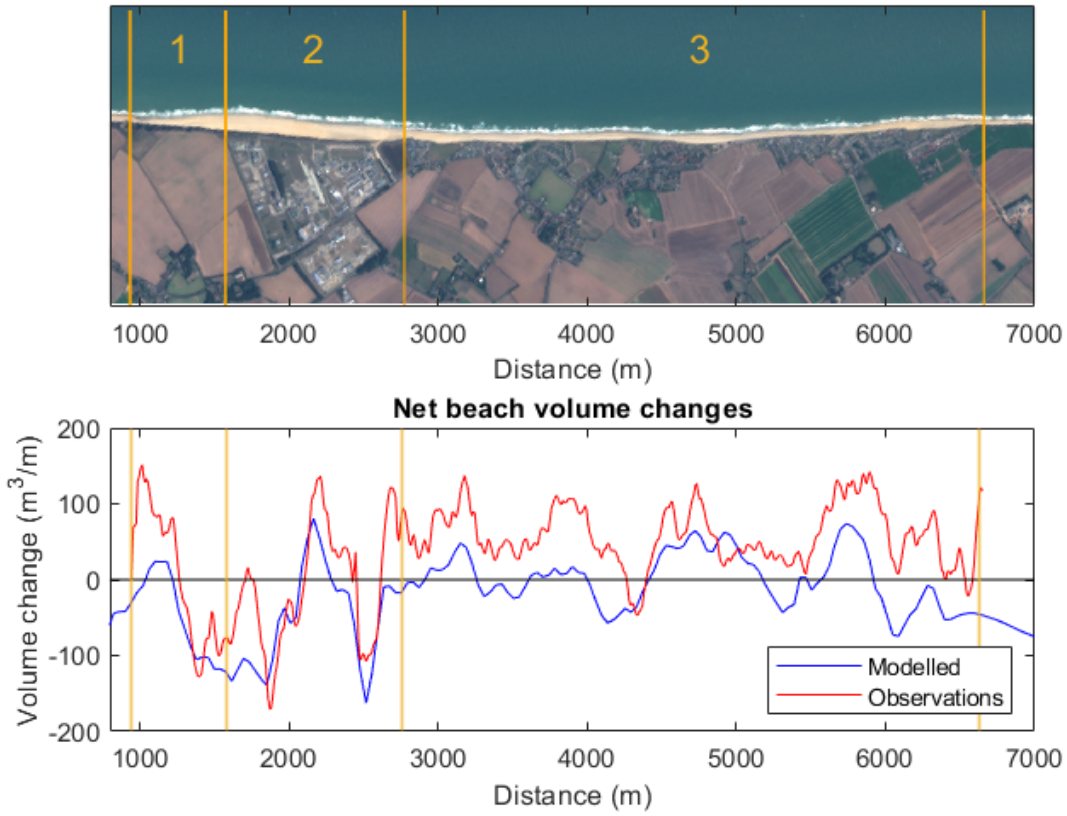

Figure 6.3: Modelled net volume changes (blue) compared to the observed volume changes (red). In yellow the section boundaries and numbers are indicated.

The modelled volume change pattern shows good agreement with the measured pattern. The peaks and troughs show mostly similar locations. However, the accretion of the submerged beach is under predicted as was described before. This results in the fact that accretion of the net volume changes is also under predicted. Calculating the Brier skill score for the net volume changes results in a Brier skill score of 0.12 (reasonable). This is slightly worse than the Brier skill score for the exact bed levels, but still a reasonable result is obtained. The brier skill score is a statistical based formula and using a statistical method to assess morphological model results comes with a downside. Models that show a desired variability may well score the same skill as models that under predict this variance [40][5]. Therefore, the brier skill score will only be used as a positive or negative indication. The BSS model shows the right pattern but at some places it shows erosion instead of accretion and the Brier skill score is largely lowered by this. To further analyse the model results the volume changes are split up in the sub-aerial beach and submerged beach volume changes. This results in a better overview of the model performance. The volume changes per running meter for both the sub-aerial beach and the submerged beach that are calculated by the model are compared to the observations in Figure 6.4. The model shows a good agreement between the patterns found in the observations. The peaks and troughs of the sub-aerial volume changes are well captured by the model. However, the first peak in Section 2 around the 2000m mark is underestimated. The sub-aerial beach erosion of Section 3 is on average overestimated and the small accretion peaks are not visible in the model. Despite these minor differences the sub-aerial beach volume changes score 0.82 on the Brier skill score, which is excellent for a morphological model, according to Sutherland et al. [39]. The positive Brier skill score indication combined with its capability to follow the alongshore variability shows the model's excellent capabilities.

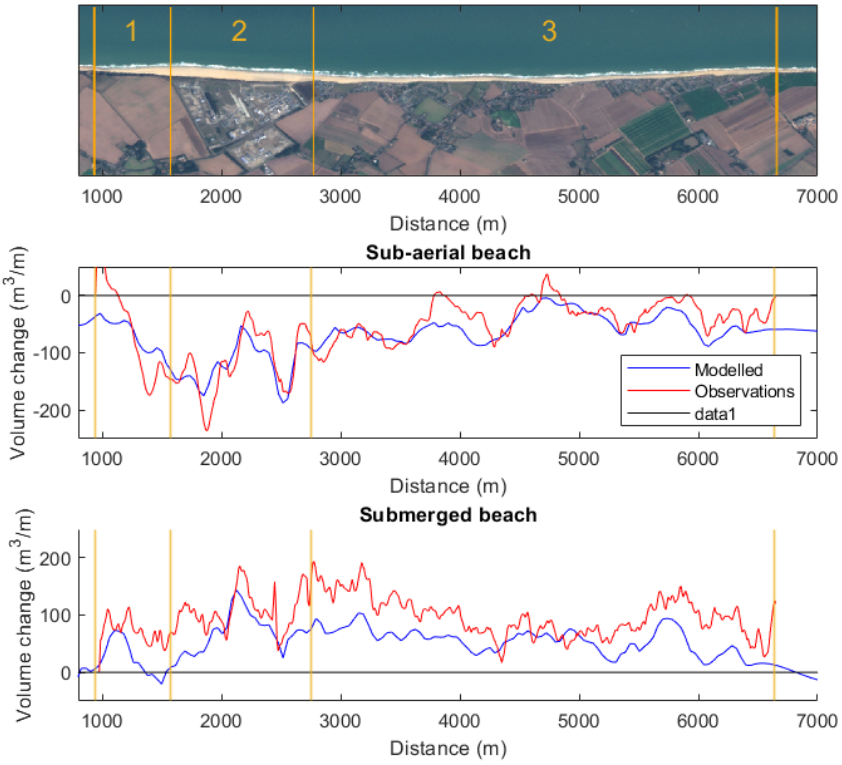

Figure 6.4: Modelled volume changes (blue) compared to the observed volume changes (red). In yellow the section boundaries and numbers are indicated.

The modelled submerged beach volume changes show a similar pattern as the observations, but seems to underestimate the accretion across the entire domain. The observations showed a net sediment input (see Chapter 5) which is largely deposited in the submerged beach area. A net sediment input requires a known sediment influx rate. A sediment boundary condition is therefore required at the open boundary [23]. The average influx of the system is unknown and is probably depending on cliff erosion events and other sediment sources outside the model domain. Therefore, adding a sediment boundary would be complicated. This also explains why the model underestimates the total accretion found for the submerged beach. As the accretion patterns are similar the difference between the model and the observations is largely due to the missing sediment influx. Even though, the submerged volume changes have a Brier skill score of 0.76. Combining this with its ability to follow the alongshore variability of the submerged beach volume changes, is a very positive indication of the model's performance.

In Chapter 5 a connection between the sub-aerial beach volume changes and the submerged beach volume changes was found. High local erosion of the sub-aerial beach was linked to low local accretion of the submerged beach. Likewise, low local erosion of the sub-aerial beach was linked to high local accretion of the submerged beach. The model seems to capture this behaviour quite well. Especially, Section 2 and Section 3 show this behaviour. As peaks of high erosion match with troughs of low erosion.

The model performance is also checked for the period between October 2019 - March 2020. However, it must be noted that the in model bathymetries are used for the analysis. This results in that the computed bed levels of October 2019 are compared to the computed bed levels in March 2020. This also means that no extra model runs were performed with the bathymetry from the survey in October 2019. This limits the viability of the analysis of this period and therefore, the result of this analysis has to be taken carefully. The volume changes per running meter for this period are shown in Figure 6.5. The model follows the alongshore variability of the sub-aerial beach again very well. However, erosion is largely over predicted and no accretion is found for the sub-aerial beach. The model predicts less alongshore variability for the submerged beach as found in the observations. The magnitude of the accretion is however, more in line with the observations

compared to the entire simulation. The Brier skill score is not used for this simulation as this is not possible, as the model uses the computed bed levels in October 2019 instead of the surveyed bathymetry in October 2019.

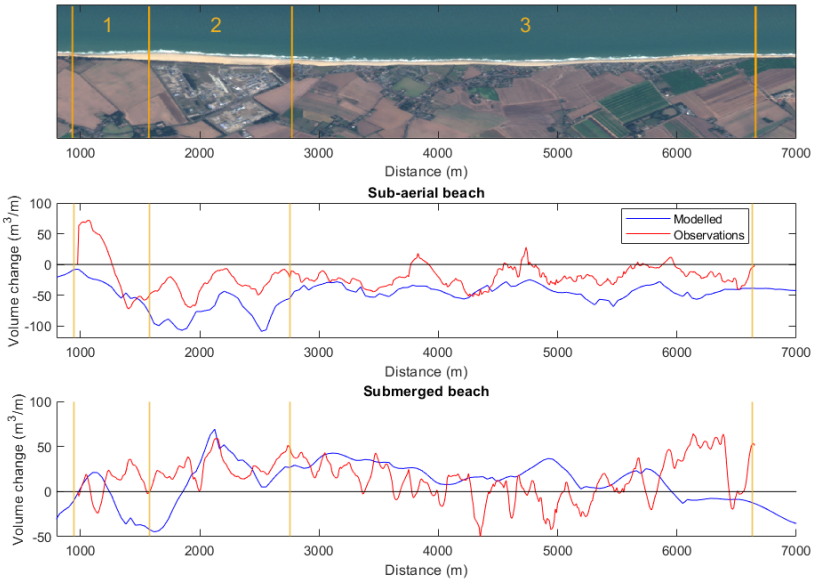

Figure 6.5: Modelled volume changes (blue) compared to the observed volume changes (red) for the period Oct 2019-Mar 2020. In yellow the section boundaries and numbers are indicated.

To further explain the model behaviour the absolute volume changes are described. These give an insight in the exact sediment losses and gains. The volume changes per section for the model and the observations are shown in Table 6.2. The table shows the exact overestimation of the sub-aerial beach erosion of Section 3 and the underestimation of the submerged beach volume changes. The model underestimates the submerged beach volume changes by roughly 243,000 m^3. This is a similar amount as the total net influx of the observations of 218,867 m^3. Further indicating that the model's underestimation is due to the missing net influx instead of the model's inability to model the morphology of the submerged beach. Further, the model predicts a total loss of 101,120 m^3 in the system. A large part of this eroded sediment is traced back in the area below -10m which is not used for the analysis. This area contains 45,000 m^3 and the other part of the eroded sediment is transported out of the model. The sediment that is still in suspension is negligible compared to the loss that is observed.

Section	Observed sub-aerial beach [m^3]	Modelled sub-aerial beach [m^3]
Section 1	-44,025	-48,255
Section 2	-138,511	-147,590
Section 3	-151,450	-214,720
Total	-333,986	-410,565
	Observed submerged beach [m^3]	Modelled submerged beach [m^3]
Section 1	+44,383	+15,422
Section 2	+129,056	+81,923
Section 3	+379,414	+212,100
Total	+552,853	+309,445
	Observed total [m^3]	Modelled total [m^3]
Section 1	+358	-32,833
Section 2	-9455	-65,667
Section 3	+227,964	-2,620
Total	+218,867	-101,120

Table 6.2: A comparison between the observed and modelled volume changes for each section for the period August-March

6.3. Model observations

This paragraph describes the observed erosion volumes caused by waves. This gives insight in which significant wave heights and directions dominate the erosion process of the BSS. Luijendijk et al. [27] showed that the largest 12 wave events were responsible for 60% of the erosion of the main area that is supposed to feed the adjacent coast. This paragraph analyses whether this is also the case for the BSS or if other wave conditions determine the morphological behaviour.

The average significant wave height per day is used to calculate the volume changes for each of these days. The volume changes are calculated for the sub-aerial beach of Section 2 as this section is supposed to feed the adjacent coast. The average significant wave height per day and the average wave direction are plotted against the daily erosion volumes in Figure 6.6.

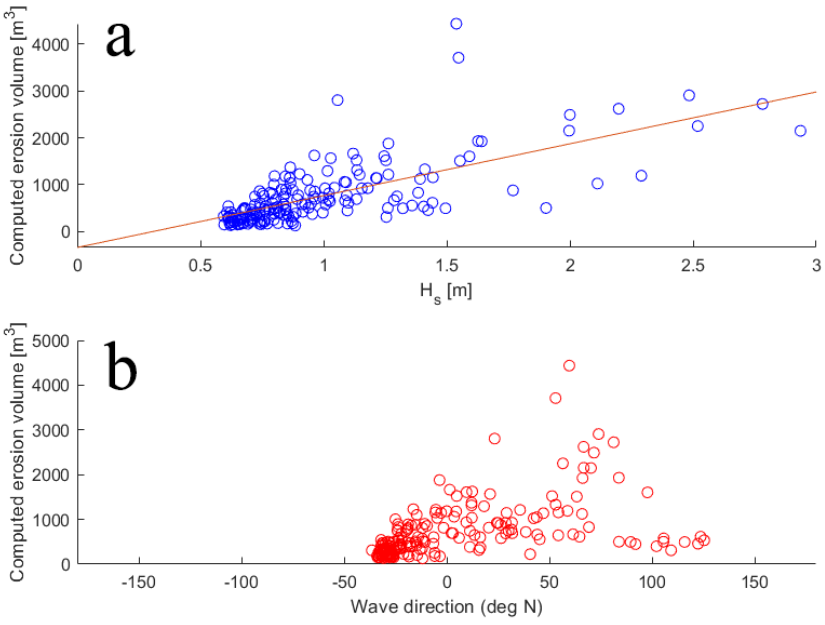

Figure 6.6: a) Computed erosion volumes for the average wave heights at the boundary of the Delft3D model.b) Computed erosion volumes for average wave directions in degree north.

The figure shows that there is a relationship between the wave height and the computed erosion volume of Section 2. Increasing wave heights lead in general to an increase in the computed erosion volume as might

be expected. However, the most erosive events are caused by significant wave heights of around 1.5 m. It must be noted that the majority of the computed erosion events are caused by significant wave heights below 1m. Wave conditions below 1m are observed during 123 days of the half year simulation and these are responsible for 57% of the total erosion of Section 2. Figure 6.6 also shows that in general the most erosive events are directed from around +50 degrees north. This goes to show that wave direction is more important than the significant wave height. In addition, Figure 6.7 shows that the 34 days with the highest significant wave heights is only responsible of eroding 50,500m^3 of the total 139,000m^3 that has eroded from Section 2, which corresponds to 36% of the total erosion. Luijendijk et al. [27] showed that the 12 largest wave events (duration is roughly 1 month as well, but for a one year simulation) are capable of eroding 60% of the total observed erosion. This means that for Bacton milder wave conditions also play an important role and that the largest wave events do not dominate the total erosion. On the other hand,the significant wave heights in the research of Luijendijk et al. [27] are typically much higher than for Bacton. this could be an explanation of higher wave events being more dominant.

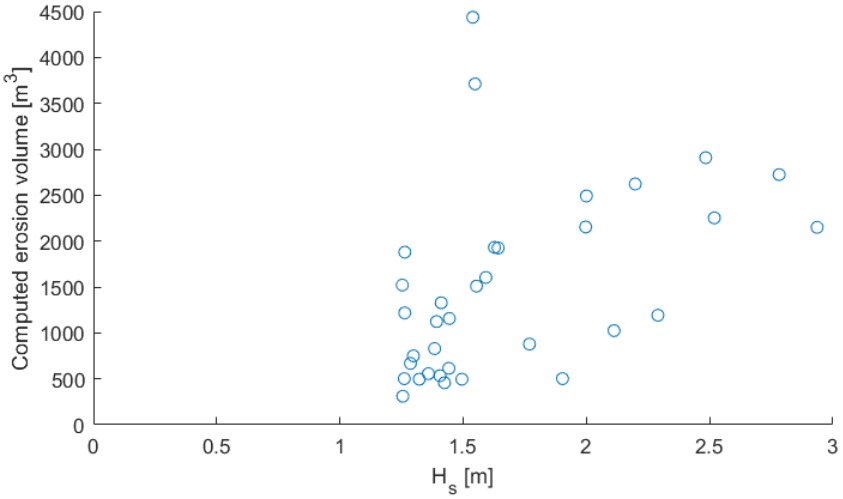

Figure 6.7: Computed erosion volumes of Section 2 for the 34 days with the highest average significant wave heights.

6.4. Model prediction capacity for secondary research questions

This paragraph summarises the model's capability to model beach volume changes as well as it's capability to provide results for the requirements analysis. First the beach volume modelling capacity is described and secondly the requirements capacity is discussed.

6.4.1. Beach volume

One of the secondary research questions is to describe the effect of different wave event intensities and grain size on the sub-aerial beach volume changes, it is therefore essential that the model captures the morphological variability in alongshore direction. It is more important that the model captures the volume changes from the sub-aerial beach than it is able to simulate the submerged beach volume changes. However, it is still necessary that the model captures the alongshore volume fluctuations of the submerged beach. From the volume analysis performed in this chapter it is evident that the BSS model is well capable of simulating the morphological patterns. Hence, The brier skill score for the submerged beach is 0.75 and for the sub-aerial beach the brier skill score is 0.82, which gives a positive indication. Besides the Brier skill score, the net volume changes per section showed that the model is overestimating the erosion of the sub-aerial beach and is underestimating the accretion of the submerged beach. In addition, the net sediment influx observed in the measurements is not captured in the model. To assess the effect of beach volume changes due to wave events and grain size, the strengths and weaknesses of the model are of great importance. As the model captures the sub-aerial beach volume quite well, it is assumed that the model is also capable of simulating other grain sizes and forcing conditions with similar accuracy for sub-aerial beach volume changes. For the sub-aerial beach volume analysis it is also important to incorporate the forcing conditions and grain size effects on the submerged beach. As the model is well capable of simulating the submerged patterns it is able to indicate

what effects are present at the submerged beach. However, it has to be taken into consideration that the submerged beach will always be an underestimation of what would have happened in reality. Moreover, the sub-aerial beach volume changes are likely to be an overestimation of reality.

6.4.2. Requirements

The requirements of the BSS form the basis of one of the secondary research questions and it is therefore essential to quantify if the model is able to assess the BSS at the end of its lifetime. The requirements are assessed per section. For each of the requirements it is explained how the BSS model is able to assess them. The model's strengths and limitations are described in how they will affect the ability to simulate the requirements.

1. Section 1
    - Section 1 has no requirements and therefore no description is necessary on how the model is able to asses this section.
2. Section 2
    - Requirement 1: maintain a beach width of 20m at +7m MSL.
      To assess this requirement the bed levels at the end of the 15 year simulation are computed. The bed levels at the end of the simulation are then used to create cross-shore profiles. The width of at the base of the cliffs are evaluated and checked whether they maintain a beach width of 20m at +7m MSL. The grid size resolution and the capability of the model to erode the higher beach are of importance when assessing this requirement. The grid size resolution is 17 to 21 meters at the base of the cliff, this results in a minimum width at +7 m MSL of 1 grid cell at the base of the cliff. As described before, with the use of the ThestSed parameter the model is well able to erode higher parts of the beach. The model should therefore be able to model the higher beach erosion and thus assess the beach width at +7m MSL. In conclusion, the requirement is met when at the end of the simulation the 15 year simulation the beach width is still larger than 1 grid cell at the base of the cliff.
    - Requirement 2: Water level may not reach base of the cliff
      At the end of the 15 years simulation it is assessed whether the water level has reached the base of the cliffs at +7m MSL. During simulation the water levels are computed for each time step. The wave run up is incorporated in the Delft3D software and allows the water to reach higher parts of the beach. The Delft3D software is therefore, able to assess whether the base of the cliffs are reached by the water. On the other hand, storm surge levels are not incorporated in the BSS model and it will not be able to assess the water level for these conditions.
3. Section 3
    - Requirement 1: No erosion at the toe of the Seawall. With the known seawall toe location it can easily be checked whether sediment is still covering the toe of the structure. The model is used to assess the bed levels at the base of the cliff. If the bed levels of the cliff are below the toe of the cliff, the toe will be exposed.

Most of the requirements have to be inspected visually as it is not possible to assess the requirements using the volume analysis. At each individual cross-section of the model the requirements are checked. The model's capability to model exact bed levels are reasonable and a rough estimate of the requirements can be made with the model.

6.5. Concluding remarks

The numerical BSS model was both quantitatively and qualitatively validated using the same calibration parameters from the calibration process. The visual validation showed that the erosion and sedimentation intensity matches very well with the survey data. The model's prediction of the most intense erosion is in line with the location of the scarp in the measurements. Both the model and the surveys show that most accretion of the submerged beach is present for the area between +-0m MSL and -5m MSL. Furthermore, the model

showed more morphological changes below -8m MSL than the surveys, which are due to profile adjustments in the model.

The quantitative validation showed that the model's capability to simulate the net volume changes is reasonable and it follows the alongshore variability quite good. However, the main strength of the model is to simulate the volume changes of the sub-aerial beach. The model performs excellent and shows the alongshore variability very well. The maxima and minima are also very well represented by the model in both their location and magnitude. For the submerged beach volume changes, the alongshore variability is also very well represented, although scoring just a bit lower than the sub-aerial beach. A similar cross-shore behaviour as in the surveys is observed. High sub-aerial beach erosion areas lead to lower sedimentation of the submerged beach. Likewise, low sub-aerial beach erosion areas leads to higher sedimentation of the submerged beach. This goes to show that the model is capable of representing the cross-shore connection between the sub-aerial and submerged beach.

The absolute volume differences of the sub-aerial beach are very similar to the observation. The model predicts almost identical volume losses for the sub-aerial beach for Section 1 and Section 2. On the other hand, the sub-aerial beach volume loss of Section 3 is overestimated.

Lastly, the model predicted that significant wave heights lower than 1 meter are responsible of 57% of the observed erosion of Section 2 and that the erosive behaviour is not dominated by large wave events. Moreover, the model predicted that waves directed from +50 degrees north cause the most erosion overall.

7

Sediment, wave event intensity and long run scenarios results

This chapter describes the results of all the model runs of the different scenarios described in Chapter 3. The different scenarios contain different wave conditions, different sediment conditions and one long run simulation to assess the requirements of the BSS. These scenarios will answer the secondary research questions. First, the the results of the wave scenarios are discussed, afterwards the results of the sediment scenarios are discussed. Subsequently, the results of the combined effect of both sediment size and wave conditions are described. Finally, the results of the two long runs are presented.

7.1. Wave scenarios

This paragraph describes the results of the different wave scenarios. Three different wave events were selected based on the alongshore transport rates. For every selected event, an intensified and a reduced version of the wave event is made. This is done to assess the sensitivity of wave events on morphology. For all these scenarios the volume changes of the sub-aerial and submerged beach are presented. This shows the influence of the event itself and the impact of the intensified or reduced wave conditions. The impact of each event is then compared to the volume changes of the total simulation.

7.1.1. Results of wave scenarios

The results of the wave scenarios are obtained via brute force simulations and are presented in two ways. The first, is that the morphological effects of the single events are discussed. The second, is that the effects of the events on the total morphology after half a year are described. All these volume changes are calculated per section and per running meter. The differences between the three wave scenario runs determine their effect on the morphological behaviour of the first half year. In addition, the morphological changes induced solely by the events is calculated as well. This means that volume changes are calculated with the bed levels from just before the storm and just after the storm.

First the event characteristics and the volume changes solely induced by the events are described. Secondly, the volume changes on the total morphological behaviour of the BSS is discussed.

Results per wave event

This paragraph discusses the results of morphological changes induced solely by the selected events. The characteristics of the events and the volume changes during the events are described per section and afterwards the volume changes per running meter. The results of the total volume changes per section per event is shown in Table 7.1. These volume changes are used to describe the effects of each of the events. Lastly, a summary of the similarities between the effect of the events is given.

November 2019

The waves of the event of November 2019 are directed from 0° to 80° North. The results of Table 7.1 show that if wave intensity increases, the erosion volume of the sub-aerial beach of the Section 2 increases. On the contrary, Section 1 and 3 show less erosion as wave intensity increases. Section 2 functions as a feeder for Section 1 and 3. Increasing wave power leads to a higher capacity of waves to transport sediment. The eroded sediment of Section 2 ends up partly in Section 1 and 3. In addition, the intensified wave events are causing deposition in the submerged beach for Section 2 and Section 3. The intensified waves have higher orbital

velocities and are capable of transporting more sediment from deeper water to the area of the submerged beach (0 to -10m MSL). For the event of November, it can be concluded that an increase of wave energy is beneficial for spreading sediment from the feeder Section to the adjacent sections. Moreover, reduced wave events show to only reduce the erosion of the sub-aerial beach of Section 2, but increase the erosion for Section 1 and 3.

December 2019
The waves of the event of December 2019 are directed from 10° to 90° North. The event shows similar behaviour as the event in November. Intensified waves are eroding more of the sub-aerial beach of Section 2 and this eroded sediment is spread out to Section 1 and 3. It even leads to accretion of the sub-aerial beach in Section 3. Onshore sediment transport from deeper areas to the submerged beach is less pronounced across Section 2 and 3 compared to the event in November. Moreover, Section 1 is showing more erosion for both the sub-aerial beach and the submerged beach for intensified wave events.

January 2020
The event in January is causing the most erosion across the entire domain of all the events. The event in January is also the longest event as it lasts for 13 days. Wave direction ranges from 10° to 80° North. Similar to the events of November and December the second Section is showing more erosion of the sub-aerial beach and less erosion of the Sub-aerial beach of Section 3 for increased power of wave events. For intensified wave events, large sediment volumes are deposited in the Submerged beach of Section 2 and Section 3, while Section 1 shows large erosion volumes. Another indication that stronger events lead to more sediment spread from Section 2 to Section 3. Section 1 seems to not fully benefit from the feeder mechanism of Section 2 as most of the sediment is transported south.

Summary of events
Summarising the behaviour of the three events leads to the conclusion that intensified waves are causing more erosion of the Sub-aerial beach in front of the Gas terminal (Section 2). This eroded volume is transported mostly in the direction of Section 3 to both the sub-aerial beach and the submerged beach. Therefore, less erosion is observed for Section 3. Section 1 shows a less pronounced behaviour as the effect of the events vary. Mostly this section shows an increase of erosion of the Submerged beach for increased wave events. This sediment is either transported out of the domain or into Section 2.
The secondary research question regarding the behaviour of the Sub-aerial beach under different forcing conditions is partly answered by the results of these three events. Higher waves are more capable of eroding the feeder part of the nourishment and transport this sediment to the sub-aerial beach of Section 3. However, this transport seems to be insufficient compared to the erosive effects of the wave events on Section 3, as a net erosion is still observed for this Section. Only the intensified event of December is capable of accreting Section 3 in the Sub-aerial beach. The sub-aerial beach of Section 1 is not benefiting of the intensified wave events, erosive processes are generally greater for intensified events.

Event	Wave scenario	Section 1 Sub-aerial	Section 1 Submerged	Section 2 Sub-aerial	Section 2 Submerged	Section 3 Sub-aerial	Section 3 Submerged
Nov 2019	Wave events -20%	-1,341	-924	-10,045	+547	-6,684	+1475
Nov 2019	Wave events +0%	-1,266	-5,273	-12,458	-850	-3,313	-767
Nov 2019	Wave events +20%	-1,242	-803	-13,313	+5,394	-9	+21,066
Dec 2019	Wave events -20%	-419	-911	-5,172	-791	-1,880	-294
Dec 2019	Wave events +0%	-485	-4,405	-6,664	-1,850	+223	-953
Dec 2019	Wave events +20%	-639	-7,916	-6,972	+3,235	+3,400	+3,235
Jan 2020	Wave events -20%	-2,113	-1,895	-11,822	+4,190	-12,062	+4590
Jan 2020	Wave events +0%	-1,187	-5,900	-14,342	+3,301	-10,706	+4104
Jan 2020	Wave events +20%	-2,456	-10,198	-15,760	+10,035	-7,532	+21,090

Table 7.1: Absolute volume changes per section for the three different wave scenarios in m^3. The negative sign indicates erosion and the positive sign indicates accretion.

To further analyse the behaviour of the sub-aerial beach volume after the three events, the volume changes per running meter are shown in Figure 7.1a and 7.1c. It further shows the effect of stronger wave events erod-

ing more volume in Section 2 and causing either less erosion or more accretion of the sub-aerial beach in Section 3. In addition, Figure 7.1 shows that morphological changes to the sub-aerial beach are more prominent in Section 2 compared to both Section 1 and 3. Lastly, erosion and accretion patterns maintain similar for all events except for the event in January where less accretive behaviour of the sub-aerial beach is observed overall. The submerged beach shows more accretion for Section 3 if wave events are intensified. Larger amounts of the sub-aerial beach are deposited at lower areas and more sediment from offshore is transported onshore. The wave events are generally transporting sediment southward, therefore erosion is observed in Section 1 as less sediment is provided from Section 2 to the first Section. This further illustrates that more intense events are beneficial for the Sub-aerial beach of Section 3 but not for Section 1.

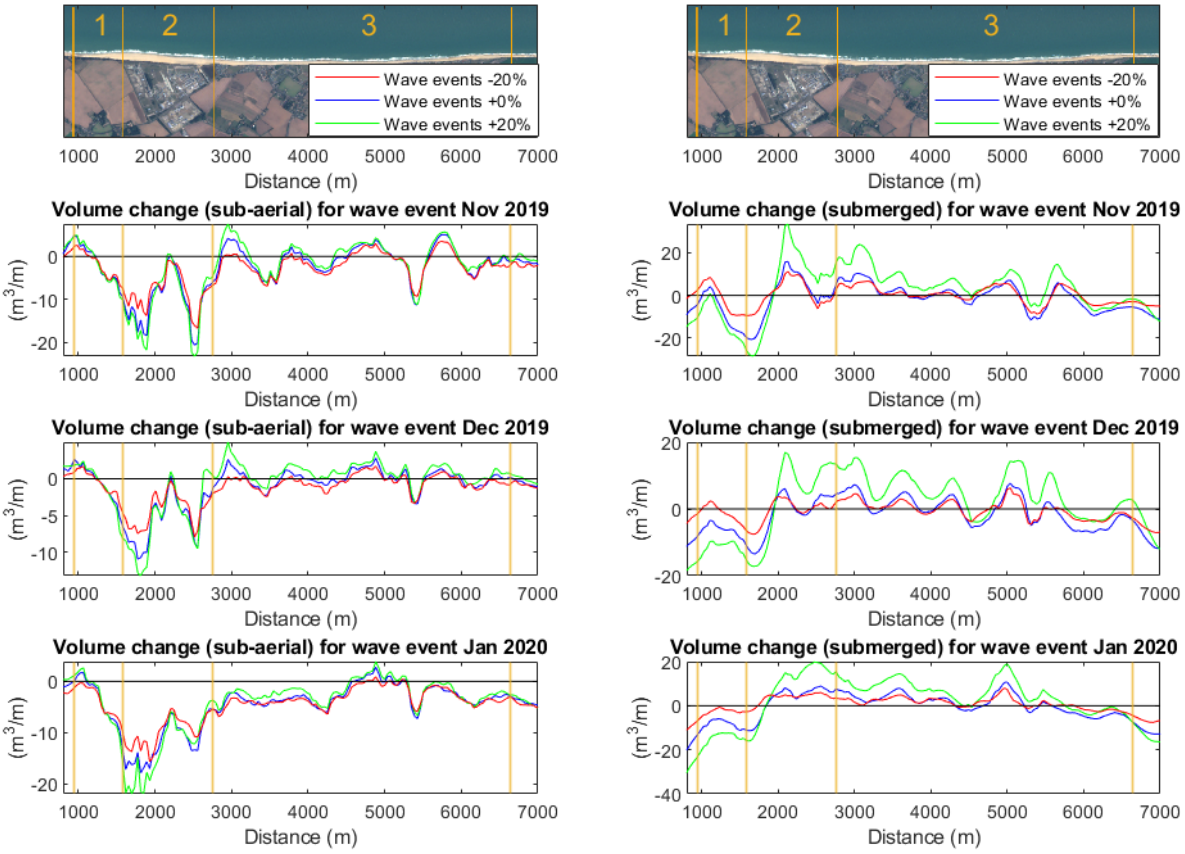

Figure 7.1: The volume changes induced by wave events for different wave intensities for the sub-aerial and submerged beach. In yellow the Section numbers and boundaries are indicated. The top two figures function as a location indicator

Total volume changes

The total volume changes per section determine the total influence of each wave scenario on the total morphological behaviour of the BSS. It shows which sections are most affected by different wave events and shows the total affect of erosion of the sub-aerial beach. Table 7.2 shows these volume changes of the sub-aerial and submerged beach per section for the first half year of the BSS. The table shows that the intensified wave events cause for slightly more erosion of the sub-aerial beach of Section 1 and 2 compared to the reference scenario. As intensified wave events result in higher orbital velocities and higher shear stresses, it is logical that more erosion is caused for the sub-aerial beach in Section 2. However, Section 3 shows less erosion of the sub-aerial beach even though wave events are more dominant. The selected wave events are responsible for the major alongshore sediment transport in the southern direction. Therefore, an increase in wave heights results in more alongshore transport. As Section 2 was designed as the feeder part of the BSS, it is likely that the eroded sediment from Section 2 has transported to Section 3, resulting in less total erosion of the Sub-aerial beach in Section 3. However, the described effects on erosion and sedimentation are only minimal. This small effect is also present for the reduced ware events. Less alongshore transport happens during these events and Section 3 has less sediment input from Section 2.

The submerged beach shows an increase of accretion for both Section 2 and Section 3 for intensified wave

events. As waves move onshore and waves start feeling the bottom, their orbital velocity decreases until waves start breaking where the velocity increases again. The orbital velocity starts dropping around the -10m MSL mark and this leads to sediment deposition in the deeper parts of the submerged beach. Intensified wave events result in more onshore sediment transport and therefore the deposition in the submerged beach is also larger for these events. Calculations happen in depth averaged mode so these effects can still be noticed in deeper waters. On the other side, the submerged accretion of Section 1 decreases as wave events intensify. Possibly, the southward sediment transport route is too powerful to result in more deposition of sediment in Section 1 for the submerged beach. The morphological behaviour of the submerged beach is more affected by the wave event intensity than the sub-aerial beach. However, the aforementioned differences between the wave scenario runs maintain to be minimal, as the alongshore variability is not much affected by different wave event intensity. The individual storm analysis showed larger differences between the individual runs, but the effect on the total morphology is less.

Wave scenario	Section 1 Sub-aerial	Section 1 submerged	Section 2 Sub-aerial	Section 2 submerged	Section 3 Sub-aerial	Section 3 submerged
Wave events -20%	-47,356	+28,165	-139,720	+81,482	-216,240	+139,720
Wave events +0%	-48,255	+15,422	-147,590	+81,923	-214,720	+212,100
Wave events +20%	-48,212	+4,296	-149,140	+100,590	-202,860	+266,790

Table 7.2: Volume changes per section for each wave event. A positive sign indicates accretion and a negative sign indicates erosion.

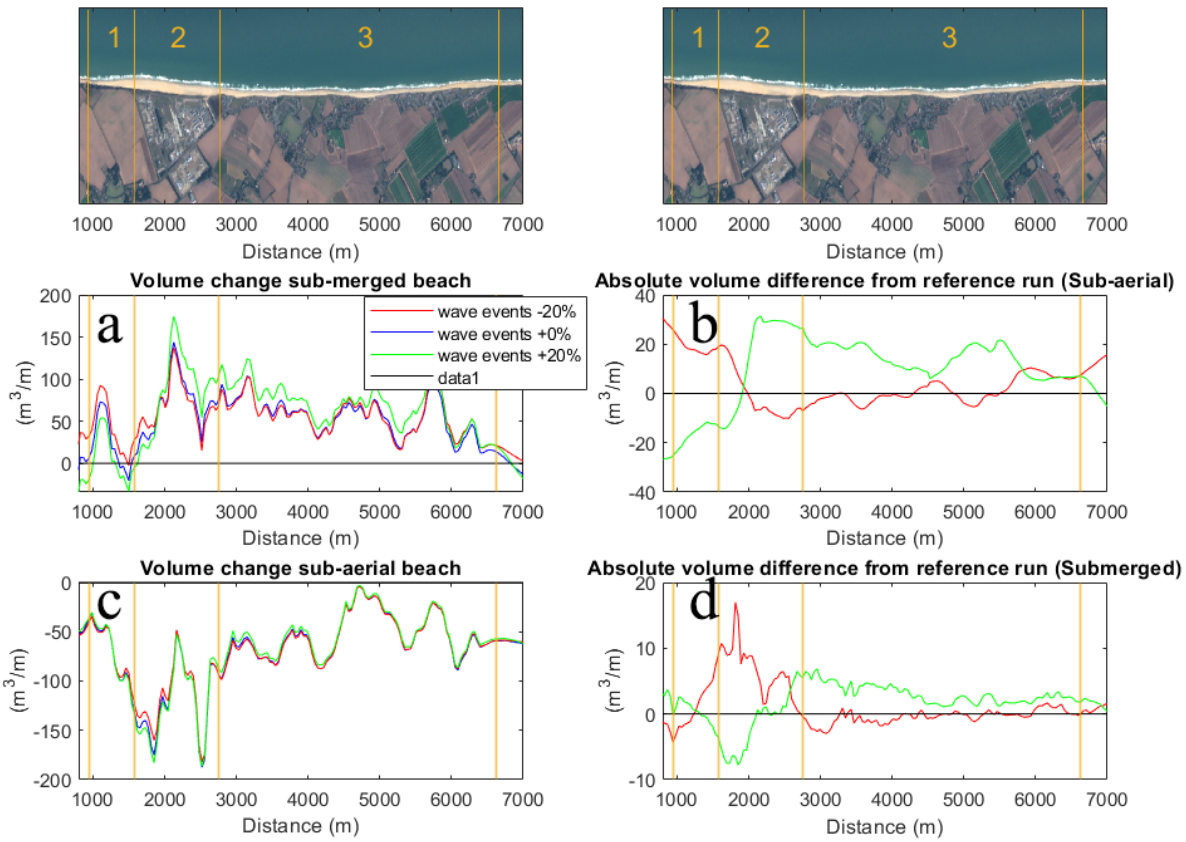

Figure 7.2: a) Volume change of the submerged beach for different wave scenarios. b) The absolute volume differences of the submerged beach for the intensified and reduced wave event compared to the reference wave event. A positive value indicates more accretion and a negative value indicates less accretion c)Volume change of the sub-aerial beach for different wave scenarios. d) The absolute volume differences of the sub-aerial beach for the intensified and reduced wave event compared to the reference wave event. A positive value indicates less erosion and a negative value indicates more erosion. In all figures the section numbers and boundaries are indicated in Yellow. The top two figures function as a location indicator

The absolute volume differences from Figure7.2b and 7.2d further illustrate that intensified events are

transporting the eroded sediment from Section 2 to Section 3, both for the submerged beach as the sub-aerial beach. Reduced wave events are less eroding the sub-aerial beach of Section 2 but do not show a benefit to Section 3. Section 1 seems to benefit more from the reduced wave events as accretion is observed for the submerged beach. The reduced wave events reduce the alongshore transport in southward direction and can therefore also explain the increase in sediment deposition in Section 1, as this section is located northward.

The submerged beach shows marginally more accretion for Section 2 and Section 3 as waves intensify, indicating the earlier described behaviour of onshore sediment deposition from deeper parts of the submerged beach. On the contrary, the accretion of the submerged beach of Section 1 is slightly increasing when wave events are reduced. The reduced wave events provide less transport southward and allows for more sediment deposition in Section 1 than for rougher conditions. To conclude, intensified wave events are slightly increasing the feeder mechanism of Section 2, since sediment is fed to Section 3. The sub-aerial beach volume shows some dependence on the intensity of the events for all sections, but the net effect is still not very large.

7.2. Sediment scenarios

This paragraph discusses the effect of sediment grain size on the morphological behaviour of the BSS. Again the total volume and the volume changes per running meter are discussed. The events from the previous paragraph are not incorporated in the sediment analysis, as the combination of sediment and events is discussed in a later paragraph. This results solely in the effect of sediment grain size on the erosion and sedimentation patterns. The total volume changes for different grain sizes is shown in Table 7.3. The results show a slight decrease in erosion of the sub-aerial beach for all sections for an increase in grain size. Sub-aerial beach volume changes of Section 3 are the least affected by the grain size and the largest volume changes are observed for Section 1.

Grain size Grain size	Section 1 Sub-aerial	Section 1 Submerged	Section 2 Sub-aerial	Section 2 Submerged	Section 3 Sub-aerial	Section 3 Submerged
300	-50,467	+11,387	-150,600	+82,269	-217,160	+212,110
350	-48,255	+15,422	-147,590	+81,923	-214,720	+212,100
400	-46,490	+17,054	-144,270	+80,629	-210,920	+210,390

Table 7.3: Absolute volume changes per section for the three different grain sizes

Smaller grain sizes are getting easier into suspension. This results in more erosion of the sub-aerial beach in all sections. However, the smaller grain size also results in a lower settling velocity in the water column. The sediment deposits in deeper water and therefore higher accretion is observed for the submerged beach. For larger grain sizes it takes more effort to get into suspension but settling velocity increases. Therefore, the increased grain size is eroding less and also depositing less in lower areas of the submerged beach, since the sediment is more likely to sink to the bottom at higher velocities than for a sediment with a lower settling velocity. However, the observed differences are very small and are having less effect on the morphological behaviour than the wave event intensity. Showing that grain size is even less important.

Figure 7.3 shows volume changes per running meter for the three different sediment classes. For the sub-aerial beach a larger grain size is always less eroding than a smaller grain size for all sections. No clear pattern is found for the submerged beach as erosive and accretive patterns switch around in the sections themselves and is likely to be affected by local bathymetry. For the submerged beach of Section 1 a clear pattern is found, a smaller grain size reduces the accretion of the submerged beach and a larger grain size increases the accretion. However, all the changes are again very small and the model predicts that the effect of grain size is insignificant for the morphological development of the nourishment.

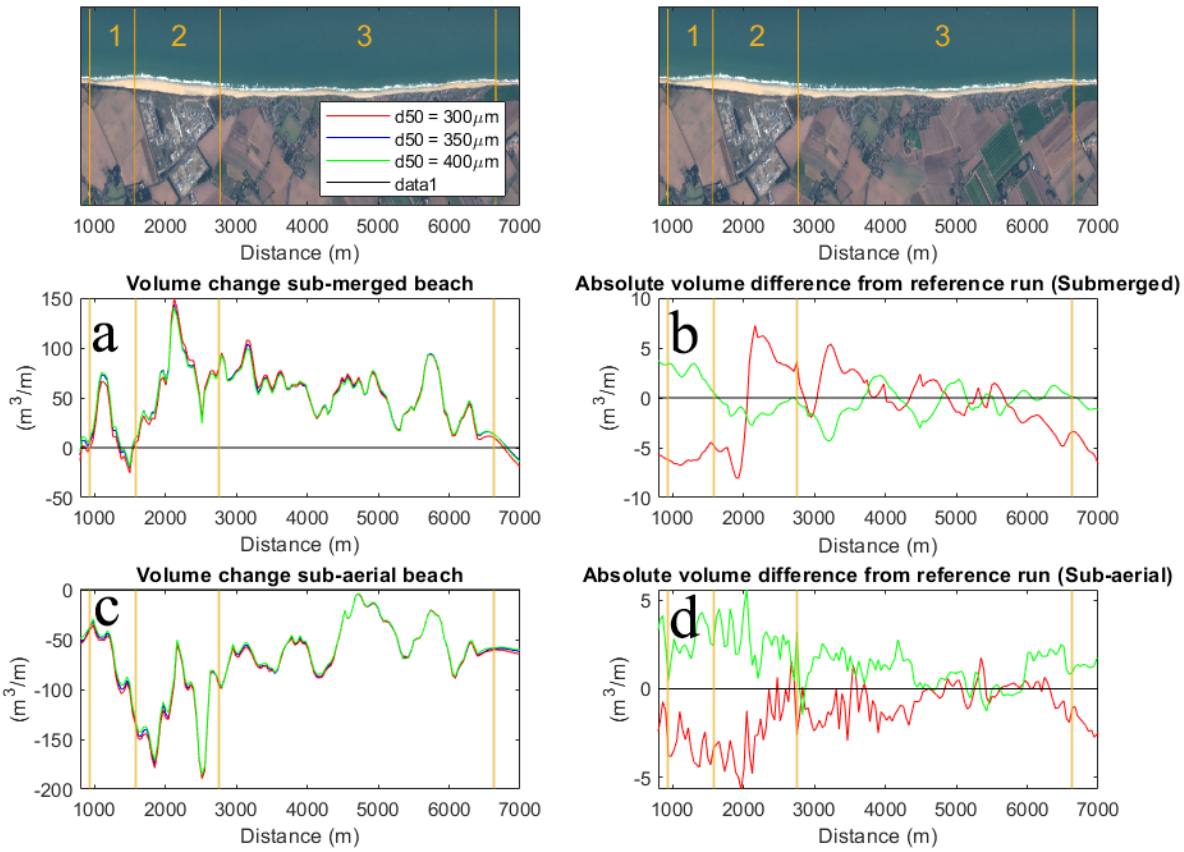

Figure 7.3: a) Volume change of the submerged beach for different sediment scenarios. b) The absolute volume differences of the submerged beach for 300 μm and 400 μm compared to the reference grain size (350 μm). A positive value indicates more accretion and a negative value indicates less accretion or more erosion. c) Volume change of the sub-aerial beach for different wave scenarios. d) The absolute volume differences of the sub-aerial beach for 300 μm and 400 μm compared to the reference grain size (350 μm). A positive value indicates less erosion and a negative value indicates more erosion.. In all figures the section numbers and boundaries are indicated in Yellow. The top two figures function as a location indicator

7.3. Conclusion Sediment and Wave event intensity scenarios.

The sensitivity of wave event intensity and grain size is a secondary objective of this thesis. The result of the individual sensitivity of wave event intensity and grain size showed to have minimal effect on the alongshore variation of the BSS. The combined runs show no significant difference from these results. Therefore, the results of the combined sediment and wave runs are presented in Appendix F. It is therefore, concluded that both grain size and wave event intensity do not significantly affect the morphology of the BSS.

7.4. Long run scenarios

This paragraph describes the results of the two long run scenarios. The requirements from Table 7.4 are assessed for both runs and an answer to the last secondary research question is obtained. The requirements that are checked in these results are the following:

Table 7.4: Requirements

Section 1	Section 2	Section 3
1. No requirement	1. Maintain a beach width of 20 m at +7m MSL 2. No erosion at the toe of the cliffs, therefore the water level may not reach the toe of the cliffs	1. No erosion at the toe of the seawall

First the requirements of Section 2 are discussed. Secondly, the requirements of Section 3 are discussed. To evaluate the beach width at +7m MSL cross-section are taken from the model results at a yearly interval. The cross-section locations are shown in Figure 7.6. The results for the long run scenarios for the cross-section in Section 2 is shown in Figures 7.4 and 7.5.It is observed that after 5 years of simulation the BSS has disappeared completely according to the model. After a year of simulation a steep scarp has formed and this scarp keeps moving in onshore direction. The model predicts a very rapid movement of the scarp of around 25 meters a year. There seems to be no slowdown in this movement and erosion happens at a constant rate. Across the rest of Section 2, similar behaviour is observed when analysing other cross-sections.

The expected lifetime of the BSS is calculated to be 15 years. The predicted lifetime by Delft3D is much shorter and it seems that Delft3D is therefore over predicting the erosion rate. The Delft3D model is not calibrated for longer term periods and therefore the simulation result should be regarded in a conservative way.

In addition, the same model run is performed with a ThetSed parameter of 0.5. This is to evaluate the influence of this parameter on the onshore movement of the scarp. The result of this run is shown in Figure 7.5. The Figure shows a slower movement of the scarp in onshore direction. The onshore movement is now 17 meters a year. 7.5.

The second requirement for Section 2 assesses the water level at the base of the cliff. During the simulation, the water level is not able to reach the cliff toe as the scarp formation is too high for run-up to reach the base of the cliffs. However, after 5 years the water level is obviously able to reach the cliffs as the base of the cliff is now located at -1m MSL.

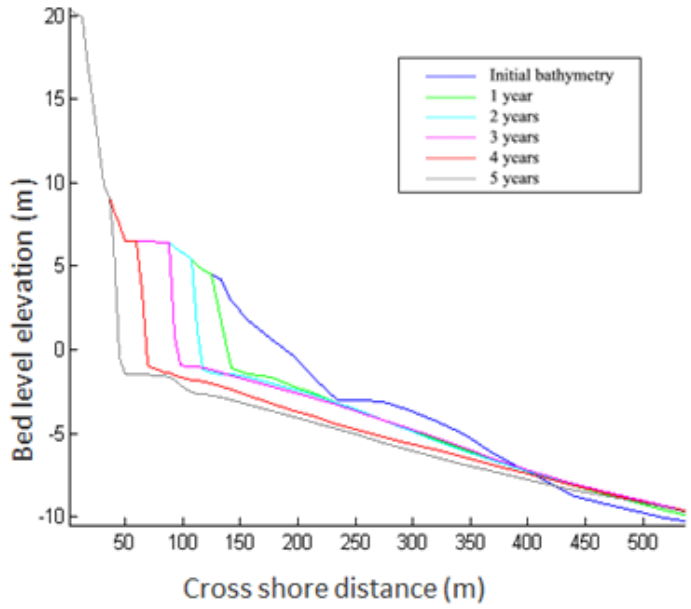

Figure 7.4: Cross-sections per year in Section 2. Simulation with a Thetsed = 1.

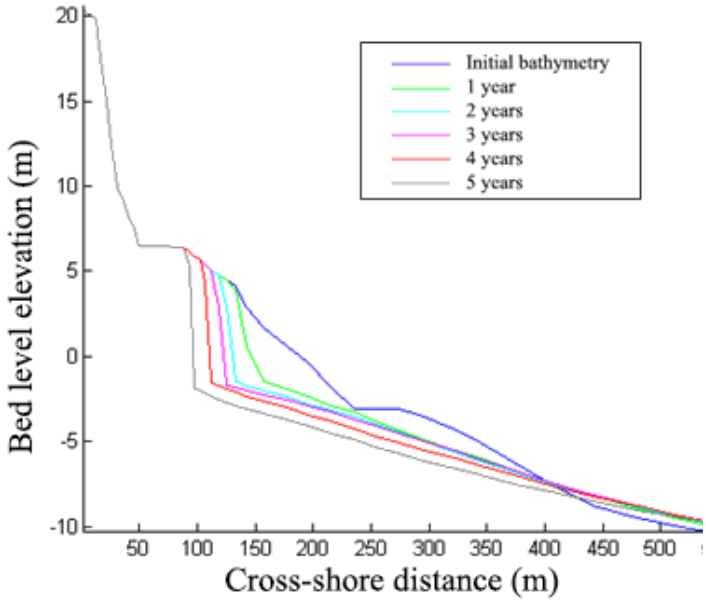

Figure 7.5: Cross-sections per year in Section 2. Simulation with a Thetsed = 0.5.

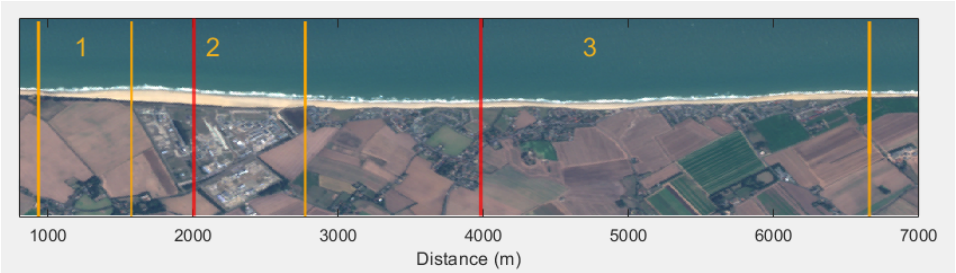

Figure 7.6: Location of the cross-sections in Section 2 and Section 3

A similar analysis is performed for Section 3. The cross-sections are analysed to show if erosion has reached the toe level of the seawall. A similar pattern is observed here, the sub-aerial beach is eroding and most of the beach has eroded after 2 years of simulation. Another model run is performed with ThetSed of 0.5 and the erosion rate is significantly slower as the seawall is now reached after 4 years. The results of the runs are shown in Figure 7.7 and 7.8.

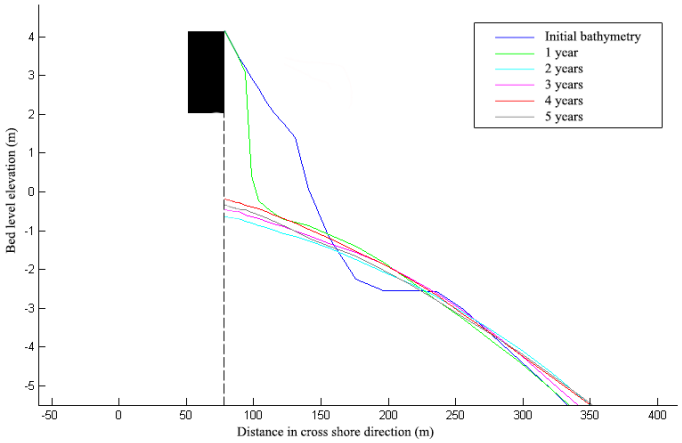

Figure 7.7: Cross-section of Section 3 for every year of the model run with ThetSed = 1. The black box indicates the location of the seawall

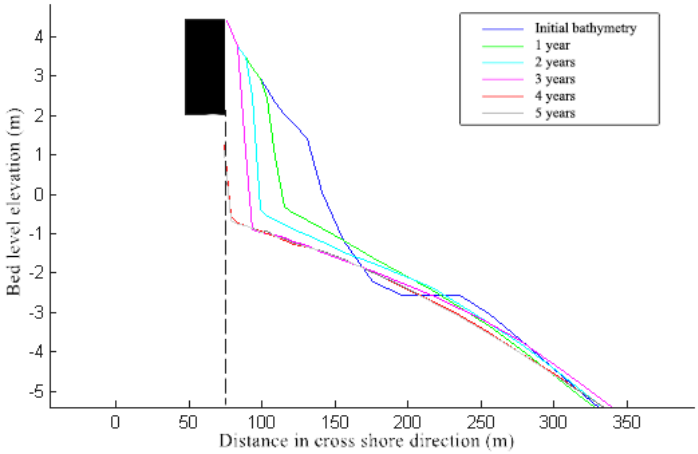

Figure 7.8: Cross-section of Section 3 for every year of the model run with ThetSed = 0.5. The black box indicates the location of the seawall

7.5. Concluding remarks

This chapter discussed the results of the scenarios to answer the secondary research questions. The sediment and wave event scenarios showed that the BSS model is very robust. Grain size and wave event intensity seem to have a minor impact on the morphological prediction. The alongshore variation is similar for all different scenarios and the differences are mostly a small percentage of the local erosion or sedimentation. The long run scenarios showed that the model predicts much shorter lifetime than initially expected. The model seems to be sensitive to the ThetSed parameter and more calibration and validation is necessary to allow for better long term simulations.

8

Discussion

Before the start of this thesis, the morphological response of the BSS was still unknown. Moreover, only a 1D model was available to assess and predict the morphological behaviour. This thesis provided more insight in the morphological behaviour of the first half year and a numerical model was created using Delft3D. This depth averaged (2DH) model allows for the assessment of more complex morphological behaviour, which was not possible with the use of a 1D model only. This chapter aims to reflect on the entire numerical modelling process. Results and model settings are compared to other modelling studies and it is assessed how this study can contribute to new modelling studies regarding feeder nourishments. In addition, the effect of model simplifications and assumptions on the model results are discussed.

8.1. Model's strengths and value

This paragraph describes the strengths of the model and how the model can be used as a valuable asset in the future. The two main strengths of the model are highlighted and an explanation on how this strength adds value to the BSS project and future nourishments.

1. Sub-aerial beach volume prediction
   The biggest strength of the model is its capability to simulate the volume changes of the sub-aerial beach. It follows the alongshore variability very well and the cross-shore interaction found in the surveys is also traced back in the model results. The model's ability to predict the sub-aerial beach with this accuracy provides more confidence in the ability of Delft3D to simulate future feeder nourishments. The Delft3D model gives more insight in the alongshore morphology of the BSS, which could not be captured by the 1D model that was present before the start of this thesis. The model can now be used to further analyse the behaviour of forcing conditions on the morphological behaviour. The model gives more insight in what happens between all the surveys and can be used in the future as well, when new surveys are conducted.

2. Robustness of the model
   The results of the sediment and wave event intensity scenarios showed that the model is robust. Changes in sediment grain size and wave event intensity showed to have limited effect on the alongshore variation of the morphological behaviour. Moreover, erosion or sedimentation increased/decreased locally in a predictable way and were not significantly different from the reference run. This shows that the model is robust and that the end result of the model simulation is highly dependent on the forcing conditions during the entire simulation. In addition, it shows that the model is not very sensitive to small adjustments, which makes it more valuable in analysing the behaviour.

8.2. The BSS compared to other studies

This paragraph discusses the results of the BSS study to other studies. It compares the use of wave calibration parameters and the morphological changes to the waves.

- Morphological effect due to waves: The BSS model predicted that 57% of the total erosion observed in Section 2 was caused by significant wave heights lower than 1m (entering the model at a depth of -14m MSL). An important finding from Luijendijk et al. [27]for the Sand Engine at the Delfland coast, is that 60% of the observed erosion was caused by the 12 largest high energy wave events during the first year. In this study, these events have a total duration of roughly 30 days. The highest wave events for the

BSS that take up 34 days of time cause only 36% of the observed erosion for a half year simulation. At the Delfland coast, the average significant wave heights for these events are typically higher than 2m, with the highest average significant wave height of 3.7m. However, for the BSS average significant wave heights are typically lower than 2m and certainly not higher than 3m. This could well be the explanation for the lower dependence of erosion on the high energy wave events at the Bacton coast. This means that average conditions play a more important role as well.

- Calibration factors for transport by waves: The factor for suspended transport by waves (SUSw) and the factor for bed-load transport by waves (BEDw) are important parameters for modelling coastal morphology, as they determine the sediment transport by waves. In a 2DH model, wave undertow is largely under predicted due to the depth averaged velocity calculation. Therefore the onshore sediment transport by waves is not balanced by the return current, which transports sediment in offshore direction. A reduction of the SUSw and BEDw lead to less onshore sediment transport and seem to be the most viable options. In the study of Luijendijk et al. [27], values of 0.20 for both SUSw and BEDw were used to obtain optimal results. In shoreface nourishment studies of Walstra et al. [46] and Grunnet et al. [14], a value of 0.3 for SUSw was used to reduce the onshore transport by waves. In this thesis, a value of 0.35 was used for both SUSw and BEDw, which is similar to the other studies, but slightly higher. This is an indication that the default values of 1 are not applicable for coastal application and also feeder nourishments. Values between 0.2-0.4 give in general better predictions.

8.3. Discussion on survey analysis

A large net sediment input of 200,000 m^3 was observed for the period of August 2019 - October 2019. However, the sediment volume seemed to be on the high side, especially considering the net sediment input for the period October 2019 - March 2020, as it is a factor 10 smaller (20,000 m^3) than for the period August 2019 - October 2019. Possible reasons for this input were identified as cliff erosion and measurement inaccuracies of the first survey in August. In literature a value of 400.000 m^3 cliff erosion is mentioned, but this seems to be an unrealistic value as this would result in major cliff line retreat across the entire coast from Cromer up until Bacton (20km distance) each year. It is much more likely that a combination of a smaller cliff erosion event and measurement errors are the cause for the observed accretion in the submerged beach (see paragraph 5.4 for a more thorough explanation on these possible measurement errors). The observed net sediment input is limited to the area of the submerged beach. This means that sub-aerial beach measurements are unaffected. Therefore, the model results of the sub-aerial beach are also unaffected by these possible survey errors.

8.4. Model simplification choices

The BSS model has several limitations regarding its capacity to predict the bed levels at the end of the simulation. The simplifications of the model are listed below and the effect of the limitations on the model outcome is discussed as well.

- Groynes
  A vast amount of wooden groynes is present at the coast of Bacton. During construction these groynes were largely buried by the nourishment. Therefore, their effect on the nourishment's behaviour is assumed to be of less importance. Moreover, the groynes are largely open wooden structures that let sediment pass through. However, on the long term these groynes could start playing a larger role as more sediment starts to erode from the nourishment and groynes could become visible again and affect the morphological behaviour. This would influence the alongshore transport rates and also affect the feeder behaviour, since part of the sediment transport is being blocked by the groynes. However, the BSS model shows a good agreement between the modelled alongshore variability of erosion compared to the measurements. The effect of the groynes seems to be minimal in this first half year. Especially, considering that the groynes are not incorporated in the model.

- Grid resolution
  The BSS model has a grid resolution of 17 meters in cross-shore direction and 40 meters in alongshore direction. To put this into perspective: the nourishment has a length of 6 kilometers and a width of just 100 meter up until the +0 MSL mark. The dry beach of the nourishment consists therefore only of about 6 to 8 grid cells in cross-shore direction. This limits the accuracy of predicting the exact bed levels at higher levels of the dry beach. This limitation does not influence the outcome of the first half

year significantly, as volume prediction are in line with the observations. However, for future longer simulations the grid resolution may not satisfy as the sub-aerial beach will consist of too few grid cells.

- Storm surge level
  Storm surge levels are not incorporated in the Delft3D model of the BSS, since no surge level data is available. This means that high storm surge levels during the first half year are not taken into account. This could be an explanation on why in reality more erosion on higher parts of the sub-aerial beach is observed. The erosion on the higher sub-aerial beach is now largely determined by the ThetSed parameter as the water levels are not reaching the higher elevations. It is assumed that the storm surge levels are not of major importance for the first half year as the model is well able to predict the volume changes of the sub-aerial beach. This would definitely not be the case if storm surge levels played an important role.

- Uniform sediment class
  The coastal area of Bacton consists of different sediment classes that vary in cross-shore direction of the coast. Grain sizes are ranging from 200 μm at the base of the cliffs to 450 μm at the foreshore. It was chosen to use a uniform grain size in the Delft3D software, which implicates that grain size sorting mechanisms are not included. It was chosen to do so, since adding sediment fractions adds to the computational time as well as the complexity of the model. Moreover, no sediment samples were taken during post construction surveys, which makes validating a non uniform sediment model much harder, as this would require sediment size distributions of the entire area. On the other hand, the sediment scenario's showed that changing the grain size was not influencing the morphological behaviour of the BSS significantly. It is therefore expected that the choice for a uniform sediment class for the entire area is not affecting the total outcome in a significant way.

9 Conclusions

This research has assessed the morphological behaviour of the first half year of the BSS with the use of survey data. This gave insight in the initial morphological response of the BSS. With this knowledge, a morphological model was set up with the use of Delft3D. It was assessed how Delft3D is capable of simulating the first half year. This gives an answer to the main research questions of this thesis. The research questions with the answers are listed below.

1. What is the morphological response of the BSS in the first half year?
   During the first half year, mainly erosion is observed for the sub-aerial beach and accretion is observed for the submerged beach. The erosion of the sub-aerial beach has led to a scarp formation in Section 2 in October. The scarp continued to grow in height from October 2019 to March 2020 until a height of 4 meters. Besides the scarp formation, beach flattening was observed for the entire alongshore stretch.

   The erosion observed in the first six weeks is 4.5 times higher than the months following. This shows a strong initial response of the BSS. Especially considering the winter period with higher wave conditions. The accretion of the submerged beach also decreased in this period.

   A cross-shore link between the morphological behaviour of the sub-aerial and submerged beach is found. Higher local erosion of the sub-aerial beach is coupled with lower accretion of the submerged beach. Likewise, lower local erosion of the sub-aerial beach is coupled with higher accretion of the submerged beach. Alongshore variability is observed as Section 2 shows the highest erosion of the sub-aerial beach and Section 1 and 3 show on average less erosion.

2. How well is Delft3D at simulating the morphological behaviour of the BSS?

   The BSS model is well able to simulate sub-aerial and submerged beach volume changes. A Brier skill score is obtained of 0.82 and 0.76, respectively. Both predictions scored in the excellent range [39]. The alongshore variability was very comparable to the measurements and the same cross-shore link was found as well. The model slightly under predicted the exact coastline retreat, but the erosion of the higher dry beach was still represented well enough by the model with the use of the ThetSed parameter set to 1 (allowing for dry cell erosion). On the other hand, submerged beach accretion is under predicted. However, the alongshore variability of the sedimentation of the submerged beach is again very well represented. Furthermore, the model is less able to predict exact bed levels due to grid size resolution and Delft3D's capabilities to exactly represent cross-shore profiles. However, a reasonable to almost good score is still obtained.

   The wave event intensity and grain size scenarios showed that the BSS model is robust and is not very sensitive to changes of the three major wave events and of grain size. The scenarios showed almost no effect on the alongshore variability of the nourishment and only showed an increase in erosion or sedimentation across the entire alongshore stretch.

Besides the two main research questions, there were two secondary research questions. These are answered below:

1. What is the sensitivity of wave event intensity and grain size on the morphological behaviour of the BSS?

   Wave event intensity is affecting the alongshore transport of the feeder nourishment. The effect is mostly noted when observing the differences before and after the storm events. However, the effect

of wave event intensities on the final bed levels of the BSS are insignificant.
Grain size determines the rate of erosion; a smaller grain size gets easier into suspension and therefore leads to more erosion overall. However, the effect is even less than the effect of wave event intensity. Erosion is only slightly enhanced for a smaller grain size and slightly reduced for a larger grain size. This shows that grain size is not an important parameter for the alongshore behaviour of a feeder nourishment.

2. Do the functional requirements of the nourishment still hold at the end of the design lifetime?

   For the long run scenario, it is observed that the beach width requirement in front of the gas terminal is not met at the end of fifteen years. According to the model, the majority of the nourishment has eroded after five years. In addition, the model predicts a more rapid erosion in front of the seawall. The model prediction has to be regarded in a conservative way, as the model has not yet been validated and calibrated for longer periods of time. A possible seasonal behaviour has not been evaluated during validation. Moreover, the erosion of the nourishment seems to be highly dependent on the ThetSed parameter and future measurements can indicate the exact value of this parameter. Luijendijk et al. [26] showed that erosion of a mega feeder nourishment slowed down after the first year of construction. The BSS model does not show this behaviour for now and could therefore lead to a conservative estimate of the lifetime of the BSS. It is therefore considered as a worst case scenario.

10 Recommendations

This chapter discusses recommendations for the BSS project itself, the BSS model improvements, requirement assessment and future feeder nourishments.

10.1. Sediment budget assessment

The analysis of the surveys showed that a large amount of sediment has transported into the system. Several causes of this sediment input were given, but it still remains highly unlikely that this large amount of sediment has transported into the system in such a short amount of time. Further surveys should point out whether the amount of sediment input is justified or that the cause is due to errors made in the first survey. It is therefore, very important to identify and further research the cause of this sediment input. If the cause lies outside the system (e.g. cliff erosion events outside the domain), their input should be added to the numerical model via a sediment boundary conditions. A sediment boundary condition could force a different sediment concentration at the boundary, which could add a net influx to the system.

10.2. Model Improvements

1. *Include groynes if they show to affect the morphological behaviour of the BSS*
   The groynes that are present in this coastal system are left out of the numerical model as their effect on the morphology was assumed negligible. However, if they show to affect the morphological behaviour of the BSS they could be included in the Delft3D model in the future.

2. *Increase grid size resolution of the sub-aerial beach in cross-shore direction*
   Increasing the grid size resolution of the sub-aerial beach in cross-shore direction for longer simulations increases the accuracy of the model. As the sub-aerial beach starts eroding more, the amount of grid cells representing this area is decreasing. At a certain point the sub-aerial beach is represented by too few grid cells to predict volume changes accurate enough. Increasing the grid size of the entire model would come at great computational costs and it is therefore advised to only increase the grid size resolution for the sub-aerial beach area.

3. *Apply more efficient acceleration techniques for the long term scenarios*
   For this thesis the Brute Force Filtered technique in combination with a morfac is used for the long run scenarios. This results in an 8 times faster simulation compared to a standard Brute force simulation. This simulation time could even be reduced further if the Brute force merged [26] technique is used. This is strongly recommended if more long term runs are required to asses the morphological behaviour. For the short term simulations this method is not necessary.

10.3. Model performance

1. *Asses model performance in the future*
   It is advised to further assess the model's performance when future surveys are performed. This will show if the model still performs satisfactory for longer periods than the first half year of the BSS. With these future measurements the model can be fine tuned to match these surveys. It is essential to check the calibration parameters that influence the alongshore transport as well as the calibration parameter for dry cell erosion. The alongshore transport of the area is still uncertain and future surveys can provide more insight. The calibration parameters will largely determine the rate of erosion of the BSS.

If the model skill is still scoring high enough, it is an indication that the model is very well suitable for longer time simulations. This will enlarge the reliability of the model to predict the expected lifetime of the BSS as well as the need for future renourishments.

2. *Enhance the model's performance for the submerged beach.*
   It is advised to further enhance the model's capability to predict volume changes of the submerged beach. Future measurements could provide more insight in the sediment budget and accuracy for the submerged beach could be increased.

10.4. Future feeder nourishments

This paragraph discusses two recommendations regarding the design and modelling of future feeder nourishments.

1. Feeder nourishment calibration
   The BSS numerical model used wave calibration parameters similar to studies of Luijendijk et al. [27] andWalstra et al. [46] in the Netherlands. This resulted in a very good performance of the BSS model. The assumption that wave calibration parameters are more or less independent from site specific conditions could improve the calibration procedure of future (feeder) nourishment model studies. It is advised to use wave calibration parameters in the range of 0.2-0.4 in future studies, to further investigate if this is indeed true.

2. Feeder nourishment design parameters
   The results of the sediment and wave event intensity scenarios showed that grain size and wave event intensity are not affecting the morphology of the BSS significantly. Only minor changes in the cross-shore direction are observed and almost no alongshore variation are caused by grain size and wave event intensity. Therefore, it is advised to not focus on the grain size diameter and wave event intensity in future feeder nourishment design phases.

10.5. Assessing requirements

1. *Change all functional requirements to volume based requirements*
   The requirement in front of the gas terminal is based on the exact beach width at +7m MSL. However, the constructed nourishment shows levels that vary between +7m and +6m MSL. This makes it harder to define the beach width at one exact level. Moreover, the starting point and end point of this beach width may become harder to define when time progresses. Parts of this higher beach may erode due to aeolian transport and also a gradual slope may occur at this beach. It is not clear if a total lowering of the beach in front of the gas terminal is allowed or where the end of the beach at +7m is defined. Changing these conditions to a certain volume loss per running meter makes it easier to assess the entire domain and also makes it better to evaluate the requirements using the Delft3D model. Volume changes are independent of the exact beach height and are therefore less subjective. Also, the model scores excellent at volume changes and is less accurate at exact bed levels. The model could then also assess the requirement at a volume base, which would be more accurate than the current cross-shore profile analyses

Bibliography

[1] About Bacton gas plant. https://www.shell.co.uk/about-us/meeting-todays-demands/processing-oil-and-gas/bacton-gas-plant/about-bacton-gas-plant.html. [Online; accessed 18-11-2019].

[2] Living with coastal erosion in europe: Sediment and space for sustainability. part i - major findings and policy recommendations of the eurosion project. service contract b4-3301/2001/329175/mar/b3 "coastal erosion – evaluation of the need for action", 2004.

[3] Bacton sand engine monitoring, field report t1, w201806-04 uk bactonsandengine, 2019.

[4] Bacton sand engine monitoring, field report t0, w201806-04 uk bactonsandengine, 2019.

[5] J. Bosboom, A.J.H.M. Reniers, and A.P. Luijendijk. On the perception of morphodynamic model skill. *Coastal Engineering*, 94:112 – 125, 2014. ISSN 0378-3839. doi: https://doi.org/10.1016/j.coastaleng.2014.08.008.

[6] Judith Bosboom and Marcel .J.F Stive. *Coastal dynamics I, lecture notes CIE4305*. Delft Academic Press, 2015. ISBN 978-90-65662-3720.

[7] S.M. Brooks and T. Spencer. Temporal and spatial variations in recession rates and sediment release from soft rock cliffs, suffolk coast, uk. *Geomorphology*, 124(1):26 – 41, 2010. ISSN 0169-555X. doi: https://doi.org/10.1016/j.geomorph.2010.08.005.

[8] N.E. Carpenter, M.E. Dickson, M.J.A. Walkden, R.J. Nicholls, and W. Powrie. Effects of varied lithology on soft-cliff recession rates. *Marine Geology*, 354:40 – 52, 2014. ISSN 0025-3227. doi: https://doi.org/10.1016/j.margeo.2014.04.009.

[9] K.M. Clayton, I. Mccave, and Christopher Vincent. The establishment of a sand budget for the east anglian coast and its implications for coastal stability. institution of civil engineers (eds) shoreline protection. proceedings of a conference organised by the institution of civil engineers, university of southampton, 14–15 september 1982. thomas telford. *London*, pages 63–68, 01 1983.

[10] H.J. de Vriend, M. Capobianco, T. Chesher, H.E. de Swart, B. Latteux, and M.J.F. Stive. Approaches to long-term modelling of coastal morphology: A review. *Coastal Engineering*, 21(1):225 – 269, 1993. ISSN 0378-3839. doi: https://doi.org/10.1016/0378-3839(93)90051-9. Special Issue Coastal Morphodynamics: Processes and Modelling.

[11] Huib J. de Vriend, Mark van Koningsveld, Stefan G.J. Aarninkhof, Mindert B. de Vries, and Martin J. Baptist. Sustainable hydraulic engineering through building with nature. *Journal of Hydro-environment Research*, 9(2):159 – 171, 2015. ISSN 1570-6443. doi: https://doi.org/10.1016/j.jher.2014.06.004. Special Issue on Environmental Hydraulics.

[12] Robert George Dean and Chul-Hee Yoo. Beach-nourishment performance predictions. *Journal of waterway, port, coastal, and ocean engineering*, 118(6):567–586, 1992.

[13] Ye Yincan et al. Chapter 7 - coastal erosion. In Ye Yincan et al, editor, *Marine Geo-Hazards in China*, pages 269 – 296. Elsevier, 2017. ISBN 978-0-12-812726-1. doi: https://doi.org/10.1016/B978-0-12-812726-1.00007-3.

[14] Nicholas M. Grunnet, Dirk-Jan R. Walstra, and B.G. Ruessink. Process-based modelling of a shoreface nourishment. *Coastal Engineering*, 51(7):581 – 607, 2004. ISSN 0378-3839. doi: https://doi.org/10.1016/j.coastaleng.2004.07.016. URL `http://www.sciencedirect.com/science/article/pii/S0378383904000729`.

[15] Christopher Hackney, Stephen E. Darby, and Julian Leyland. Modelling the response of soft cliffs to climate change: A statistical, process-response model using accumulated excess energy. *Geomorphology*, 187:108 – 121, 2013. ISSN 0169-555X. doi: https://doi.org/10.1016/j.geomorph.2013.01.005.

[16] Jim W Hall, Ian C Meadowcroft, E.Mark Lee, and Pieter H.A.J.M van Gelder. Stochastic simulation of episodic soft coastal cliff recession. *Coastal Engineering*, 46(3):159 – 174, 2002. ISSN 0378-3839. doi: https://doi.org/10.1016/S0378-3839(02)00089-3.

[17] L Hamm, M Capobianco, H.H Dette, A Lechuga, R Spanhoff, and M.J.F Stive. A summary of european experience with shore nourishment. *Coastal Engineering*, 47(2):237 – 264, 2002. ISSN 0378-3839. doi: https://doi.org/10.1016/S0378-3839(02)00127-8. Shore Nourishment in Europe.

[18] H Hanson, A Brampton, M Capobianco, H.H Dette, L Hamm, C Laustrup, A Lechuga, and R Spanhoff. Beach nourishment projects, practices, and objectives—a european overview. *Coastal Engineering*, 47 (2):81 – 111, 2002. ISSN 0378-3839. doi: https://doi.org/10.1016/S0378-3839(02)00122-9. Shore Nourishment in Europe.

[19] John B. Herbich and Tom Walters. *WAVE CLIMATEWave climate*, pages 922–922. Springer US, Boston, MA, 1987. ISBN 978-0-387-30749-7. doi: 10.1007/0-387-30749-4_195. URL `https://doi.org/10.1007/0-387-30749-4_195`.

[20] W. S. Jäger and O. Morales Nápoles. A vine-copula model for time series of significant wave heights and mean zero-crossing periods in the north sea. *ASCE-ASME Journal of Risk and Uncertainty in Engineering Systems, Part A: Civil Engineering*, 3(4):04017014, 2017. doi: 10.1061/AJRUA6.0000917.

[21] E.M. Lee. Coastal cliff behaviour: Observations on the relationship between beach levels and recession rates. *Geomorphology*, 101(4):558 – 571, 2008. ISSN 0169-555X. doi: https://doi.org/10.1016/j.geomorph.2008.02.010.

[22] Laura Lemke and Jon K. Miller. Eof analysis of shoreline and beach slope variability at a feeder beach constructed within a groin field at long branch, new jersey. *Coastal Engineering*, 121:14 – 25, 2017. ISSN 0378-3839. doi: https://doi.org/10.1016/j.coastaleng.2016.11.001.

[23] G.R. Lesser, J.A. Roelvink, J.A.T.M. van Kester, and G.S. Stelling. Development and validation of a three-dimensional morphological model. *Coastal Engineering*, 51(8):883 – 915, 2004. ISSN 0378-3839. doi: https://doi.org/10.1016/j.coastaleng.2004.07.014. Coastal Morphodynamic Modeling.

[24] Patrick W. Limber, A. Brad Murray, Peter N. Adams, and Evan B. Goldstein. Unraveling the dynamics that scale cross-shore headland relief on rocky coastlines: 1. model development. *Journal of Geophysical Research: Earth Surface*, 119(4):854–873. doi: 10.1002/2013JF002950. URL `https://agupubs.onlinelibrary.wiley.com/doi/abs/10.1002/2013JF002950`.

[25] B.C. Ludka, R.T. Guza, and W.C. O'Reilly. Nourishment evolution and impacts at four southern california beaches: A sand volume analysis. *Coastal Engineering*, 136:96 – 105, 2018. ISSN 0378-3839. doi: https://doi.org/10.1016/j.coastaleng.2018.02.003.

[26] A.P. Luijendijk, M.A. de Schipper, and R. Ranasinghe. Morphodynamic acceleration techniques for multi-timescale predictions of complex sandy interventions. *journal of Marine Science and Engineering*, 7:78, 2019. doi: https://doi.org/10.3390/jmse7030078.

[27] Arjen P. Luijendijk, Roshanka Ranasinghe, Matthieu A. de Schipper, Bas A. Huisman, Cilia M. Swinkels, Dirk J.R. Walstra, and Marcel J.F. Stive. The initial morphological response of the sand engine: A process-based modelling study. *Coastal Engineering*, 119:1 – 14, 2017. ISSN 0378-3839. doi: https://doi.org/10.1016/j.coastaleng.2016.09.005.

[28] Shilong Luo, Yuheng Liu, Ruifang Jin, Jinpeng Zhang, and Wei Wei. A guide to coastal management: Benefits and lessons learned of beach nourishment practices in china over the past two decades. *Ocean Coastal Management*, 134:207 – 215, 2016. ISSN 0964-5691. doi: https://doi.org/10.1016/j.ocecoaman.2016.10.011.

[29] A. McLachlan and A.C. Brown. 14 - human impacts. In A. McLachlan and A.C. Brown, editors, *The Ecology of Sandy Shores (Second Edition)*, pages 273 – 301. Academic Press, Burlington, second edition edition, 2006. ISBN 978-0-12-372569-1. doi: https://doi.org/10.1016/B978-012372569-1/50014-8.

[30] R.J. Nicholls, I.H. Townend, A.P. Bradbury, D. Ramsbottom, and S.A. Day. Planning for long-term coastal change: Experiences from england and wales. *Ocean Engineering*, 71:3 – 16, 2013. ISSN 0029-8018. doi: https://doi.org/10.1016/j.oceaneng.2013.01.025. Sea Level Rise and Impacts on Engineering Practice.

[31] L. Prandtl. *Über ein neues Formelsystem für die ausgebildete Turbulenz*, pages 6–19. 216, 326. Springer Berlin Heidelberg, Berlin, Heidelberg, 1945. ISBN 978-3-662-11836-8. doi: 10.1007/978-3-662-11836-8_72. URL https://doi.org/10.1007/978-3-662-11836-8_72.

[32] Roshanka Ranasinghe, Cilia Swinkels, Arjen Luijendijk, Dano Roelvink, Judith Bosboom, Marcel Stive, and DirkJan Walstra. Morphodynamic upscaling with the morfac approach: Dependencies and sensitivities. *Coastal Engineering*, 58(8):806 – 811, 2011. ISSN 0378-3839. doi: https://doi.org/10.1016/j.coastaleng.2011.03.010.

[33] L.A. Robinson. Marine erosive processes at the cliff foot. *Marine Geology*, 23(3):257 – 271, 1977. ISSN 0025-3227. doi: https://doi.org/10.1016/0025-3227(77)90022-6.

[34] Dano J.A. Roelvink and Dirk-Jan Walstra. Keeping it simple by using complex models. volume 6, 01 2005.

[35] B. Rostaing, G. Guthrie, C. Adnitt, and J. Flikweert. Bacton gas terminal coast protection stage 1 report - options appraisal, 2015.

[36] Olavo Santos, Ada Scudelari, Yuri Costa, and C Costa. Sea cliff retreat mechanisms in northeastern brazil. *Journal of Coastal Research*, 01 2011.

[37] T. Sunamura. Rocky coast processes: with special reference to the recession of soft rock cliffs. *Proceedings of the Japan Academy. Series B, Physical and biological sciences*, 91,9:481–500, 2015. doi: https://doi.org/10.1002/2013JF002950.

[38] James Sutherland, David S Brew, and Alun Williams. Southern north sea sediment transport study, phase 2 sediment transport repor, 2002.

[39] James Sutherland, A. Peet, and R. Soulsby. Evaluating the performance of morphological models. *Coastal Engineering - COAST ENG*, 51:917–939, 10 2004. doi: 10.1016/j.coastaleng.2004.07.015.

[40] Karl E. Taylor. Summarizing multiple aspects of model performance in a single diagram. 106:7183–7192, 2001. doi: https://doi.org/10.1029/2000JD900719.

[41] P.K. Tonnon, B.J.A. Huisman, G.N. Stam, and L.C. van Rijn. Numerical modelling of erosion rates, life span and maintenance volumes of mega nourishments. *Coastal Engineering*, 131:51 – 69, 2018. ISSN 0378-3839. doi: https://doi.org/10.1016/j.coastaleng.2017.10.001.

[42] M.J.P. van Duin, N.R. Wiersma, D.J.R. Walstra, L.C. van Rijn, and M.J.F. Stive. Nourishing the shoreface: observations and hindcasting of the egmond case, the netherlands. *Coastal Engineering*, 51(8):813 – 837, 2004. ISSN 0378-3839. doi: https://doi.org/10.1016/j.coastaleng.2004.07.011. Coastal Morphodynamic Modeling.

[43] Vera Vikolainen, Jaap Flikweert, Hans Bressers, and Kris Lulofs. Governance context for coastal innovations in england: The case of sandscaping in north norfolk. *Ocean Coastal Management*, 145:82 – 93, 2017. ISSN 0964-5691. doi: https://doi.org/10.1016/j.ocecoaman.2017.05.012.

[44] C.E. Vincent. Longshore sand transport rates — a simple model for the east anglian coastline. *Coastal Engineering*, 3:113 – 136, 1979. ISSN 0378-3839. doi: https://doi.org/10.1016/0378-3839(79)90013-9.

[45] M.J.A. Walkden and J.W. Hall. A predictive mesoscale model of the erosion and profile development of soft rock shores. *Coastal Engineering*, 52(6):535 – 563, 2005. ISSN 0378-3839. doi: https://doi.org/10.1016/j.coastaleng.2005.02.005.

[46] D.J.R. Walstra, C. Briere, A.B. Cohen, A.P. van Dongeren, L.J.P. Elshoff, C. Hoyng, M. Ormondt, S. Quartel, B. de Sonneville, P.K. Tonnon, and L. Uunk. Monitoring and modelling of shoreface nourishment, 2008.

[47] D.J.R. Walstra, R. Hoekstra, P.K. Tonnon, and B.G. Ruessink. Input reduction for long-term morphodynamic simulations in wave-dominated coastal settings. *Coastal Engineering*, 77:57 – 70, 2013. ISSN 0378-3839. doi: https://doi.org/10.1016/j.coastaleng.2013.02.001.

[48] Xujie Zhang, Pengcheng Zhao, Qingwu Hu, Mingyao Ai, Datian Hu, and Jiayuan Li. A uav-based panoramic oblique photogrammetry (pop) approach using spherical projection. *ISPRS Journal of Photogrammetry and Remote Sensing*, 159:198 – 219, 2020. ISSN 0924-2716. doi: https://doi.org/10.1016/j.isprsjprs.2019.11.016. URL http://www.sciencedirect.com/science/article/pii/S092427161930276X.

A

Cliff erosion modelling

There are several methods to model cliff erosion which will be summarised below.

1. **Stochastic simulation**: A probabilistic prediction method is used to simulate the cliff recession with its uncertainty. Monitoring data of the cliff line is often scarcely available and cliff retreat is often highly episodic. Cliff retreat is modelled as an episodic random process and can be evaluated with different distributions for the retreat. Therefore this model is only valid for areas where no interventions are taken to prevent the erosion. At Bacton a nourishment is placed in front of the cliff to prevent the erosion and therefore a stochastic model will not be valid.

2. **Energy approach**: The wave energy approach relates the cliff line retreat (CLR) to the amount of wave energy at the toe of the cliff (Ω). An energy threshold level (Ω_c) is set at the toe of the cliff and the energy surpassing this level is computed. These energy levels are then coupled to the known CLR rates of the area to determine a CLR formula for the whole cliff area [15]:

$$CLR = \int_{t=0}^{t} f((\Omega(t) - \Omega_c) + c)\,dt \tag{A.1}$$

   The parameter 'c' is a constant which can be calculated With given historical data. However, this method doesn't include the strength of the cliffs [15].

3. **Linking beach levels to recession rate**: In this method the beach area above Mean High Water (MHW) is coupled to the erosion rate. This beach area has been studied by Lee [21] for the cliffs in the area of Bacton. It was found that if the beach area is large enough, almost no erosion will be present. Some variability in the results was found and it cannot be concluded that a specific beach area will result in no erosion during more stormy conditions.

4. **SCAPE+**: This is a long-term coastal model which incorporates the cliff erosion process at the toe in a 2D morphological model. Besides the cliff erosion it also calculates the morphology of the beaches with a simple 1D approach. This model seems to be less suitable for complex nourishment intervention and is rather used to assess the cliff erosion on the scale of decades. This can therefore in a less extent simulate the erosion during a single storm.

B

Nourishments

A nourishment is a "soft engineering" alternative for traditional "hard engineering" solutions to counteract shoreline erosion and increase shoreline protection [29]. These hard engineering solutions include structures as groynes, revetments, and breakwaters. It is well known that these hard solutions have a large impact on their surroundings and don't necessarily solve the erosion problems. Most often the problem is solved locally, but increases erosional effects further down drift. Therefore nourishments have been introduced to reduce the effects down drift and increase the coastal safety [25]. Nourishments can be characterised into 3 main categories: Beach nourishment, shoreface nourishment and mega-nourishment. These categories will be described in the upcoming section to get a better understanding of the different schemes that are present.

B.1. Beach nourishment

A beach nourishment is characterised by a location in between the dune foot and the mean low water level [6]. This creates a wider dry beach which allows for more recreational space and is able to absorb more wave energy [13]. An increased beach width will not reduce the erosional effects that are present in the area, but will provide the system with more sediment and act as a buffer. Besides, a beach nourishment has no unfavourable effects on the longshore transport processes either up drift and down drift [12].

B.2. Shoreface nourishment

A shoreface nourishment is located in the active zone of the coastal system and is submerged in all conditions. The nourishment is expected to reach the beach in several years [42]. Unfortunately, not all the sediment supplied in the nourishment will reach the beach. Accordingly, larger amounts of sediment are needed to supply the beach with enough sediment. The costs of shoreface nourishments on the other hand, are significantly lower than for beach nourishments, which compensates for the extra sediment needed. These large deposits can have a mayor impact on the local bar system that is present. [6].
Furthermore, a shoreface nourishment can behave as a detached breakwater. Due to a local reduction in water depth, waves start breaking over the nourishment, which causes milder wave conditions onshore, however it also causes a return current. Due to the local wave breaking and the return current, a shoreface nourishment will have impact on both the cross shore and longshore sediment transport rates. The return current is able to transport large amounts of sediment off shore (as is the case in Egmond (the Netherlands)) [42] while the nourishment itself can block the onshore sediment flow from further offshore. The waves energy that is dissipated over the shoreface nourishment causes a local decrease in wave energy behind the nourishment area. This decrease in wave energy will cause less sediment transport in the lee of the shoreface nourishment. Therefore, local shoreline erosion will be present further down drift of the shoreface nourishment and in the lee of the shoreface nourishment accretion will take place (see also Figure B.1(a)).

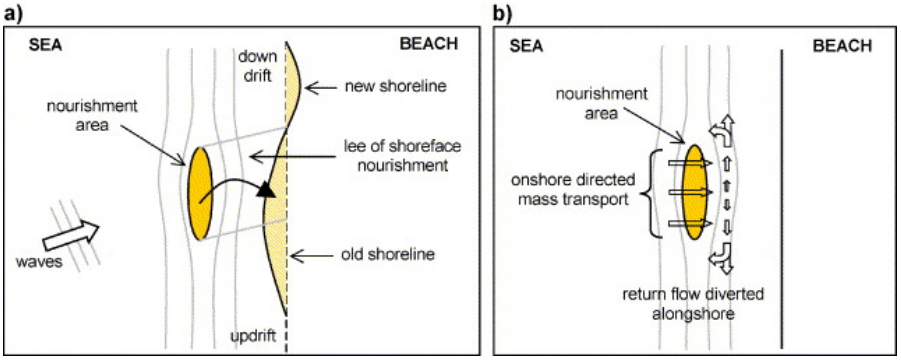

Figure B.1: Effects of a shoreface nourishment.(Adapted from van Duin et al. [42].)

B.3. Mega-nourishment

Mega-nourishments are, as their name may suggest, very large nourishments with volumes in the order of tens of millions of m^3. According to Tonnon et al. [41] Mega-nourishments can be divided into 2 categories:

- Feeder type: Nourishment is designed in such a way that the nourishment will spread out and 'feed' the adjacent beaches with sediment.
- Permanent type: The nourishment must maintain a minimum shape and size and the nourishment will not function as a feeder.

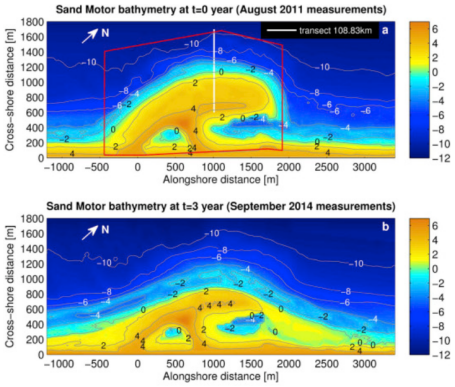

Figure B.2: Diffusive behaviour of SE in a 3 year period. Adapted from Tonnon et al. [41]

Although the BSS cannot be considered as a mega nourishment, it can be considered a feeder nourishment. The feeder nourishments constructed in the past are a smaller feeder nourishment in New Jersey [22] and the Sand Engine located at the Delfland coast in the Netherlands. Findings of the latter show that a feeder nourishment will reshape quite quickly into a 'bell shape' like feature [41] which behaves in a diffusive way. Therefore the feeder redistributes sediment in both alongshore directions.

C

Scarp formation

Figure C.1: Scarp (2m high) in October, adapted from [4]

Figure C.2: Scarp (4m high) in February, adapted from [3]

D

Profile locations

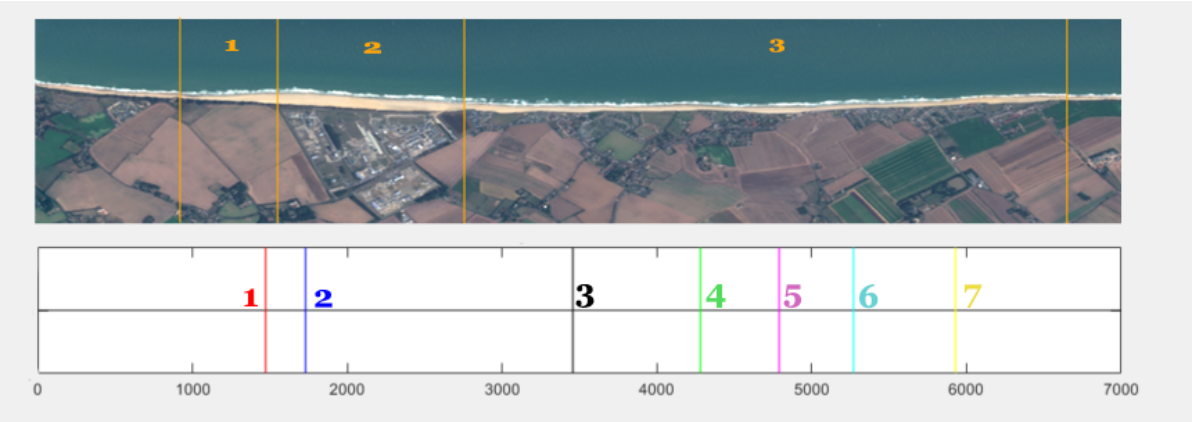

Figure D.1: locations of the cross-sections shown in Figures below

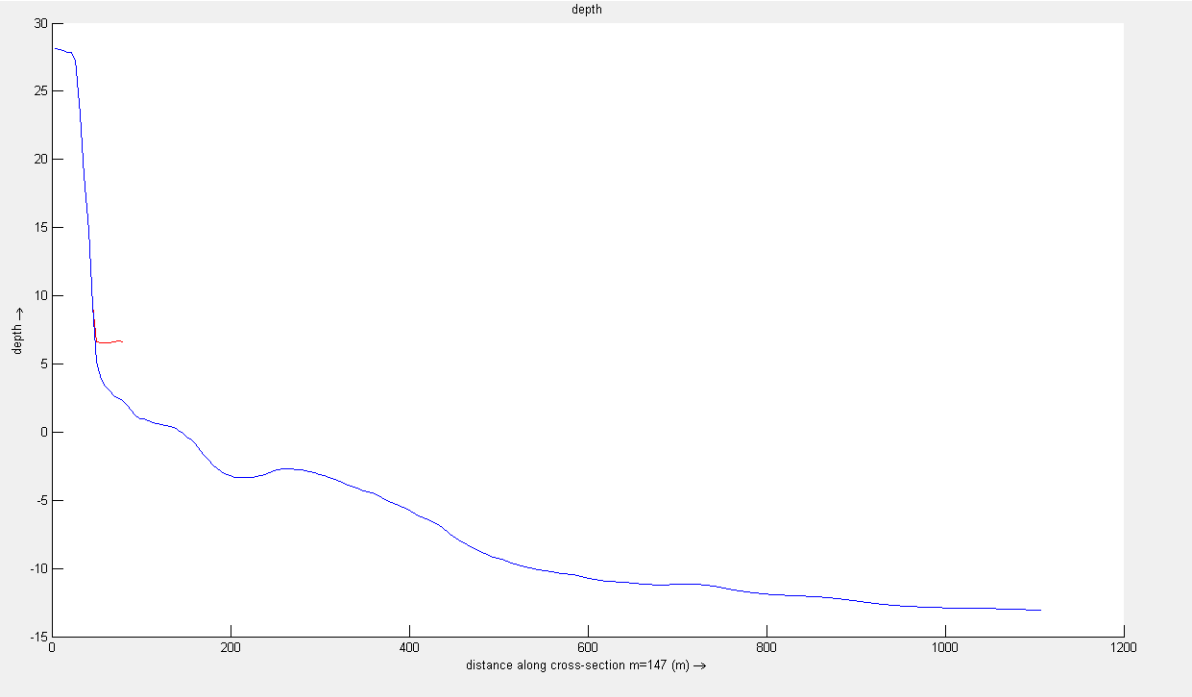

Figure D.2: Mismatch location 1

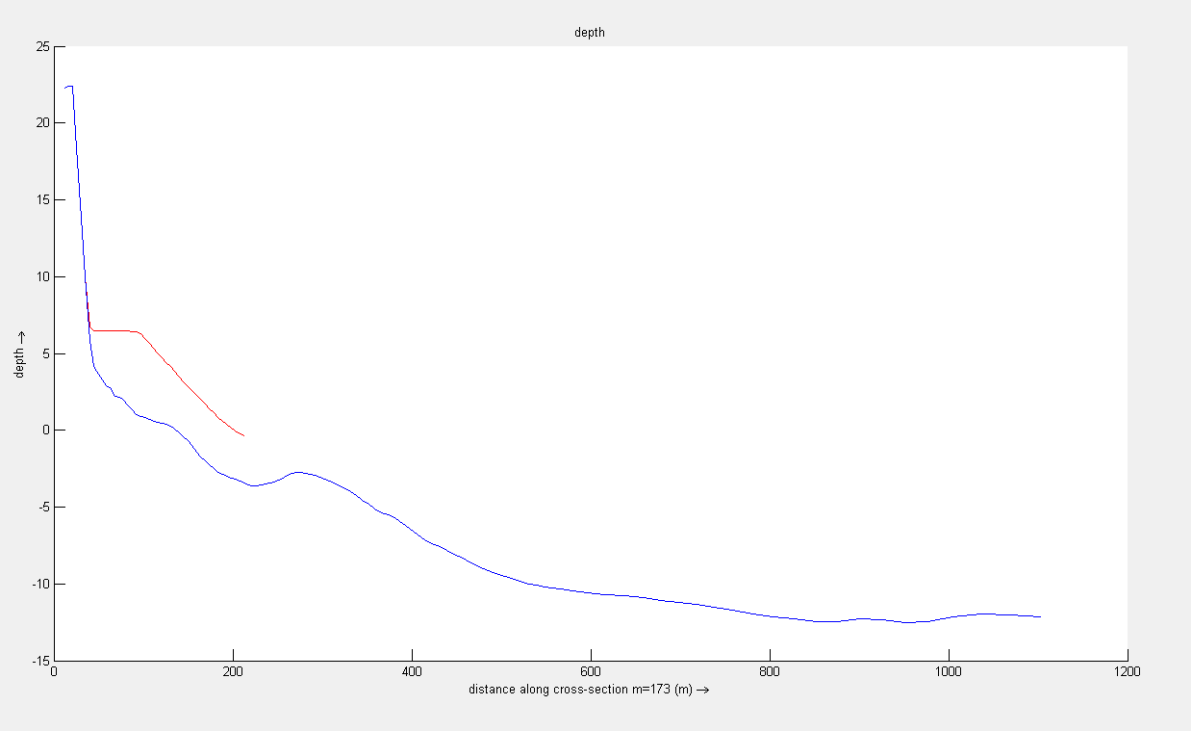

Figure D.3: Mismatch location 2

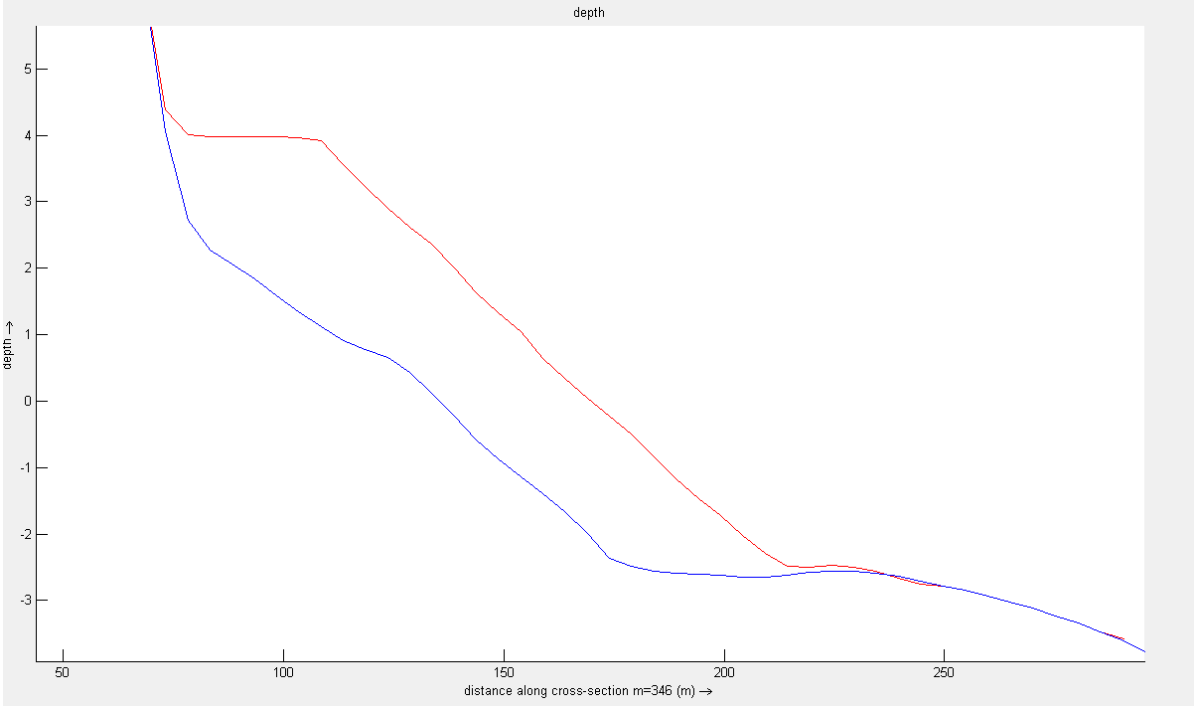

Figure D.4: Good match at location 3

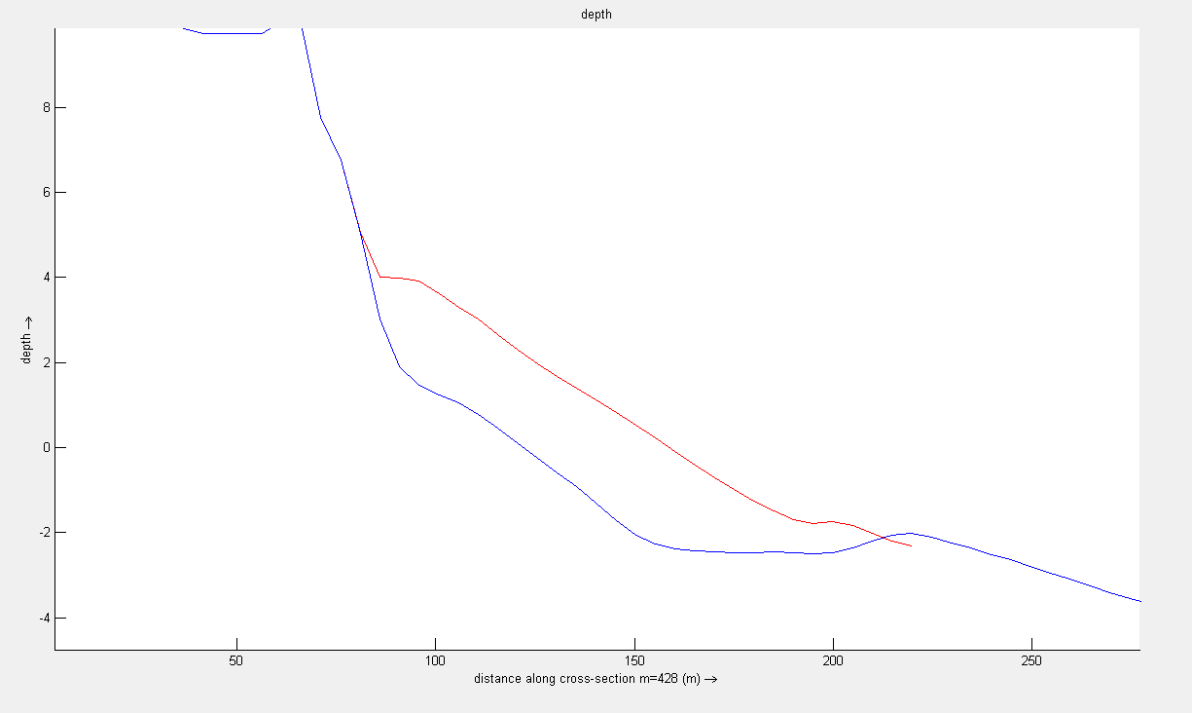

Figure D.5: Mismatch location 4

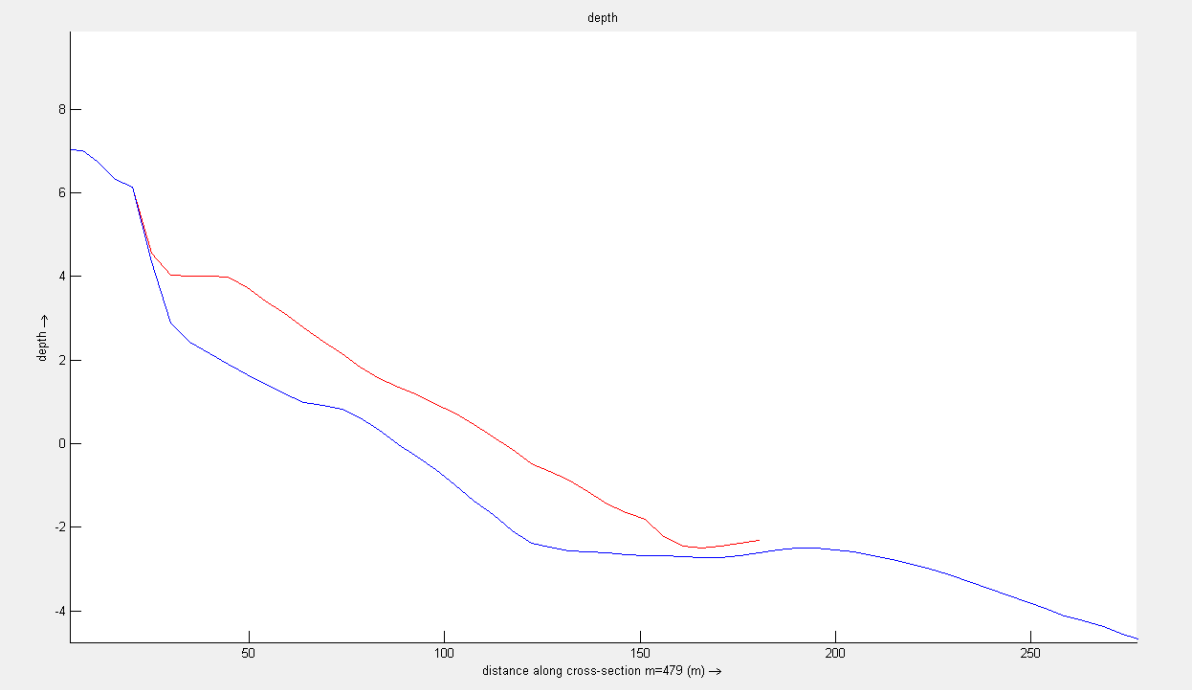

Figure D.6: Mismatch location 5

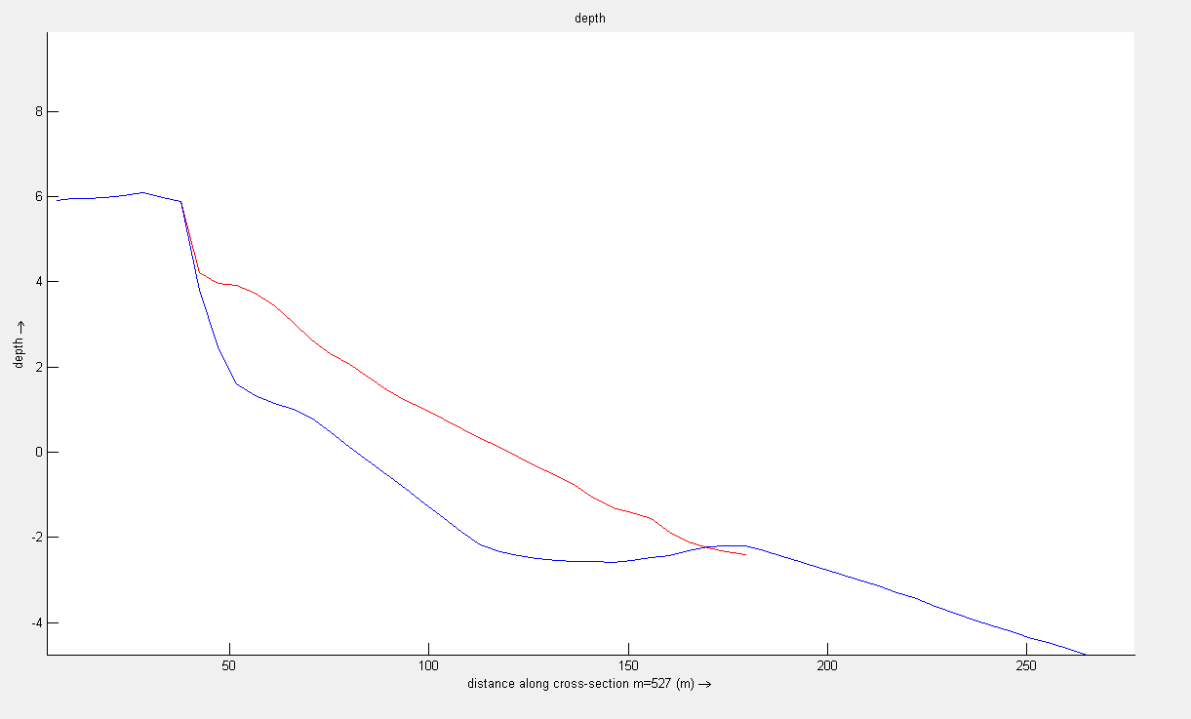

Figure D.7: Mismatch location 6

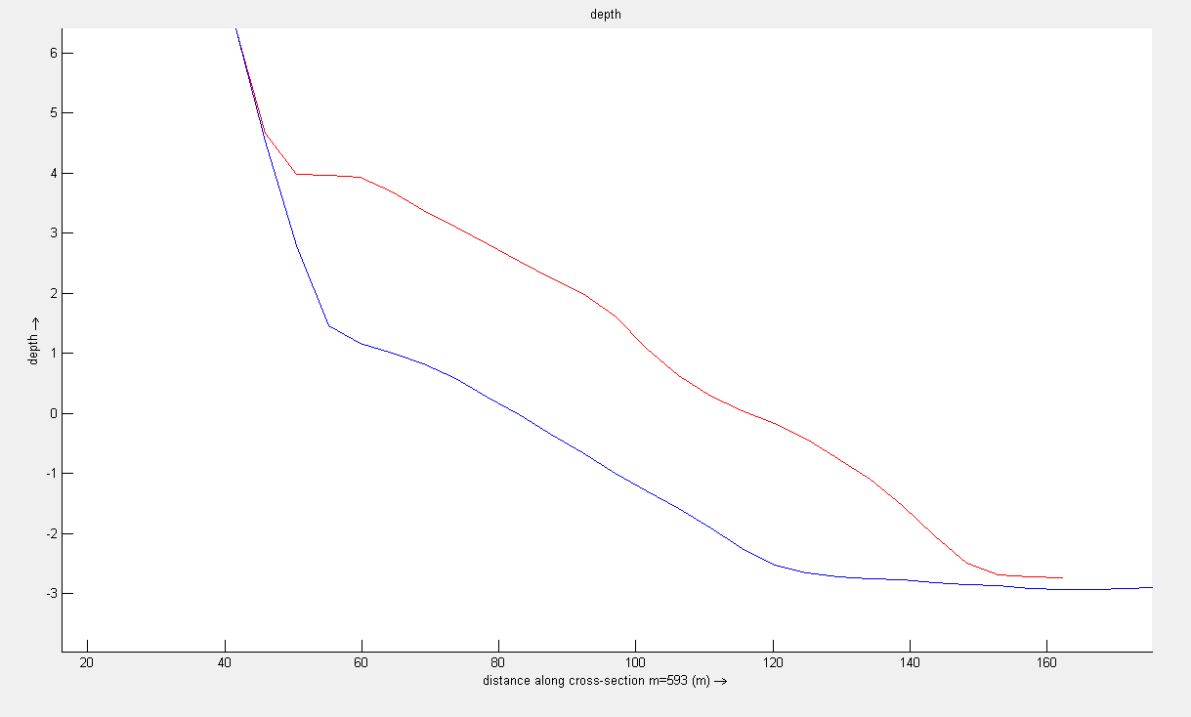

Figure D.8: Mismatch location 7

E

Wave transformations

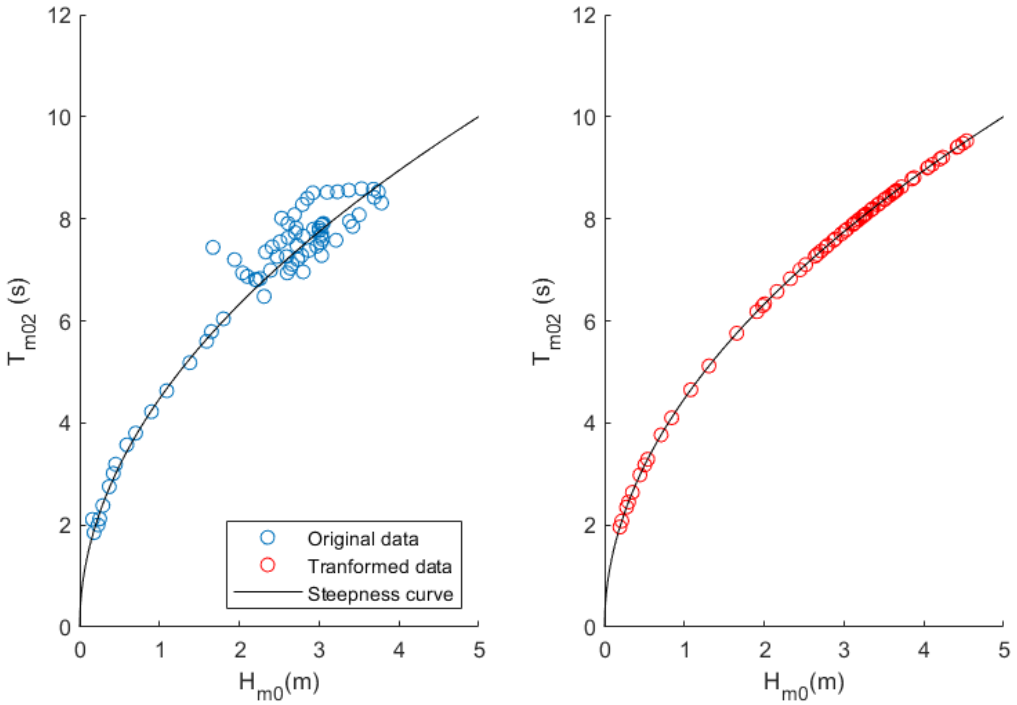

Figure E.1: Wave transformation for the event in November 2019 (+20%)

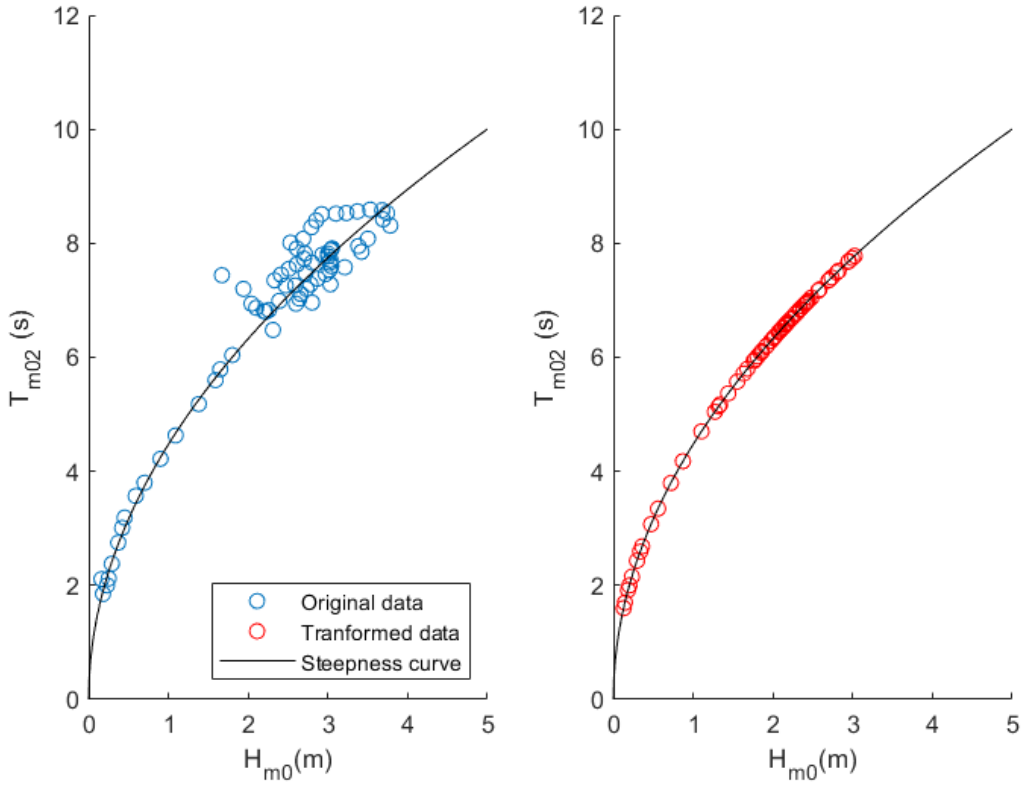

Figure E.2: Wave transformation for the event in November 2019 (-20%)

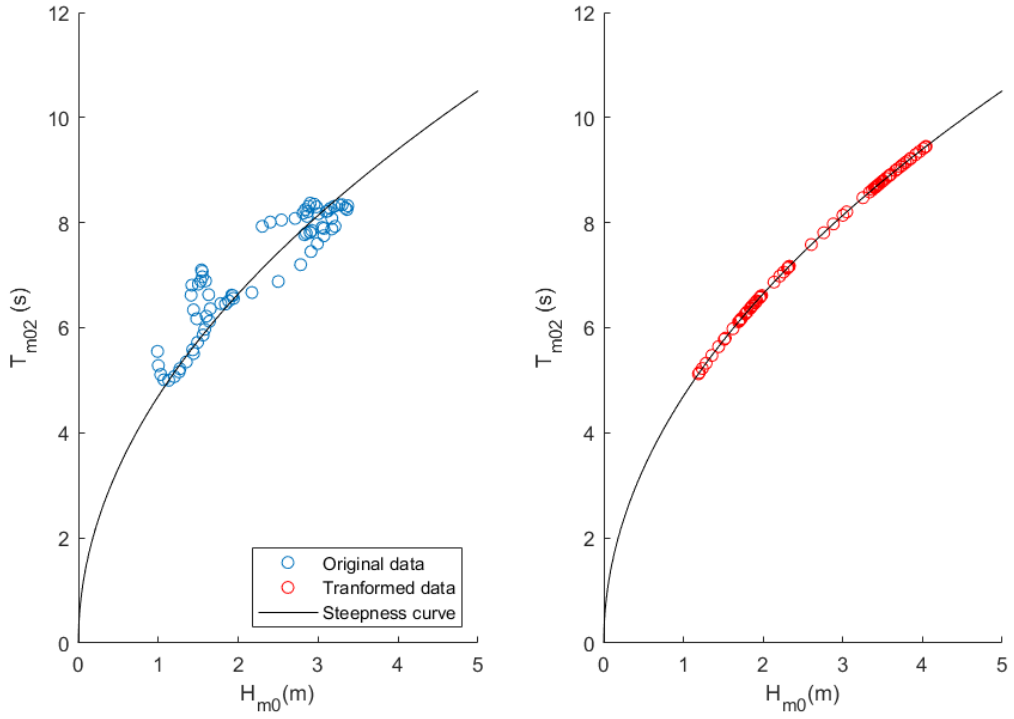

Figure E.3: Wave transformation for the event in December 2019 (+20%)

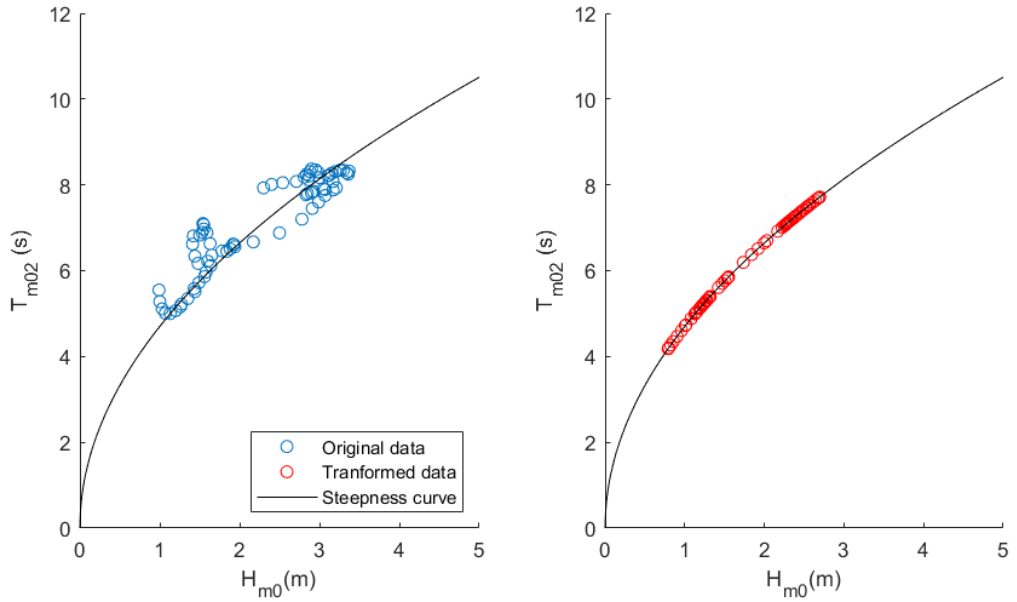

Figure E.4: Wave transformation for the event in December 2019 (-20%)

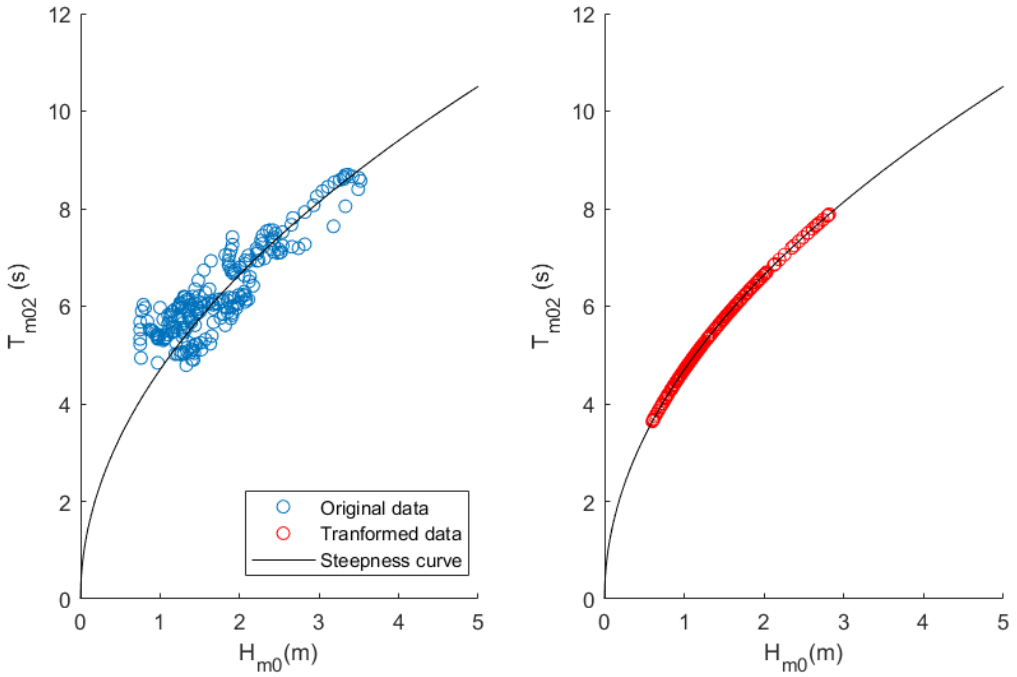

Figure E.5: Wave transformation for the event in January 2020 (-20%)

F

Extended results of sediment, wave and long run scenarios

The volume differences for the sub-aerial beach per scenario are listed from least erosive to most erosive in Table F.1. A smaller grain size than the reference grain size of 350 μm seems to be unfavourable for the BSS as the top three most erosive scenarios always contain 2 scenarios with a grain size of 300 μm. Likewise, the most erosive scenario for Section 1 and 2 is with a grain size of 300 μm with the intensified wave events. For Section 3 the most erosive scenario is also with a grain size of 300 μm but with reduced wave events. The least erosive scenarios include mostly the larger grain size of 400 μm and again for Section 1 and Section 2 less erosion is observed for reduced wave events and for Section 3 less erosion is observed for intensified wave events. Moreover, for all grain sizes the pattern is similar. As wave events intensify, more sediment is eroded for Section 1 and 2 and less sediment is eroded from Section 3. More intense wave events tend to erode more from the first two Sections and part of this sediment is transported to the last Section. When wave events are reduced, their transport capacity reduces as well. Less sediment is transported to Section 3 and also less is eroded from the first two Sections. However, the volume changes per scenario do not differ significantly and just goes to show that the model is very robust.

Section 1				Section 2				Section 3			
#	Grain size	Wave events	Vol. change	#	Grain size	Wave events	Vol. change	#	Grain size	Wave events	Vol. change
2.3	400μm	-20%	-46,091	2.3	400μm	-20%	-136,610	1.2	350μm	+20%	-202,860
2.1	400μm	+0	-46,490	1.3	350μm	-20%	-139,720	2.2	400μm	+20%	-203,730
2.2	400μm	+20%	-46,702	2.1	400μm	+0%	-144,270	2.1	400μm	+0%	-210,920
1.2	350μm	+20%	-48,212	3.3	300μm	-20%	-144,970	2.3	400μm	-20%	-213,010
1.1	350μm	+0%	-48,255	2.2	400μm	+20%	-147,540	3.2	300μm	+20%	-213,700
3.3	300μm	-20%	-50,217	1.1	350μm	+0%	-147,570	1.1	350μm	+0%	-214,720
3.1	300μm	+0%	-50,467	1.2	350μm	+20%	-149,140	1.3	350μm	-20%	-216,240
1.3	350μm	-20%	-51,443	3.1	300μm	+0%	-150,600	3.1	300μm	+0%	-217,160
3.2	300μm	+20%	-52,637	3.2	300μm	+20%	-156,260	3.3	300μm	-20%	-223,790

Table F.1: Sub-aerial beach erosion volumes per section for all scenarios in m^3. Hashtag indicates the scenario number.

The results of Table F.1 show that a smaller grain size results in slightly more erosion. Sediment gets earlier into suspension and bed load transport is enhanced as well, as less shear stresses are required to transport sediment. The easier transportation does not result in more sediment deposition in the sub-aerial beach region of Section 3. It is likely that the smaller grain size also enhances erosive processes in Section 3 and are not compensated by sediment input from Section 2. The largest grain size shows to be the least erosive for Section 1 and 2 as the sediment requires higher wave power to be transported in the first place. The reduced erosion of Section 3 is then also likely to be caused by the reduction of erosion itself, rather than an increase of sediment input from Section 2 to Section 3. There seems to be a balance in erosive capacity and transport capacity of the sediment grain size. The 350 μm grain size sits in the middle of the other two grain sizes and shows in general more erosion of Section 1 and 2 compared to the larger grain size. However, when wave events intensify the 350 μm grain size shows less erosion of Section 3 than any other scenario for 400 μm. Again, volume differences between the scenarios are very small and show almost no change in alongshore

variability.
The volume changes per running meter for all scenarios are shown in Figure F.1. These results also show the behaviour of the submerged beach. In general, the submerged beach accretion is enhanced by smaller grain sizes and reduced for larger grain sizes. Intensified wave events also show to be beneficial for the accretion of the submerged beach. These results do therefore not differ from the earlier observations from the results of the sediment scenarios and the wave scenarios. The results per running meter for the sub-aerial beach show no major differences with the results and analysis of the volume changes per Section. Larger grain sizes show less erosion of Section 1 and 2 and intensified wave events show less erosion for Section 3.

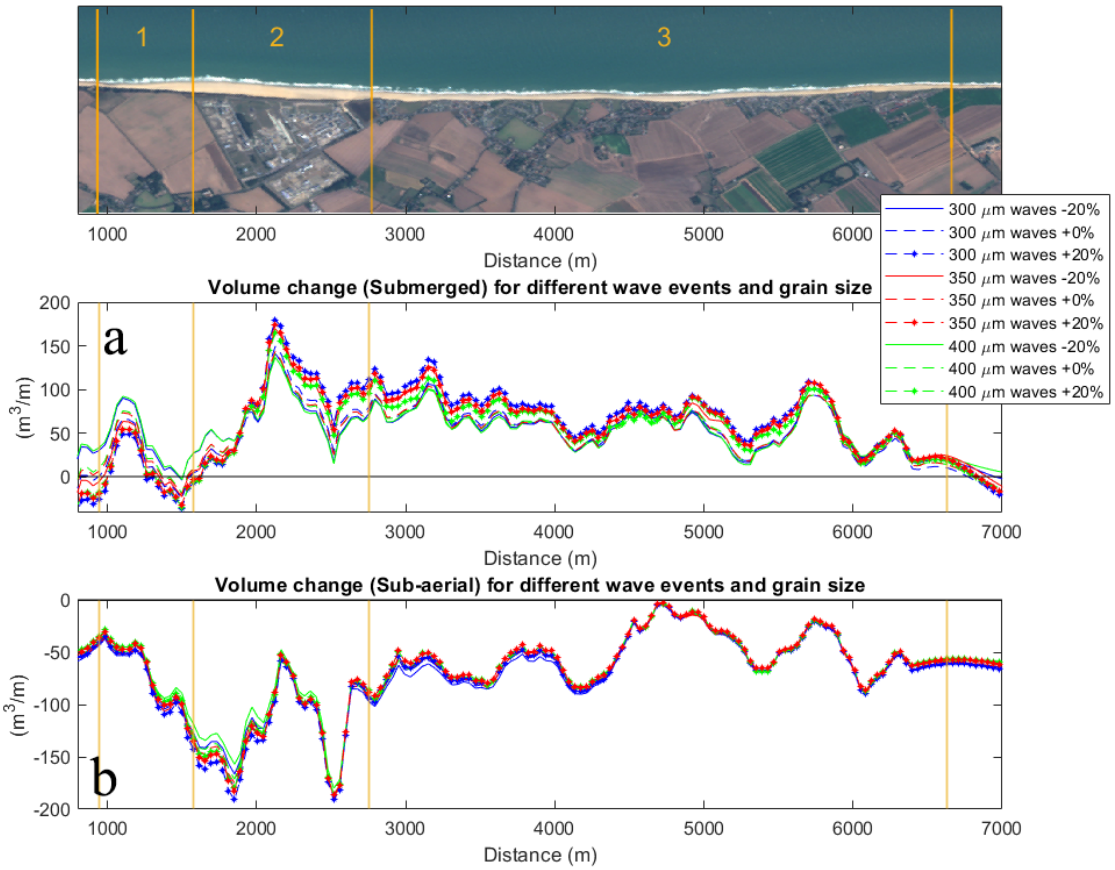

Figure F.1: a) Volume changes of the submerged beach for all scenarios. b) Volume changes for the sub-aerial beach for all scenarios. In all figures the Section numbers and boundaries are indicated in Yellow. The top figure functions as a location indicator

F.1. Summary of results

The results of the last paragraphs are presented in normalised erosion rates and erosion percentages. First the normalised erosion rates are discussed and secondly the percentage results. The erosion of the sub-aerial beach is normalised per section. The following formula is used for normalisation:

$$z_i = \frac{x_i - x_{ref}}{x_{max} - x_{min}} + 1 \tag{F.1}$$

Where z_i is the normalised erosion rate, x_i the erosion rate of a specific scenario,x_{ref} is the erosion rate of the scenario with 350μm and waves +-0%, x_{min} is the minimum observed erosion rate of a section and x_{max} is the maximum observed erosion rate of a section. This results in a value between 1 and 2 for each of the scenarios per section. A value of 1 means that the scenario results in the least erosion for that specific section and a value of 2 means that the scenario results in the most erosion for that specific section. A value between

1 and 2 shows the normalised difference between the scenarios. This results in a clearer way of analysing the earlier presented results. The normalised results are shown in Figure F.2.

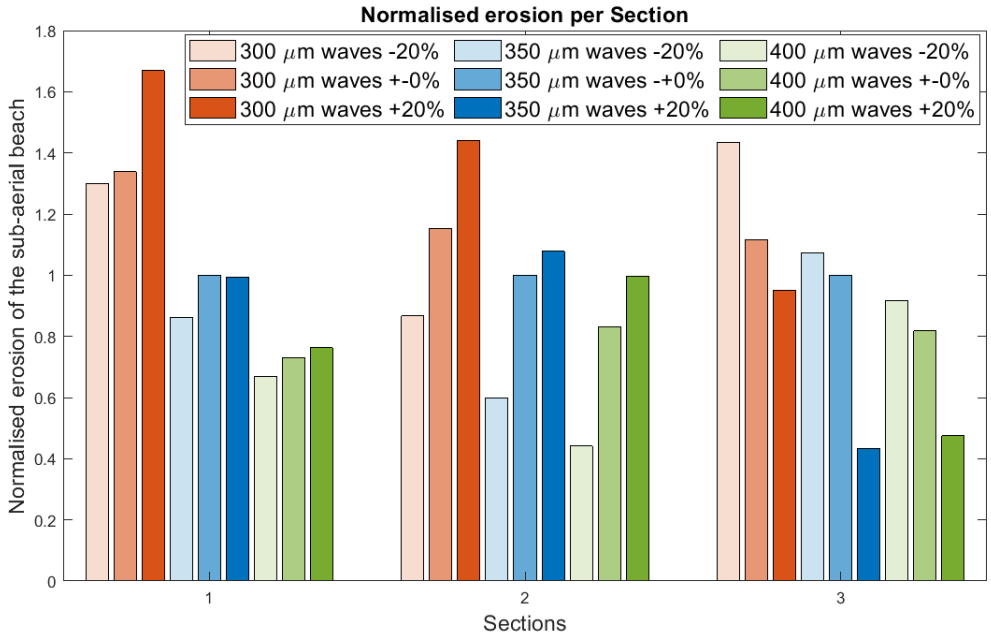

Figure F.2: Normalised erosion of the sub-aerial beach. Normalisation of the scenarios is performed per section. The results are normalised with the results of 350μm (waves +-0%) for each of the sections.

Figure F.2 shows that an increase in grain size results in overall less erosion across all sections. Intensified wave events result in more erosion of both Section 1 and 2 for all grain sizes and erosion of Section 3 decreases for intensifying wave events.